Research and application progress of welding technology under extreme conditions

Article *in* Archives of Civil and Mechanical Engineering · June 2024

DOI: 10.1007/s43452-024-00987-6

3 authors, including:

Chao Chen
Central South University
149 PUBLICATIONS **2,530** CITATIONS

Archives of Civil and Mechanical Engineering (2024) 24:182
https://doi.org/10.1007/s43452-024-00987-6

REVIEW ARTICLE

Research and application progress of welding technology under extreme conditions

Ke Xu[1,2] · **Yuxin Yin**[1,2] · **Chao Chen**[1,2]

Received: 25 December 2023 / Revised: 13 May 2024 / Accepted: 1 June 2024

Abstract
Welding technology plays a critical role in materials joining, especially in the manufacture and maintenance of space stations, ships, and nuclear equipment that operate under extreme conditions. These conditions present researchers with a wide range of research topics. This paper reviews the current research and application progress of welding technology under extreme conditions, such as microgravity, high temperature, and corrosion. Initially, the characteristics of extreme environments are introduced, and the technical bottlenecks faced by current welding technology in extreme environments are analyzed. The comprehensive performance changes of welded structures in these extreme environments are summarized. Subsequently, the influence of extreme environments, such as underwater and space, on the appearance quality, microstructure, and mechanical properties of welded joints is analyzed. The influence mechanism of environmental factors, such as temperature, gravity, pressure, and corrosion, on the performance of joints was elucidated based on typical welding cases of materials and engineering equipment. The various countermeasures studied to overcome the adverse effects of these extreme environments are compared. Finally, the current challenges in welding technology under extreme conditions are summarized and sorted out. The development and research of extreme welding technology in conjunction with engineering application needs are envisioned.

Keywords Extreme manufacturing · Welding technology · Extreme service environment · Material joining

1 Introduction

Welding technology is widely used to join components in various industries, including machinery, automotive, shipbuilding, aerospace, and energy, due to its high strength and effective sealing [1]. Welding environments gradually expand to extreme environments, such as space, oceans, and polar regions [2]. Engineering equipment requires welded structures with higher performance and longer lifespans. As a result, these structures must be able to withstand the negative impacts of various extreme conditions, such as vacuum, low temperature, corrosion, and radiation [3]. Conventional welding techniques face significant challenges when dealing with these extreme environmental conditions. Therefore, welding technology with higher durability and adaptability is necessary. Many researchers have studied welding processes, materials, and post-treatment methods to ensure the performance of welded structures.

Welded joints are the weakest points in welded structures due to their unique material composition, microstructure, and uneven properties [4]. Environmental factors can exacerbate the vulnerability of joints by generating residual stresses and defects [5]. The study of failure mechanisms of welded structures is critical to the advancement of welding technology. Indeed, the effect of environmental factors on joints can be judged by assessing criteria, such as joint quality, microstructural characteristics, mechanical properties, and corrosion resistance. For example, low temperature can cause metals to lose ductility and become brittle [6], high temperature can cause metals to creep [7], and radiation exposure can cause metals to lattice dislocate [8]. These studies drive continuous innovation in welding technology and materials technology to mitigate the negative effects imposed by the extreme environment.

In extreme environments, the welding method has a direct impact on the performance and integrity of welded

✉ Chao Chen
profchenchao@163.com

[1] Light Alloy Research Institute, Central South University, Changsha 410083, China

[2] State Key Laboratory of Precision Manufacturing for Extreme Service Performance, Central South University, Changsha 410083, China

Published online: 19 June 2024

structures. Welding techniques have progressed from arc welding (AW) [9] to contemporary approaches like laser welding (LW) [10] and friction stir welding (FSW) [11]. In response to the challenges of welding in high-temperature environments, several technological means have been developed, including high-temperature gas-shielded welding technology [12], electron beam welding (EBW) [13], and LW [14]. These methods have proven to be highly reliable in such environments. In addition, various techniques have been developed to improve the strength and mechanical properties of welded joints, including ultrasonic-assisted welding [15], magnetic pulse welding [16], and other forms of energy-based welding. These techniques take advantage of various physical and chemical effects to facilitate the welding process and improve the quality of the welded joints.

The selection of welding materials is also critical in extreme environments. In high-temperature environments, materials must possess excellent heat resistance and oxidation resistance, while materials used in low-temperature environments require higher toughness and cold resistance. Researchers have commenced investigations into novel materials to adapt to extreme environments. High-entropy alloys exhibit superior mechanical properties, corrosion resistance, and high-temperature resistance, making them suitable for use in various extreme environments [17]. Nanomaterials can change the interfacial reaction between the welding material and the welded joint and promote grain refinement during the welding soldering process. Adding nanomaterials to the welding material can significantly improve the microstructure and mechanical properties of the joint [18]. Composite ceramics are increasingly being used in equipment manufacturing as a representative of composite materials in the field of high-temperature and high-strength. They offer superior strength and durability compared to conventional materials [19]. In the design of welding equipment for extreme environments, welding equipment is becoming increasingly intelligent. The integration of automation, machine learning, and vision technology makes the welding process more precise and efficient. In addition, the intelligent welding system can monitor and adjust in real time to ensure the overall performance of the welded joints [20].

These endeavors have led to significant advancements in welding methods, materials, and equipment. This paper aims to provide a comprehensive summary and analysis of research in this field, focusing primarily on extreme service environments and welding environments. Initially, the paper outlines the distinctive characteristics of extreme environments, emphasizing influential factors, such as vacuum conditions, low temperatures, and radiation. In this paper, through a comprehensive analysis of the quality, microstructure, and mechanical properties of the weld, the mechanism of environmental factors on the performance of the welded structures is investigated. Subsequently, the paper elucidates the effects of material composition, welding techniques, and post-processing methods on welded structures. The challenges of welding technology in extreme environments are analyzed in this paper. In addition, the current progress of research and application of welding technology in extreme environments is summarized based on materials and engineering examples. Finally, the research gaps in welding technology for extreme environments are summarized by comparing existing welding methods, welding processes, and welding materials. In response to the need for high-quality welded joints in extreme environments, this paper looks at the development of advanced welding technologies suitable for such conditions.

Through a comprehensive analysis of the relevant literature, this paper aims to provide a comprehensive understanding of the various challenges facing welding in extreme environments and to provide a clear direction and focus for future research. Additionally, the key technical principles, methods, and application cases are refined to provide comprehensive reference and guidance for researchers.

2 Research and application progress under extreme conditions

2.1 Research and application progress of welding technology in the space environment

The rapid advancement in aerospace technology has highlighted the necessity of enhancing spacecraft lifespan through in-orbit manufacturing and maintenance [21]. Welding technology has become the main joining method for aircraft due to the improvement of welding strength and reliability [22]. Innovative methods, advanced materials, and intelligent equipment are required to meet space welding needs for reliable and durable welded structures for space exploration and habitation.

2.1.1 Effect mechanisms of space environment on welded structures

The mechanisms through which the space environment affects welding structures involve various factors, including extreme temperature fluctuations, vacuum conditions, and radiation exposure. These environmental conditions can affect the metallurgical properties of the welded joints, leading to changes in material strength, hardness, and corrosion resistance. Additionally, the absence of gravity in space can alter the solidification process during welding, potentially resulting in the formation of voids or cracks within the welds. Understanding these effects mechanisms is crucial for developing effective welding techniques and ensuring

the reliability and durability of welded structures in space applications [23]:

2.1.1.1 Effects of the microgravity environment on welded structures The gravitational acceleration during the operational phase of a spacecraft in low Earth orbit is only in the range of 10^{-2}–10^{-6} g_0 times that of Earth's gravity (g_0) [24]. Figure 1 illustrates the effects of gravity on porosity distribution in tungsten arc-welded seams. The distribution of pore sizes and shapes indicates that the solidification process during welding is altered. In a microgravity environment, molten metal solidifies uniformly from the top and bottom due to the absence of natural convection. Pores are evenly distributed throughout the weld seam. The weld seam is flatter than that of the conventional.

In a microgravity environment, phenomena, such as component separation, buoyancy effects, and fluid convection, induced by different densities are severely restricted.

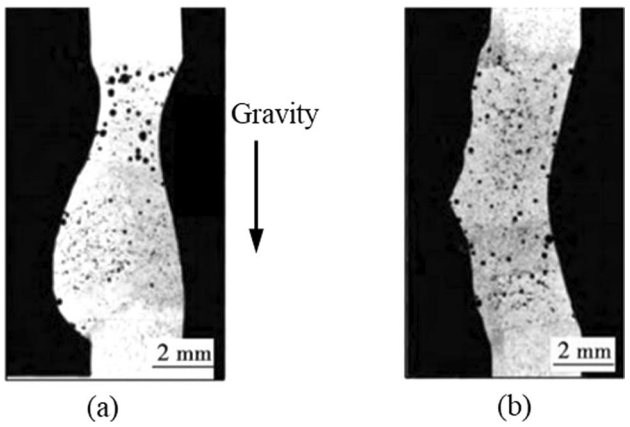

Fig. 1 Effects of gravitational level on the distribution of porosity in tungsten arc-welded seams. **a** Normal environment. **b** Microgravity environment [24]

Fluids are constrained mainly by liquid surface tension due to the absence of fluid static pressure. This absence of gravitational effects exacerbates capillary and chemical convection, and density differences no longer cause stratification phenomena [25]. Simultaneously, the surface effect of the liquid is enhanced during metal welding due to the absence of buoyancy and convection in the liquid. Additionally, the thermal conduction behaves differently in space than on Earth. Because of the lack of distinct directional boundaries, heat does not naturally rise as it does on Earth. This behavior leads to an uneven temperature distribution in the weld zone, resulting in thermal stresses and cracks [26].

Luo et al. [27] simulated the gas distribution in the weld seam under complete penetration and partial penetration welding conditions under gravity and microgravity conditions, as depicted in Figs. 2 and 3. Pore-like defects tend to accumulate in the bottom regions of the weld seam due to the influence of gravity and are distributed along the axial direction of the weld seam. However, gas pores are more likely to occur at the molten pool interface under microgravity conditions. The reason is that the effects of gravity-driven convection and natural convection are diminished, making it difficult for bubbles to escape from the molten pool. These bubbles increase the probability of pores in electron beam deep penetration welds.

In microgravity environments, workers may lose the perception of their correct orientation of the welded workpiece due to the absence of a reference to the direction of gravity. Moreover, workers are constrained in their ability to apply force and control welding equipment, which makes it more difficult to sense and control the force applied during the welding process. These factors can lead to deviations in weld position, resulting in decreased movement precision and impacting the welding process.

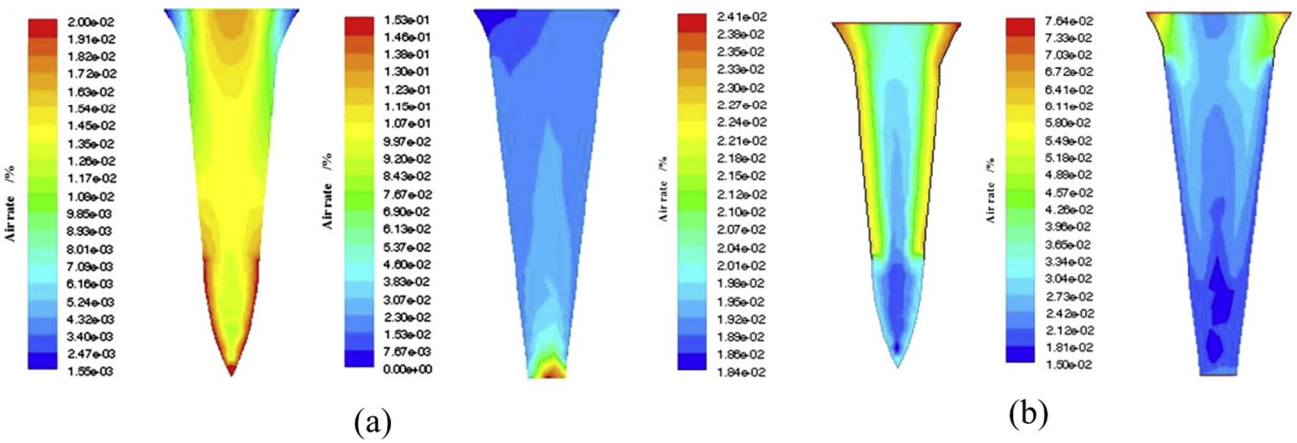

Fig. 2 Gas distribution of weld seam under different gravity and welding conditions **a** 1G. **b** 0G [27]

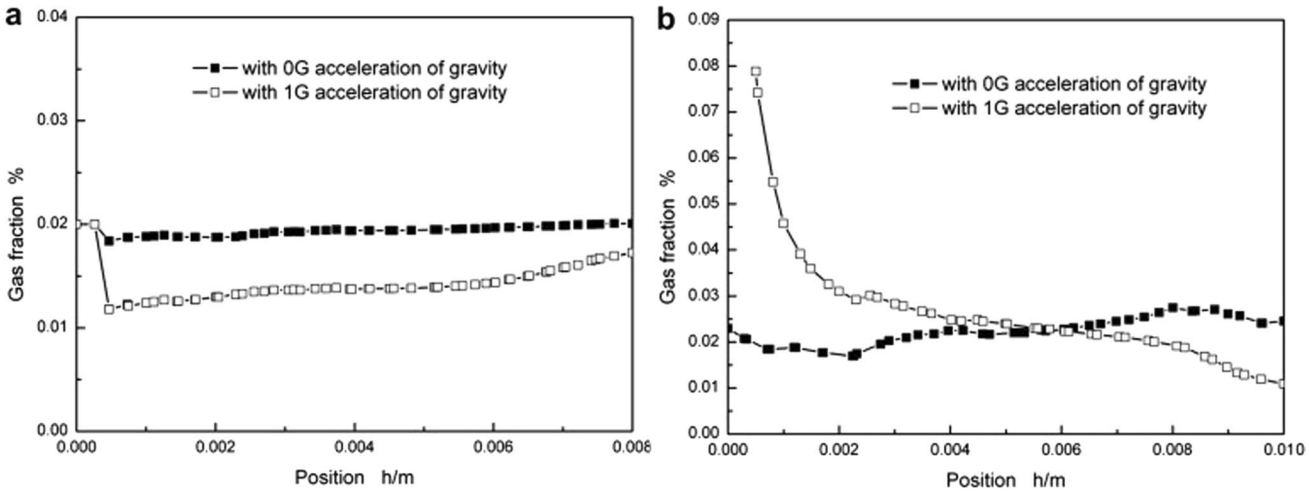

Fig. 3 Gas fraction of different types of weld seam. **a** Partial penetration welding. **b** Complete penetration welding [27]

2.1.1.2 Effects of high vacuum environment on welded structures In the space environment, atmospheric pressure diminishes exponentially with increasing altitude. Near-Earth orbit (NEO) space systems typically operate at altitudes ranging from 250 to 500 km above the Earth's surface, where the vacuum level is approximately 5×10^{-4} Pa. The effects of a high vacuum environment on welded structures are mainly in the areas of gas removal, thermal conduction, and material evaporation. There is a lack of pathways for gas diffusion and escape during welding in a vacuum environment. These gasses are trapped when the molten metal solidifies and can cause the formation of pores and cracks [23].

In the vacuum environment, the rate of atmospheric evacuation can impact both the arc and the composition of the weld seam. Due to the heightened pumping speed of the atmosphere during welding, the emission and flow of electrons may become more pronounced. The stability of arc discharge and contraction is significantly reduced [27]. Furthermore, volatile components like solutes and low-boiling-point alloy elements might evaporate instantaneously in high vacuum environments, resulting in changes in the composition of the weld zone. Such changes may potentially decrease the comprehensive performance of the welded structures [28].

2.1.1.3 Effects of light-shadow boundary on welded structures The space environment lacks atmospheric protection, causing welded zones exposed to direct sunlight to reach extremely high temperatures, while shaded regions remain relatively cold. This characteristic creates an uneven surface temperature distribution in the welded structure due to the unique boundary between illuminated and shaded regions. [29]. The temperature at the weld can vary from – 200 ℃ to 200 ℃. This large temperature gradient results in significant thermal stress within the weld seam. Thermal stress can cause deformation, stress concentration, and cracks in the joints, affecting the fatigue life and strength of welded structures [30]. Moreover, welded structures may experience diurnal temperature variations in the space environment. The periodic thermal cycles undergone by each surface of the welded structure can cause thermal deformation, stress buildup, and crack propagation. These differences in thermal expansion and contraction significantly reduce the stability of welded structures [31].

2.1.1.4 Effects of other environmental factors on welded structures In the space environment, atomic oxygen and oxygen ions are prevalent. These elements can permeate the interior of the weld during welding, which increases the amount of dissolved oxygen within the material. This heightened oxygen concentration accelerates weld corrosion, impacting its integrity and durability [32]. The weld seam is exposed to intense ultraviolet radiation due to the absence of atmospheric protection. This radiation exacerbates the oxidation of the weld upon striking the welded surface, triggering increased oxidative reactions [33].

Additionally, high-energy radiation particles in the space environment can induce ionization and displacement within materials. These defects affect the atomic structure and stability of the welded structures [34]. When these particles collide with the welded joint, they generate significant mechanical and thermal energy. This energy induces alterations in the microstructure at the joint, which can lead to localized cracking [35].

2.1.2 Current status of space welding technology development and research.

To construct the International Space Station (ISS), research and exploration into space welding began as early as the 1960s by Soviet scientists. The first instance of space welding application occurred aboard the Soyuz 6 spacecraft, where Soviet cosmonauts conducted electron beam welding (EBW), plasma arc welding (PAW), and melting electrode gas-shielded welding [36]. Researchers have conducted feasibility studies on space applications for various welding methods since then, including EBW, vacuum laser welding (VLW), PAW, and brazing.

2.1.2.1 Electron beam welding This technology utilizes a focused high-speed electron beam to generate thermal energy to heat the weld zone to melting temperature, achieving the fusion joining of materials. EBW has been successfully tested multiple times in actual space environments, and the results have shown that this technology has several advantages for space environments. The process parameters of EBW can be precisely controlled and adapted to the melting and solidification characteristics of different materials. Therefore, EBW can effectively weld different types of metals, such as aluminum alloys and titanium alloys [23]. Additionally, this technology generates a high-energy electron beam that penetrates deep into the material during the welding process, which can ensure deeper welding. This method also reduces material distortion and heat-affected zone (HAZ) by precisely controlling the focal point, resulting in high-precision and high-quality welds [13]. For this reason, EBW is also considered to be the most suitable method for space welding. Current research on EBW technology focuses on welding equipment and processes.

The EBW equipment is crucial for achieving a smooth welding process and high-performance welded joints. In space welding, all equipment for space welding must be transported by rocket to the space station, which has a limited capacity and weight for new equipment. Space missions have strict limitations on the weight of the payload, and astronauts must use lightweight and compact mechanical equipment. EBW equipment is small and lightweight, making it easy for astronauts to perform soldering work in space [23]. Figure 4 shows the EBW process and the vacuum EBW machine system.

In 1969, researchers conducted an EBW experiment using batteries as a power source on the spacecraft, marking the beginning of advancements in this field [36]. The inaugural manual EBW experiments took place in 1974, conducted by Parton Welding Investigations (PWI) in collaboration with other organizations within a sizable space simulator. The experimental outcomes substantiated the viability of artificial EBW [37]. Following this, PWI executed numerous technique experiments, both terrestrial and in space, to validate the feasibility of EBW in space. Additionally, PWI successfully engineered a specialized set of space EBW tools known as UHT, as shown in Fig. 5 [23]. To propel the practical application of EBW in space, a collaborative effort between the National Aeronautics and Space Administration (NASA) and PWI has been ongoing since 1992 through the international space welding experiment project. The project conducted a comprehensive evaluation of the UHT device at PWI. This evaluation encompassed the quality assessment of ground-simulated welds for astronauts, the potential occurrence of molten pool shedding, and the interaction dynamics between the electron beam and molten pool metal in conjunction with the spacesuit. The assessment results affirm the stability of the UHT equipment and indicate a low risk to astronaut safety [38, 39].

Welding processes are also a crucial focus of research in EBW. Fragomeni et al. [26] analyzed why molten metal is prone to detachment in space environments. They have developed a theoretical model to evaluate the influence of process parameters on detachment behavior during EBW processes in NEO. This model was subsequently employed in EBW simulations and experiments to ensure the safety of experimenters. Xiao et al. [40] researched the effect of temperature on EBW machines in ultra-low temperature and vacuum environments. Through simulation calculations and experiments, they designed a control process for welding deformation under ultra-low temperature conditions and related exacerbation. This process can effectively avoid defects, such as leakage and false soldering. Das et al. [41] determined the optimal process parameters to achieve ideal welding quality. In this study, EBW joints were fabricated using different voltages, currents, and speeds. Penetration depth, weld width, and grain boundary distribution of the EBW joints were compared under different parameters. Figure 6 displays the results of three comparative experiments. The figure demonstrates that when the I/V ratio ranges from 0.90 to 2.0, the deviations in overall penetration depth, weld width, weld volume, and grain boundary distribution are minimal, regardless of the welding parameters.

Zhai et al. [42] conducted post-weld heat treatment (PWHT) on the joints to enhance their mechanical properties. They compared the microstructure and mechanical properties changes of welded joints with different weld seam spacings. In the experiment, they used EBW technology to fabricate CLAM steel joints with different weld spacing, and the joints were tested for microhardness, impact resistance, and tensile strength under both as-welded and PWHT conditions. The spacing design is shown in Table 1. Figure 7 shows the test result of the impact resistance test of weld metal (WM) and base metal (BM) with different states. The impact resistance of the WM is lower than that of the BM under as-welded conditions. After PWHT, the

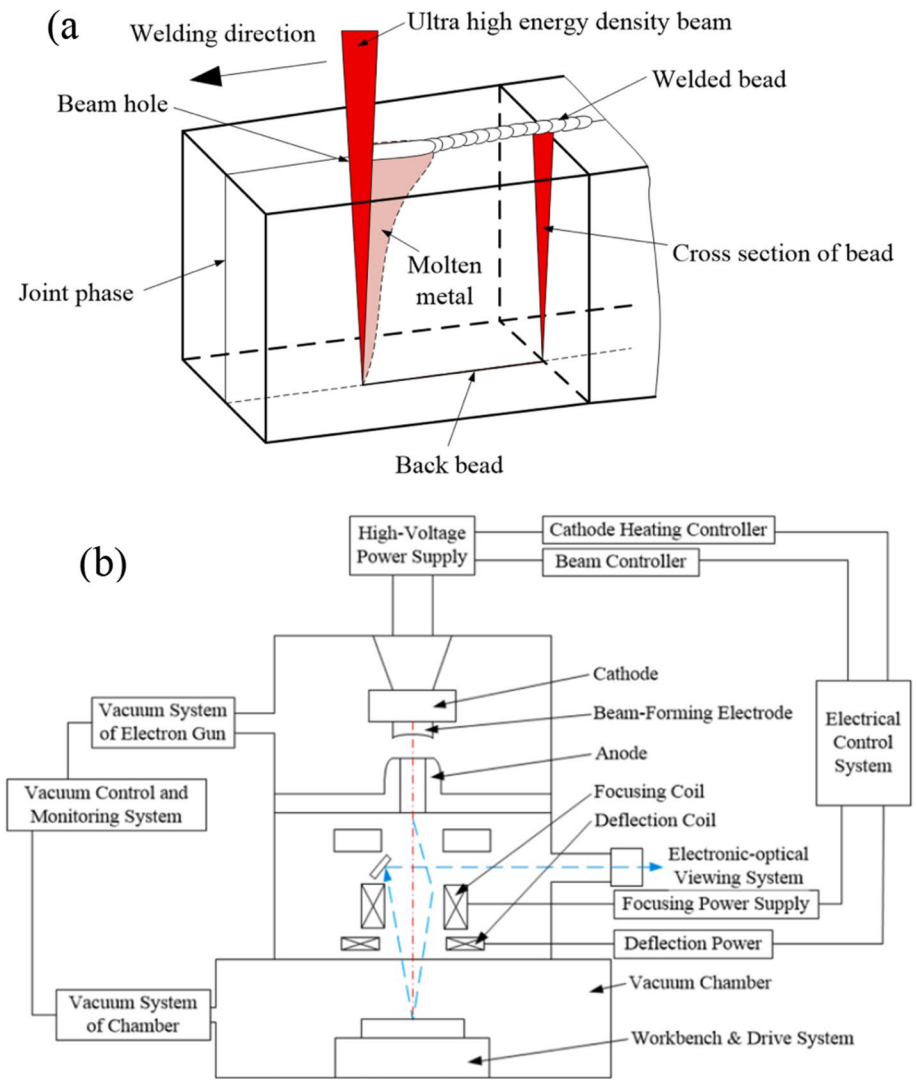

Fig. 4 The EBW process and vacuum EBW machine system. **a** The EBW process. **b** The EBW machine system [23]

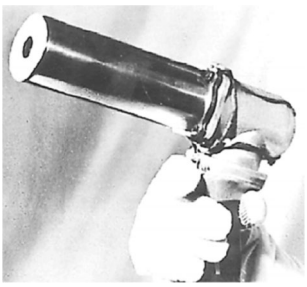

Fig. 5 Manual space EBW gun developed by PWI [23]

impact resistance of the WM is optimized, especially when the weld seam spacings are greater than 3 mm, showing stronger impact resistance than the BM. These results suggest that PWHT may improve the plasticity and toughness of welded joints.

To verify the conclusions, the microstructure of the fracture was analyzed by Zhai et al. [42] Fig. 8 shows the variation of impact fracture microstructure for welded joints with different weld spacing. In specimens 1 and 2, an apparent brittle fracture with visible grain boundaries is observed. Conversely, a ductile fracture with fuzzy grain boundaries is observed in specimens 4 and 5. This transformation may occur because the HAZ and fusion zone (FZ) of adjacent seams intersect and overlap when the spacing between weld seams is small. As a result, the microhardness of the joints increases, making them more brittle. Additionally, increasing the weld pitch refines the grain structure of the weld seam, resulting in improved joint properties, such as hardness, toughness, and ductility.

The complex operation and the high cost of equipment pose significant challenges for EBW technology. Furthermore, EBW requires large amounts of electricity to generate and accelerate the electron beam, and providing enough power in space is a challenge. Consequently, the experiments of EBW in space are relatively limited.

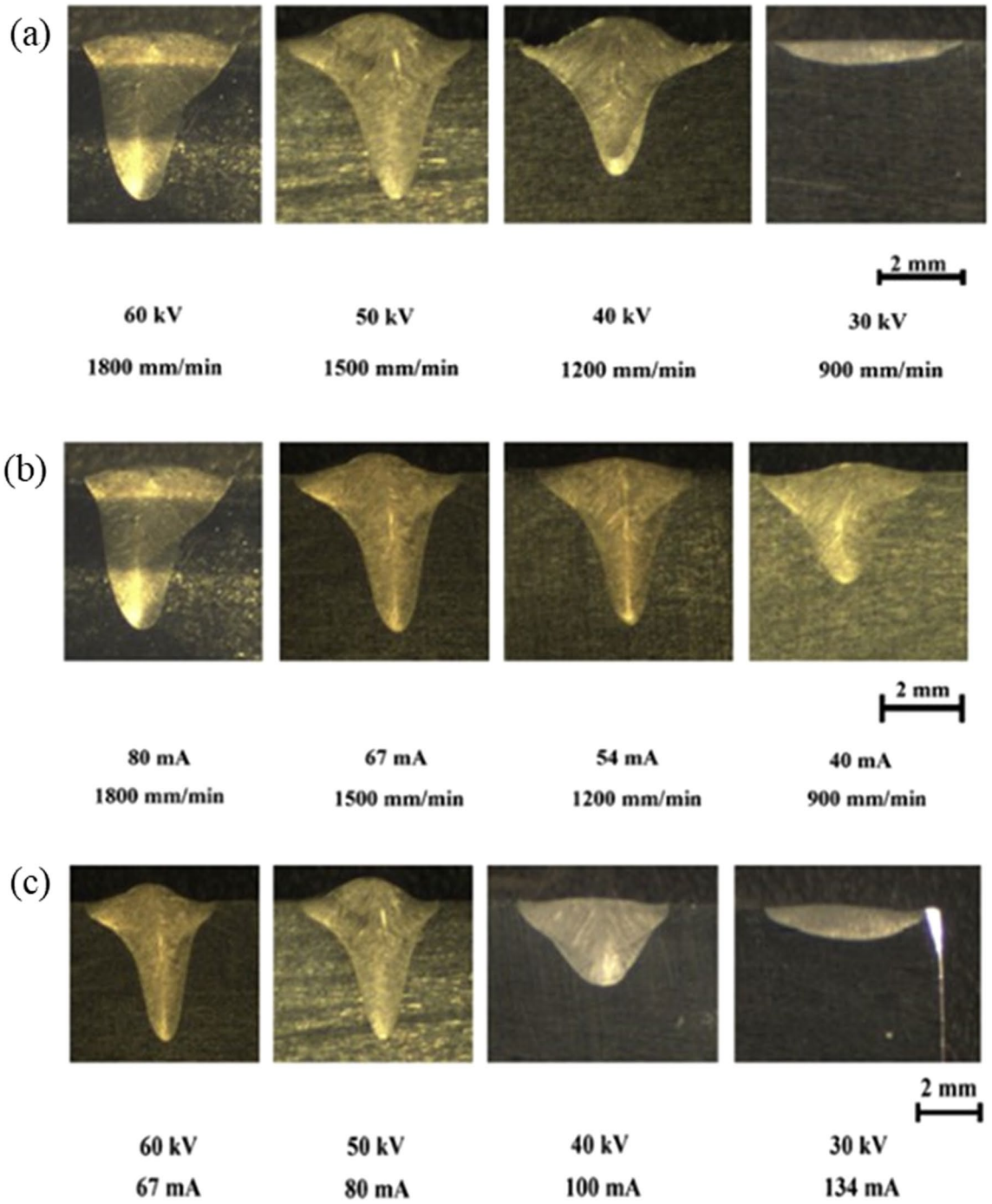

Fig. 6 The cross section of weld with different process parameters. **a** V-U. **b** I-U. **c** V-I [41]

Table 1 Weld spacings of two weld lines [42]

Specimen No.	1#	2#	3#	4#	5#
Weld spacings(mm)	2	3	4	6	8

2.1.2.2 Vacuum laser welding Laser welding technology enables the creation of high-quality welded joints, offering excellent heat resistance and corrosion resistance. These advantages ensure the stability and reliability of spacecraft in extreme environments. Vacuum laser welding (VLW) is an advanced technology that uses a laser beam in a vacuum environment. This method creates high-quality welded seams by preventing issues, such as oxidation, porosity, and other adverse effects, caused by external atmospheric influences. In the 1990s, NASA allocated funds to the space appli-

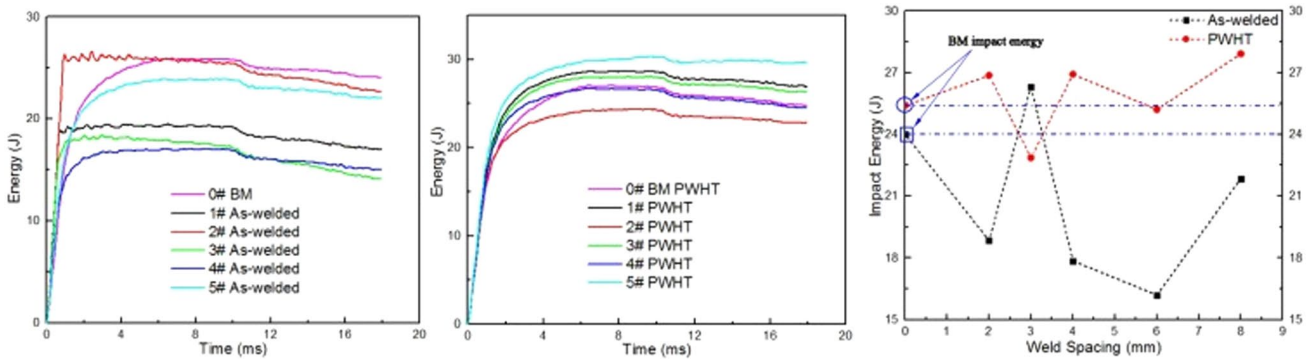

Fig. 7 The test result of the impact resistance of WM and BM with different states [42]

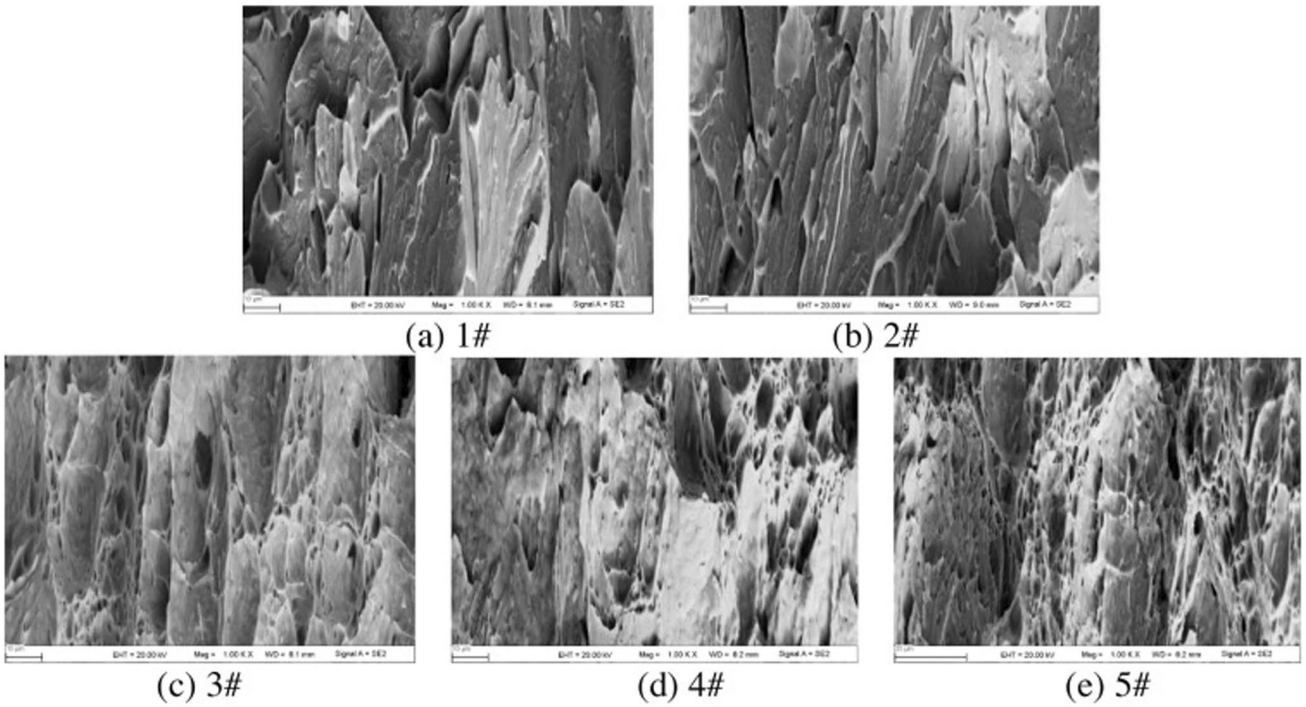

Fig. 8 Microstructure of the fracture with different weld spacing [42]

cations of industrial laser systems projects and laser welding flight experiments [43]. Gong et al. [44] conducted several laser welding experiments in the vacuum environment. Figure 9a shows the ultra-vacuum laser welding experimental system. The system consisted of a space chamber (6.33 m^3), a fiber laser, a control unit, and a particle collection system for the plasma plumes. In this study, a probe laser is used to pass the plasma plume, followed by a screen to capture the beam to test the refraction effect. Figure 9b shows the captured probe laser spot behaviors passing through the plasma plume under different pressures. It can be seen that the morphological fluctuations of the captured laser spot almost disappear and the alternation of location is very subtle. This result indicates that the attenuation effect of laser ablation by plasma is weakened in a vacuum environment, which is advantageous for laser welding.

Suita et al. [45] conducted welding experiments using a high vacuum diode laser welding system, which can simulate the vacuum environment inside the ISS. They discovered that the vacuum environment can suppress molten metal spattering. Additionally, significant changes were observed in the behavior of the laser welding plasma under vacuum conditions, with a noticeable increase in the deposition of metal vapors on the focusing lens. In a separate study, Luo et al. [46] observed a significant enhancement in surface tension-driven molten pool convection under

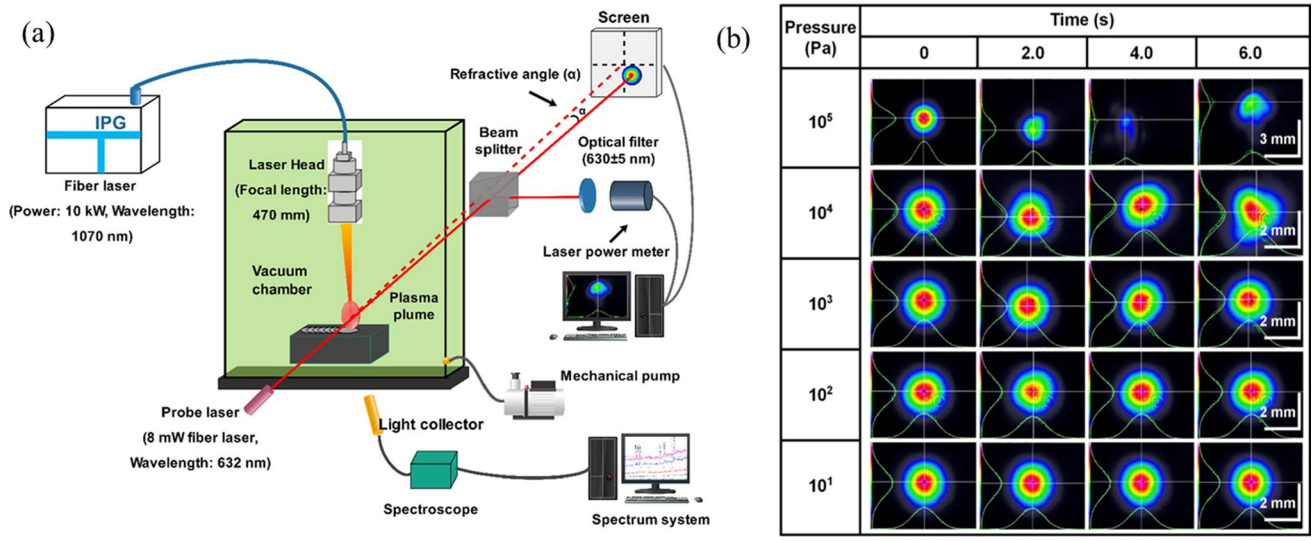

Fig. 9 Vacuum laser welding experiment. **a** The schematic diagram of the experimental system. **b** The probe laser spot behaviors passing through plasma plume under different pressures [44]

microgravity, subsequently influencing heat transfer and microstructure. As illustrated in Fig. 10, with the decrease in ambient pressure, the weld surface becomes smoother, and the weld penetration depth increases, leading to a decrease in the depth-to-width ratio of the weld. Additionally, the density and the size of plasma plumes generated during welding decrease, with a more significant reduction

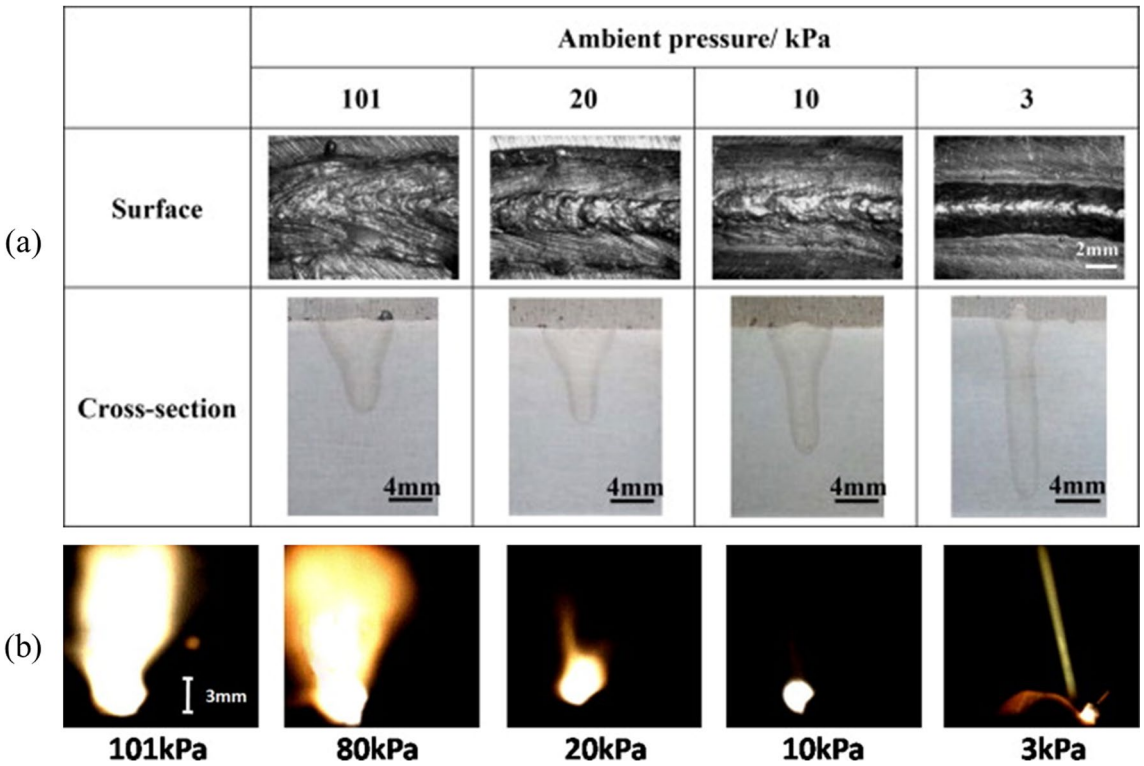

Fig. 10 The characteristics of weld and plasma plume under different ambient pressures. **a** Surface shapes and cross-section profiles. **b** High-speed photographs of plasma plumes [46]

observed at lower pressures, leading to a more pronounced suppression effect.

In contrast to EBW research, the application of VLW in space remains in the experimental stage. Further experimental validation is necessary to address the challenges in the space VLW process.

2.1.2.3 Arc welding Research on arc welding in the space environment focuses on measures to avoid or minimize the adverse effects of the vacuum environment on the welding process, where conventional arc welding methods have difficulty in initiating and maintaining a stable arc. Japanese researchers have extensively investigated gas hollow tungsten arc welding in space environments since 1992. These studies analyzed the impact of microgravity [47], vacuum conditions [48], and process parameters [49] on welding processes and joint properties. They also investigated the distribution of weld porosity and arc initiation methods. Cho et al. [50] utilized a vented hollow tungsten electrode to produce a plasma, which sustains arc combustion. The results suggested that the arc initiation and transfer may be more complex in space than on Earth. Researchers are currently investigating methods to achieve high-quality welding in this unique environment. This includes optimizing welding process parameters, improving arc-starting methods, and improving the quality and reliability of welded joints.

2.1.2.4 Other space welding methods Besides the three space welding methods discussed earlier, other techniques like brazing, heated cutting, and evaporative coating have also been acknowledged as potential methods for use in space [51, 52].

NASA has significantly advanced space brazing technology. In 2004, NASA conducted soft brazing experiments on the ISS. American astronaut Mike Fincke performed the piggyback soft brazing experiment, as depicted in Fig. 11. Figure 11b illustrates a cross-sectional view of a solder sample. The solder has a symmetrical "football" shape with numerous bubbles visible near the brazing wire. These phenomena result from the change in heat transfer mode and the absence of gravity in space. During the experiment, heat was applied to one end of the wire, resulting in a temperature gradient inside the solder. At the same time, the absence of gravity effect exacerbated the thermo-capillary convection of the liquid. Driven by the thermo-capillary convection and the temperature gradient, the bubbles inside the solder gradually moved to the joint interface between the solder and the wire [53]. This experiment established the foundation for the successful implementation of brazing in space.

The filler metal can also fill substantial brazing gaps more effectively than under Earth conditions. Brazing in space enhances capillary action and wettability of solders, reducing defects in weld seams. This welding technology minimizes assembly requirements, enabling seamless joining of diverse shapes and varying wall thicknesses without slag and fumes [54]. Despite its advantages, brazing in microgravity presents problems as the filler metal encounters difficulty transitioning to the workpiece, which can impact the overall joint shape. Additionally, the microgravity environment hinders the efficient expulsion of gasses from the joints. Severe temperature fluctuations in space can significantly impact the fatigue life of a brazed joint [55, 56]. However, these difficulties can be overcome by adjusting the brazing material and improving the process.

FSW is increasingly utilized for space welding due to its lack of requirement for additional welding materials. Jacoby et al. [57] investigated the vacuum adaptability of conventional inertial friction welding. However, the associated equipment is cumbersome, which presents challenges for practical engineering implementation. Recently, friction welding has advanced and surpassed the constraints of conventional solid-phase welding methods in space applications. This advancement has led to the development of diverse solid-phase friction welding techniques for space welding [58]. The NASA Marshall Space Flight Center (MSFC) has introduced an innovative high-speed rotary FSW technology. This technique alleviates pressure during the FSW process and enhances welding speed by utilizing tens of thousands of revolutions per minute. To address stability concerns arising from high-speed

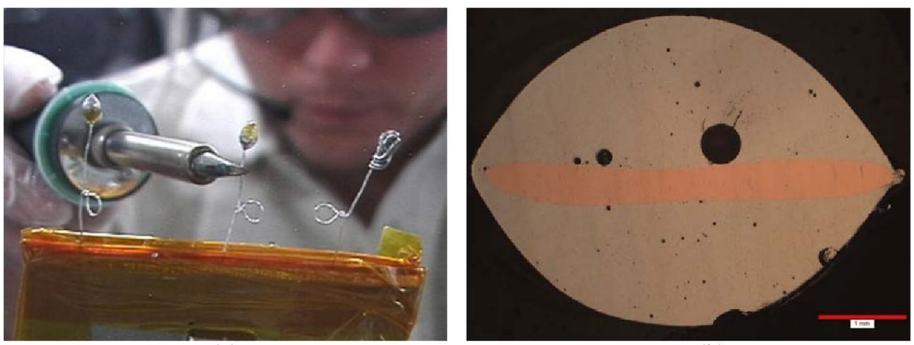

Fig. 11 Brazing experiments in ISS. **a** The soft brazing piggyback experiment. **b** An optical micrograph of solder sample [53]

rotation, MSFC has proposed solutions, such as ultrasonic friction welding and thermal friction welding [59].

Plasma arc welding (PAW) is also increasingly prominent in space applications. PAW utilizes the heat generated by a high-temperature plasma to melt and join the material [60]. During welding, an electric arc is formed between the electrode and the workpiece, followed by compression using a cooling nozzle. This results in an increase in energy density, dissociation, and temperature, resulting in a bright plasma arc. The plasma arc has higher stability, heat generation, and stability than a conventional arc, resulting in greater melt penetration and welding speeds [61]. This technology is suitable for welding different materials, such as stainless steel, aluminum alloys, and nickel alloys [62].

Several techniques offer advantages over conventional methods in space welding scenarios. Explosion welding (EXW) utilizes explosives to create high-strength welded joints. This technique is suitable for welding in microgravity environments because it is not affected by gravity. Unlike conventional thermal welding methods, EXW does not require an external heating source, which effectively addresses the issue of energy supply in space environments. These advantages make explosive welding an effective technical option for space welding. In addition, diffusion welding (DW) and cold pressure welding (CPW) are both promising techniques for creating high-integrity joints in space applications. Both methods offer advantages for space applications. DW relies on atom diffusion, while CPW operates below melting points and is compatible with specific materials.

Despite significant advancements in space welding technology, several challenges still need to be addressed. Firstly, the impact of radiation environments on welding joints is a crucial concern. While research in this area has commenced, the effects of high radiation levels on material and joint performance remain insufficiently explored. Therefore, further research is necessary to determine how to incorporate these factors into design considerations to enhance the service life of welded joints in high-radiation environments. Secondly, space missions require long-term exposure to extreme environments, which may lead to problems, such as aging, fatigue, and corrosion. Therefore, the corrosion resistance of joints in the space environment is a crucial area of research focus. Furthermore, developing new space welding processes, materials, and equipment is crucial to meet the growing demands. This may involve the development of intelligent welding technologies and highly durable materials, along with welding monitoring and control technologies in the space environment. Finally, space welding technology must address the impact of increasing space debris, for which there is currently no relevant research literature. In conclusion, these challenges provide opportunities to improve welding technology in the space environment and pose challenging questions to ensure the reliability of spacecraft and structures under extreme conditions.

2.2 Research and application progress of welding technology in the extreme temperature environment

Temperature is a crucial factor in determining the quality of the weld, particularly in extreme conditions. Weld defects can result from excessively high temperatures, while brittleness and cracking can be exacerbated by excessively low temperatures. Furthermore, extreme temperatures can alter the microstructure of the weld and impact its overall performance. Therefore, conducting thorough research in the engineering sector is crucial for developing welding techniques and materials that can withstand harsh conditions, ensuring structural integrity and reliability.

2.2.1 Effect mechanisms of environmental temperature on materials

Under high temperatures, metal materials exhibit phenomena, such as creep and relaxation. Creep refers to the slow and permanent deformation of materials under sustained mechanical stress [63]. And relaxation refers to the process of releasing stress by converting part of the elastic deformation into plastic deformation when a material is exposed to a fixed strain, even if the initial load is below its yield strength [64]. High temperatures can cause materials to soften and oxidize. During thermal cycling, welded structures may undergo periodic thermal expansion and contraction, resulting in thermal fatigue [65].

Extreme low temperatures can increase the susceptibility of metal lattice structures to dislocations and cracks, resulting in a loss of ductility and embrittlement of the metal. At low temperatures, the tensile strength of metal materials increases slightly, but they are more susceptible to brittle fracture due to impacts [66]. Low temperatures also reduce the coefficient of thermal expansion of materials, leading to significant thermal stress inside welded structures, which can cause joint deformation and cracking [67].

Therefore, the materials are challenged by thermal stresses, thermal deformation, cracking, and many other aspects under extreme temperatures. Consider specific metals or combinations at the design stage to mitigate the negative effects of extreme temperatures. The effects of temperature on welded structures in extreme environments are also extremely complex. The internal stresses and crack defects in the weld have a more significant negative effect at extreme ambient temperatures.

2.2.2 Effects of high-temperature environments on welded structures

A comprehensive exploration of these influencing mechanisms is crucial for a profound understanding of the behavior of welded structures in high-temperature environments. Research findings indicate that welded structures experience a significant decline in mechanical properties when exposed to high temperatures. Thermal expansion and high-temperature oxidation are important factors in this result. The volume of metal increases as the temperature rises, which poses a critical threat to structural integrity [68].

Guo et al. [69] explored the mechanism of temperature effect on the microstructure of WM. They found that high temperatures caused the grains in WM to grow and new phases to form gradually. Furthermore, they discovered that the tensile strength of the welded joints decreased in high-temperature environments through mechanical testing. Song et al. [63] studied the creep behavior of 2.25Cr1Mo0.25v steel at elevated temperatures. Three different creep stages in the WM were observed during their study. Under high temperatures, creep, void formation, and coalescence occurred within the microstructure of the weld, resulting in sustained softening. Figure 12 shows the results of mechanical properties tests. The stress–strain curves in Fig. 12a indicate a significant decrease in the tensile strength of both the WM and BM with increasing temperature. Meanwhile, Fig. 12b, c demonstrates that both yield strength (YS) and ultimate tensile strength (UTS) decrease at high temperatures. Specifically, at 580°C, the UTS decreases by 18.2%. This is consistent with the behavior of metal materials, which exhibit significant variations in mechanical properties at different temperatures.

Yang et al. [64] have also researched the high-temperature creep behavior of CrMoV steel. They observed a distinct three-stage creep deformation curve in the weld specimens and confirmed that the three stages of creep play a dominant role. Figure 13 shows the microstructure of creep fracture of

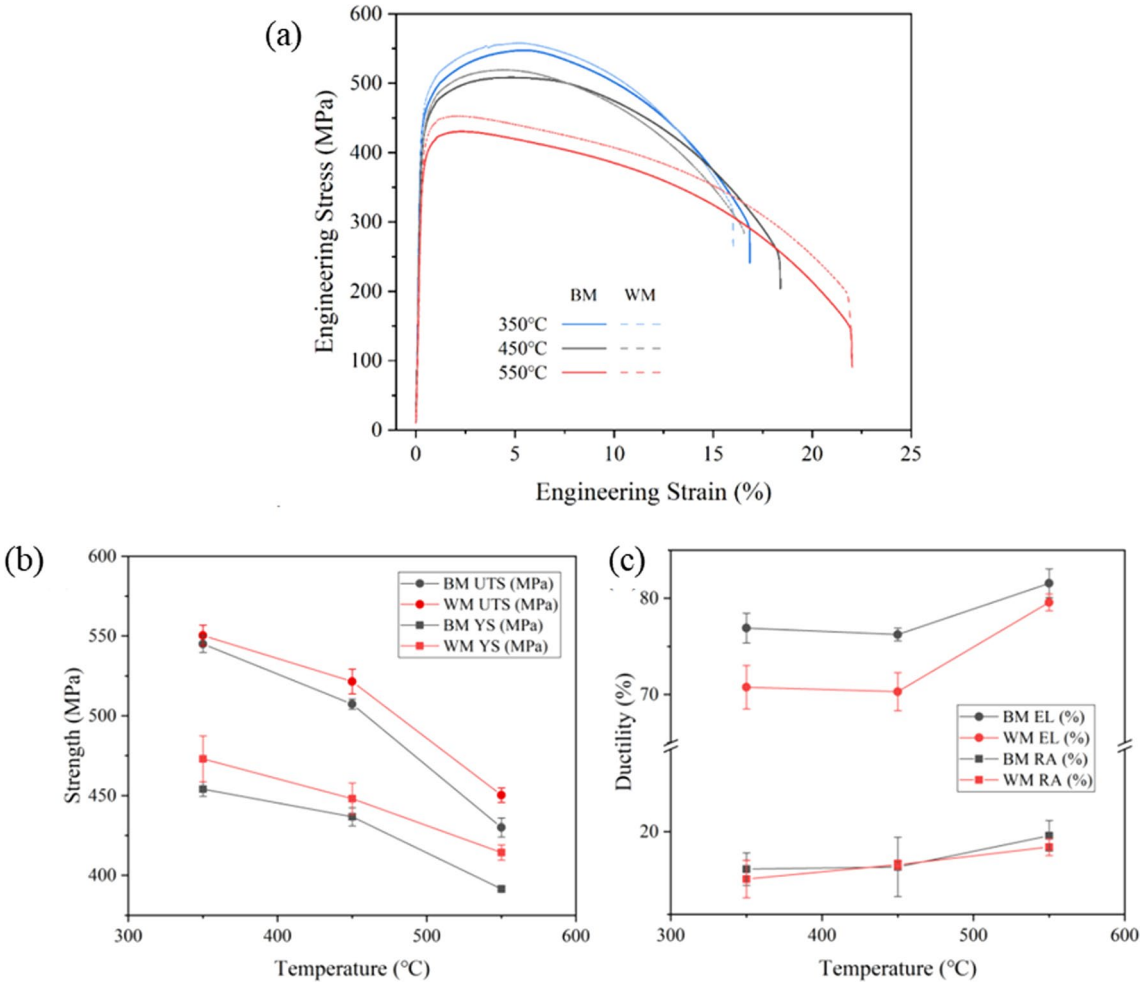

Fig. 12 Engineering stress–strain curves and tensile properties of WM and BM at different temperatures **a** Engineering stress–strain curves. **b** Variation of strengths. **c** Variation of Ductility. [63]

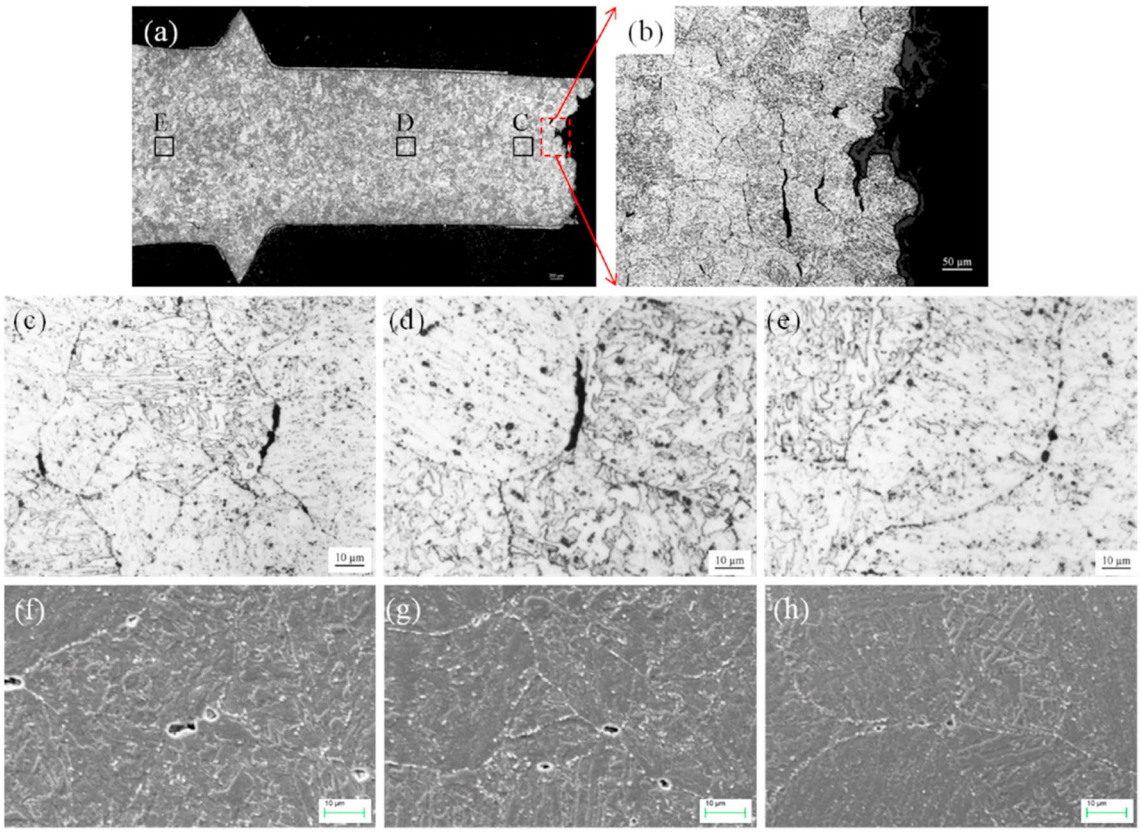

Fig. 13 Microstructure of the creep ruptured weld pass specimen. **a** The overall micrograph of creep rupture. **b** The optical microscope (OM) image of the fracture surface. **c–e** The OM images of regions C, D, and E. **f–h** The SEM images of regions C, D, and E [64]

CrMoV steel welded joints at 538°C. As shown in Fig. 13b, cracks appeared at the fracture surface. The reason for this is the sharp increase in deformation during the tertiary creep stage. In addition, creep cavities were observed in regions at different distances from the fracture surface, as shown in Fig. 13c–e. Further magnification of these regions reveals that the lowest carbide size and density is observed in region E, which is furthest from the fracture surface. These results indicate that the applied load during metal creep can promote the growth and precipitation of carbides in the microstructure.

Huang et al. [70] investigated the creep fracture behavior and microstructure changes of martensitic heat-resistant steels F92 at high temperatures. During this study, researchers utilized gas tungsten arc welding (GTAW) to fabricate welding joints of F92 and Co3W2. They observed a reduction in dislocation density and precipitate coarsening in the microstructure of F92 at high temperatures. Figure 14 shows the TEM micrographs of the HAZ at the side of F92 creep specimens at different creep times. Large amounts of dislocation lines, dislocation tangling, dislocation walls, and particles can be observed in Fig. 14a, b. Figure 14c, d demonstrates an increase in both the number and size of precipitates, along with the emergence of subgrain structures. This indicates a decrease in dislocation density and an increase in precipitate density with prolonged creep, contrasting short-term creep. Consequently, the dislocation substructure undergoes complex changes during creep processes. Pe˘si˘cka et al. [71] conducted research on the evolution of dislocation density. During this research, two types of tempered martensitic–ferritic steels underwent heat treatment, and the microstructure of the materials was observed using TEM and X-ray diffraction (XRD). The results indicated that these steels exhibited high dislocation densities in the tempered state, which decreased as the heat treatment time increased. The reason for this is that plastic deformation leads to an increase in dislocation density, which then undergoes annihilation and reorganization during prolonged creep.

Kumar et al. [72] observed significant variations in precipitate size, grain size, and substructure fraction in the WM, coarse-grained HAZ, and fine-grained HAZ of the 9Cr-1Mo steel welds at high temperatures. These variations led to changes in both the tensile strength and toughness of the WM. Sung et al. [73] reported the microstructural evolution and the creep failure mechanism of dissimilar welded joints

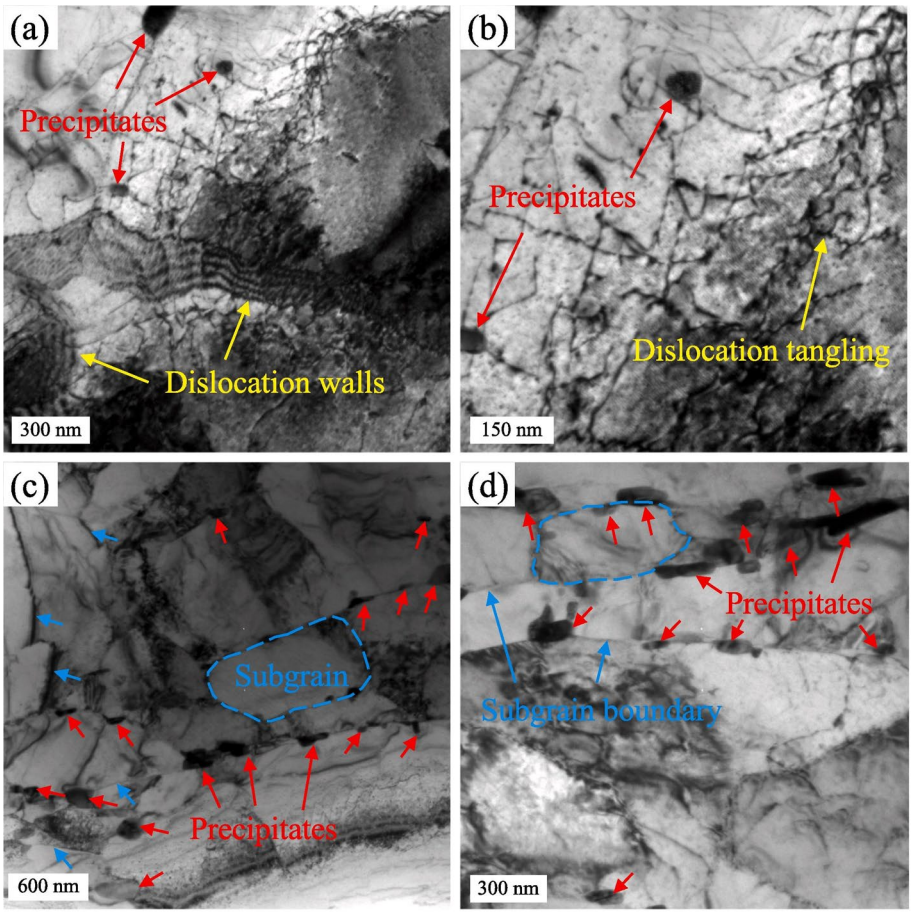

Fig. 14 TEM micrographs of the HAZ at the side of F92 creep specimens. **a**, **b** The creep specimens at 893 K, 140 MPa, and 1134 h. **c**, **d** The creep specimens at 893 K, 115 MPa, and 6051 h. [70]

of T22 and T92 heat-resistant steels. Cao et al. [74] studied the creep rupture behaviors of T92/HR3C joints. The study examined the temperature dependence of strain rate and proposed an evaluation method for the structural robustness under fire scenarios of the T92/ HR3C joints. Forni et al. [75] investigated the high-strain behavior of S355 structural steel under tension and extensive high-temperature conditions, assessing the combined effects of dynamic loading and extreme temperatures.

These research findings collectively highlight the critical importance of understanding the behavior of metal materials, particularly steel, under high-temperature conditions. Such insights aid in comprehending the mechanisms behind the degradation of mechanical properties, contributing to improved safety measures and structural design considerations in scenarios where materials are exposed to extreme heat, such as in fire incidents.

2.2.3 Effects of low-temperature environment on welded structures

At low temperatures, the temperature gradient between the HAZ of the WM and the BM increases due to the reduced ambient temperature. The low temperature accelerates the cooling process in the HAZ, forming a brittle martensitic organization. Temperature gradients and martensitic organization may lead to internal stresses and cracks in the WM and HAZ. These issues impact not only the phase transition process of the weld seam but also the mechanical properties [76].

In low-temperature environments, the yield strength and the ultimate tensile strength of structural steels are increased, and the resistance to fatigue crack propagation is improved. However, the impact toughness and fracture toughness of the structural steels will be significantly reduced [66]. Research by Stephens et al. [77] has indicated that the low-temperature fatigue performance of welded joints is significantly affected by stress concentration. Shul'ginov et al. [78] confirmed that the fatigue strength of low-alloy steel butt-welded joints increases under sinusoidal loading and low-temperature conditions and decreases under impact loading.

Liao et al. [79] conducted a study on the fatigue crack propagation behavior and fatigue properties of the Q345qD BM and WM for bridge steel at low temperatures. To improve the understanding of the effect of low temperature on fatigue crack propagation behavior, Fig. 15A–F shows the SEM fractography of BM and WM C(T) specimens at room temperature (RT), − 20 °C, and − 60 °C under the stable

propagation stage for $R = 0.1$. The fracture exhibits a quasi-dissociative pattern at RT, characterized by a short river pattern, small disintegration surfaces, and tearing edges. At − 20 °C and − 60 °C, the section displays deconstructed fractures with distinct river patterns and deconstructed steps. These findings indicate a shift in the fracture mode of crack extension under extremely low-temperature conditions, transitioning from quasi-decomposition to deconvoluted fracture.

Furthermore, Liao's research revealed that as the temperature decreases, the crack expansion rate of the BM decreases, whereas the expansion rate of the weld crack increases. Figure 16 illustrates the fatigue crack expansion rates of the BM and WM at low temperatures for different stress ratios. A comparison indicates that the expansion rate of the WM is more sensitive to stress ratio than that of the BM. It rapidly increases as the stress ratio is heightened at the same temperature. Jeong et al. [80] have demonstrated that butt-welded joints of Fe15Mn steel exhibit greater fatigue resistance at − 163 °C compared to RT. Despite these insightful findings, additional investigations are required to validate the fatigue life of welded joints at low temperatures.

2.2.4 Current application status of welding technology for extreme temperature environment

Researchers have devoted efforts to exploring and implementing new welding processes and materials to ensure the quality and life span of welded structures in extreme service environments. Temperature has a minor impact on the application of welding technology, primarily altering the internal structure of the weld due to temperature fluctuations. This characteristic enables the use of low or ultra-low hydrogen welding consumables, effectively mitigating hydrogen-induced cracks at low temperatures.

Additionally, the implementation of preheating, PWHT, and heat preservation for both the BM and the WM have been proven to be effective in ensuring the quality of welded joints [81]. Fu [82] and Jiang et al. [83] investigated the influences of different PWHT processes on the microstructure and mechanical performance of 2.25Cr1Mo0.25V steel. Results from their work showed that the time of tempering plays a vital role in regulating the microstructure and tensile strength of the material. After completing welding on the steel plate, it is essential to conduct heat treatment on both sides of the weld within a range of 2 to 3 times the thickness of the plate. The heating temperature should be maintained at 150 ℃ to 300 ℃ for 1 to 2 h. After PWHT, silica insulation cotton is utilized to shield the weld seam to facilitate a gradual cooling process. These procedures contribute significantly to the dissipation of diffuse hydrogen and prevent cold cracking caused by excessively rapid cooling [84].

Adding auxiliary elements is also an effective way to enhance the performance of welded joints. Sklenička et al. [85] found that Cr and Mo are the main alloying elements that lead to solid solution strengthening. Specifically, Cr is

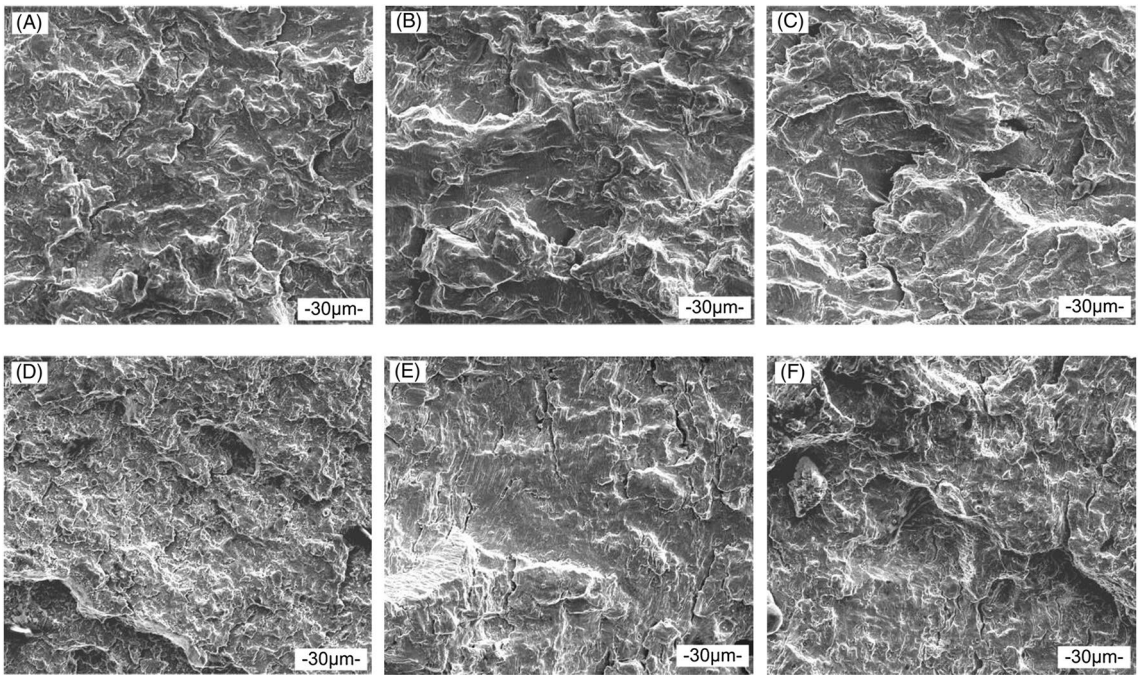

Fig. 15 Microstructure of the fracture surface. **A** The BM specimens at RT. **B** The BM specimens at − 20 °C. **C** The BM specimens at − 60 °C. **D** The WM specimens at RT. **E** The WM specimens at − 20 °C. **F** The WM specimens at − 60 °C. [79]

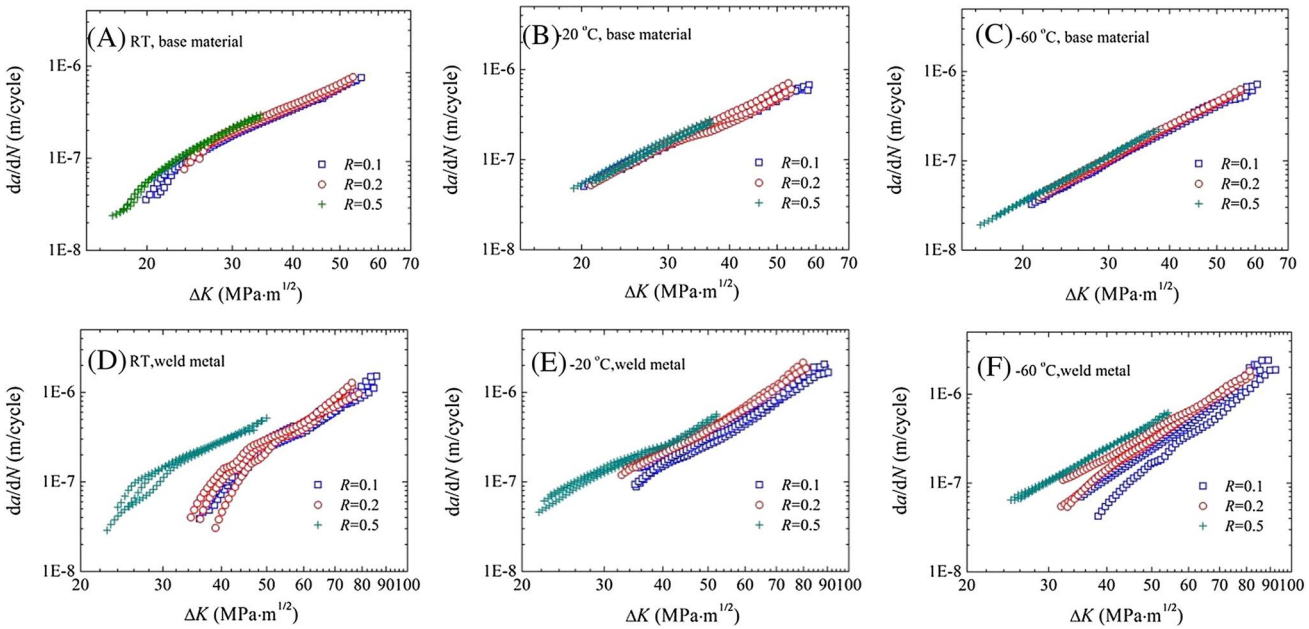

Fig. 16 Fatigue crack propagation rates for the BM and WM **A** The BM specimens at RT. **B** The BM specimens at − 20 °C. **C** The BM specimens are at − 60 °C. **D** The WM specimens at RT. **E** The WM specimens at − 20 °C. **F** The WM specimens at − 60 °C [79]

added to provide oxidation and corrosion resistance, while Mo enhances the strength of the high-temperature solid solution. Bae et al. [86] found that the addition of chemical elements such as W enhances the stability and overall performance of high-temperature alloys.

In summary, researchers have made some progress in mitigating the adverse effects on various welded joint mechanical properties under extreme temperature environments by adjusting welding processes or material compositions. However, future operating conditions may involve even higher temperature ranges, posing greater demands on welding technology. At extreme temperatures, the performance of welding materials is affected. Therefore, it is an important research direction to study the stability of materials under high-temperature conditions and to develop durable welding materials and processes suitable for high-temperature environments. In addition, since manual welding is not suitable for extreme environments, developing real-time welding monitoring and control technologies applicable to extreme temperature environments is critical. This may involve research on sensor technology, intelligent welding systems, and adaptive control of abnormal conditions.

2.3 Research and application progress of welding technology in the radiation environment

Welding technology is a crucial manufacturing and safety technology for constructing, operating, and maintaining nuclear power equipment. The defects caused by welded joints have significantly affected the operational safety and efficiency of nuclear power plants, particularly for in-service plants. These effects have posed challenges and demands on the welding techniques that are used to build and maintain nuclear power plants.

2.3.1 Effects of the nuclear radiation environment on welded structures

The effects of the radiation environment on welded structures are multifaceted. Radiation damage stands out as the most immediate consequence. High-energy radiation, including neutrons and gamma rays, can cause radiation damage in materials. This results in the formation of lattice defects and an increase in dislocations, leading to alterations in the physical and chemical properties of welded structures. Consequently, aspects, such as structural hardness, strength, and plasticity, may undergo modification [87]. Deformation microstructures of AISI 316LN austenitic stainless steel irradiated at 200 °C with 160 keV H, 360 keV He, and 3.5 MeV Fe ions produce glide dislocations and increase in separation with increasing irradiation dose and increasing strain. As illustrated in Fig. 17, vacancies and some defect-free prismatic loops were observed in the sample after irradiation with 3.5 MeV Fe ions [88].

Electromagnetic and ionizing radiation can disrupt the stability and transmission efficiency of the arc during the welding process, ultimately impacting the formation and quality of the weld seam [89]. High-energy radiation may induce localized melting or overheating in the welding area, resulting in various welding defects, such as burn-through,

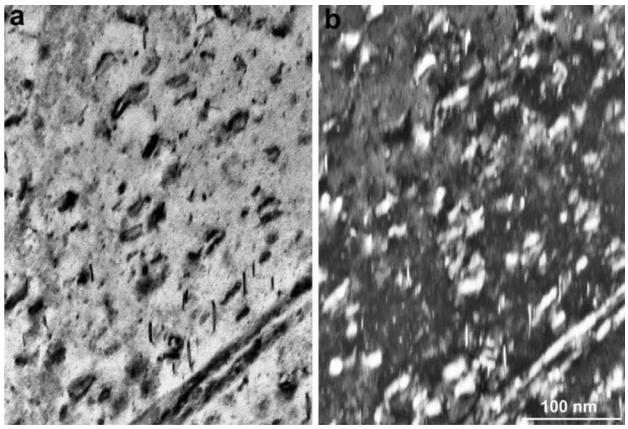

Fig. 17 Bright and dark field micrographs of the loop microstructure in 316LN austenitic stainless steel irradiated to 10 dpa at 200℃ with 3.5 MeV Fe ions [88]

cracks, and deformation [90]. Contaminants in the radiation environment, such as chemicals, gasses, and particulate matter, can lead to corrosion, porosity, and inclusions in the welding area. This can ultimately diminish the strength and corrosion resistance of welded joints [91]. Numerous research results have shown that few materials are immune to radiation damage. Therefore, when selecting welding materials, it is essential to consider factors, such as material radiation stability, resistance to radiation damage, and radiation-induced chemical changes.

2.3.2 Current status of nuclear power plant welding technology development

Welding within a radiation environment faces severe challenges due to the influence of radiation on welding materials and processes. Currently, welding and maintenance of nuclear power plant equipment primarily rely on arc welding. This encompasses mechanized and automated welding techniques, notably tungsten inert gas (TIG) welding [92, 93] and metal inert gas (MIG) welding [94]. Concurrent with the ongoing advancement in industrial laser technology, there is a growing emphasis on laser welding (LW) research within the nuclear power sector.

2.3.2.1 Tungsten inert gas welding application in nuclear power TIG welding technology is widely used in the nuclear power sector, particularly for welding stainless steel and high-alloy materials. High-quality welded structures are necessary for key components in nuclear power plants, including pressure vessels, piping systems, and reactor elements. TIG welding stands out as a preferred method in the nuclear power sector due to its attributes of high precision, low gas impurities, and excellent weld seam quality [95].

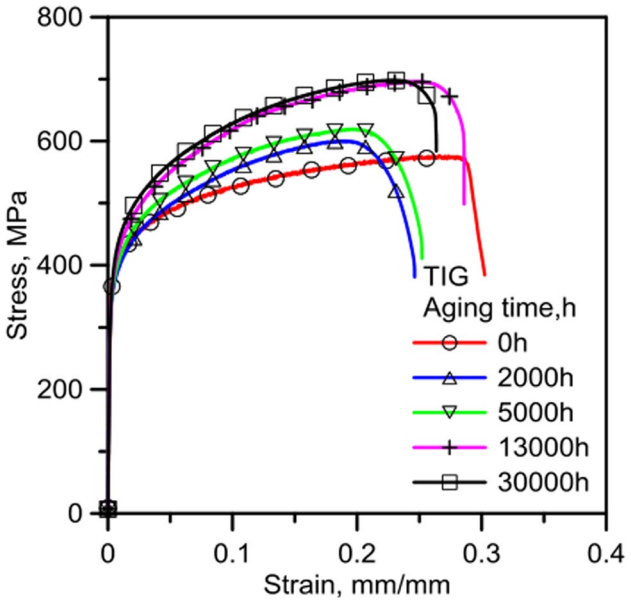

Fig. 18 Stress–strain curves from tensile tests for different aging conditions. [99]

A notable characteristic of TIG welding is using inert gas as the protective medium for the arc, ensuring that the welding area remains uncontaminated by impurities, such as oxygen and water vapor, in the environment [96]. The stable arc and the precise control offered by TIG welding enable it to meet the requirements for welding strength, sealing, and corrosion resistance of components in nuclear power plants. Advancements in technology offer potential for broader application of new techniques and processes in the field of nuclear power [97].

The conventional TIG welding technology is plagued by high energy input, diminished efficiency, and pronounced distortion. To address these issues, Yu et al. [98, 99] proposed narrow gap arc welding technology, which enables efficient welding with minimal heat input. Subsequently, this technique was applied to weld the reactor vessels in nuclear power plants. They also investigated the tensile and fatigue characteristics of welded structures during the later stages of prolonged operation. Figure 18 depicts the engineering stress–strain curves for both new material samples and aged samples. The figure illustrates a sharp rise in yield strength and ultimate tensile strength in the new material, concurrently accompanied by a reduced elongation. However, no significant differences in elongation were observed among the aged specimens. Despite the tensile strength continued to increase after 13,000 h, the deceleration of the growth trend indicates the onset of saturation. These studies indicate that welded joints operating in prolonged periods within high-radioactive and high-temperature environments may experience localized failure.

The radiation environment constrains the application of manual welding methods. As a result, the integration of TIG welding technology with automation and robotic systems is increasing steadily. This automation technology has become critical in welding and maintenance within nuclear power plants, effectively preventing radiation damage to humans. Furthermore, in-depth research and application of TIG welding technology have been conducted in the manufacturing of specific specialized components in nuclear power plants.

2.3.2.2 Laser beam welding application in nuclear power Due to its high energy density, laser beam welding (LBW) focuses the laser beam in the weld zone, resulting in less heat input than other welding methods. This results in a smaller HAZ, alleviating deformation and residual stress in the welding materials [100]. This characteristic has led to the widespread application of LBW in areas such as structural steel plates within nuclear power plants.

Many scholars have conducted in-depth research on laser welding technology. Wu et al. [101, 102] utilized a fiber laser to weld CLF-1 structural steel plates of a nuclear reactor. The plates measured 17.5 mm and 35 mm in thickness. The welding process with the fiber laser resulted in well-shaped seams for both thicknesses without any cracks, pores, or noticeable defects. Figures 19 and 20 depict the microstructure of LBW and EBW welds under the OM. The WM of both welded joints was mainly composed of lath martensite, which is wider in EBW than LBW joints. In the HAZ/FZ transitional zone around the fusion line (FL), a narrow coarse-grain heat-affected zone (CG-HAZ) composed of narrow and fine lath martensite and a few carbides was formed. In addition, a fine-grain heat-affected zone (FG-HAZ) composed of a mixture of tempered sorbites and cs was formed near the FL. This analysis revealed that for 13 mm thick steel plates, both LBW and EBW produced sound welds without gaps, cracks, or other defects. In general, the microstructure in EBW joint zones was coarser than that in the LBW joint.

Subsequently, a comparison was conducted on the mechanical properties of CLF-1 steel welds achieved through LBW and EBW. As depicted in Fig. 21, both welding methods exhibited commendable ultimate strength and average impact absorption energy. The WM demonstrated superior ultimate strength compared to the BM and closely approached the average impact absorption energy of the BM [102].

The radiation resistance of welded joints is closely related to the composition of the material. Zirconium (Zr) alloys are frequently used in pressure pipes and fuel cladding shells due to their exceptional mechanical strength and oxidation resistance, which has led to extensive research on their welding processes [103]. The weld characteristics are primarily determined by the residual stresses on the surface and the formation of metallographic phases in the weld FZ and HAZ [104]. LBW yields superior microstructures in these zones compared to conventional arc welding methods, such as TIG welding and resistance welding (RW) [105]. Consequently, LW emerges as a more suitable method for welding Zr alloys.

Bharadwaj et al. [106] investigated the impact of pulsed laser heat input on the mechanical strength and microstructure of Zr-2.5 wt.% Nb alloy weld seams. The study results

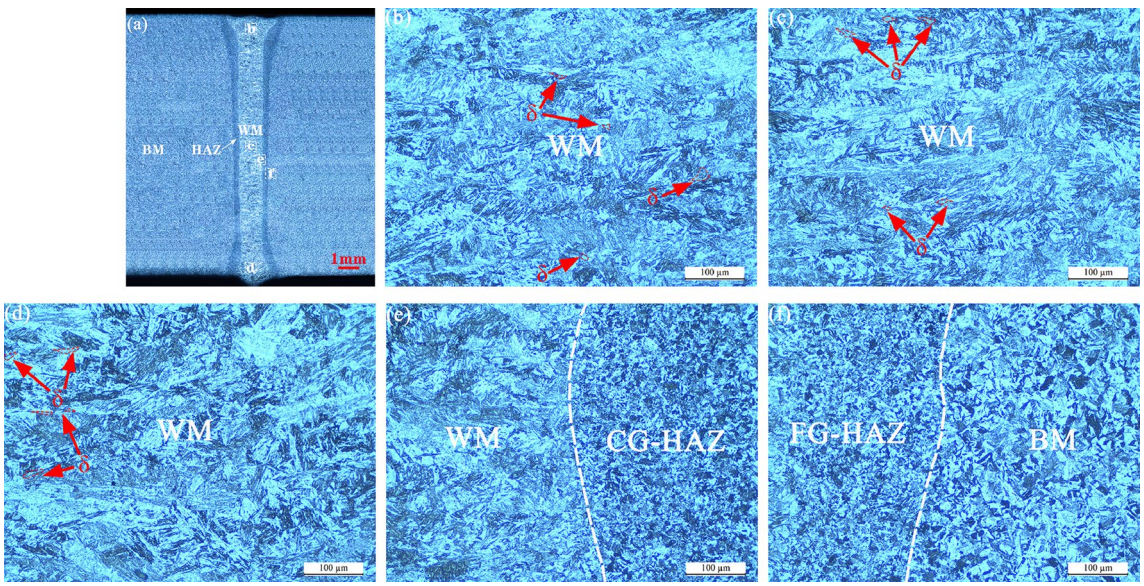

Fig. 19 Microstructure of LBW joint. **a** Weld cross-sections. **b** Upper part of the weld. **c** Middle part of the weld. **d** Bottom part of the weld. **e** FZ and CG-HAZ. **f** BM and FG-HAZ. [102]

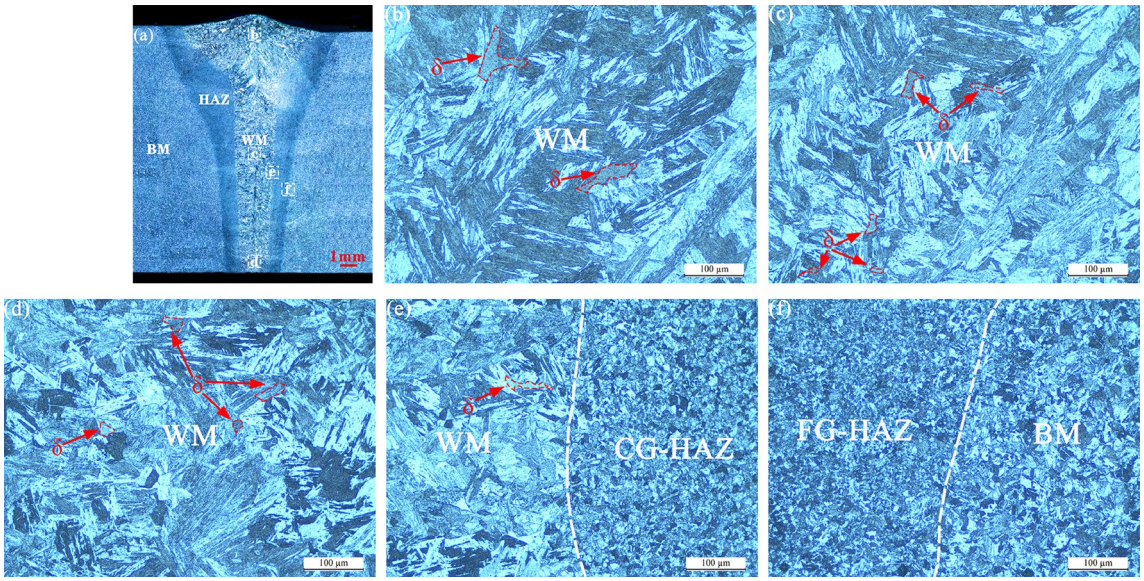

Fig. 20 Microstructure of EBW joint. **a** Weld cross-sections. **b** Upper part of the weld. **c** Middle part of the weld. **d** Bottom part of the weld. **e** FZ and CG-HAZ; **f** BM and FG-HAZ. [102]

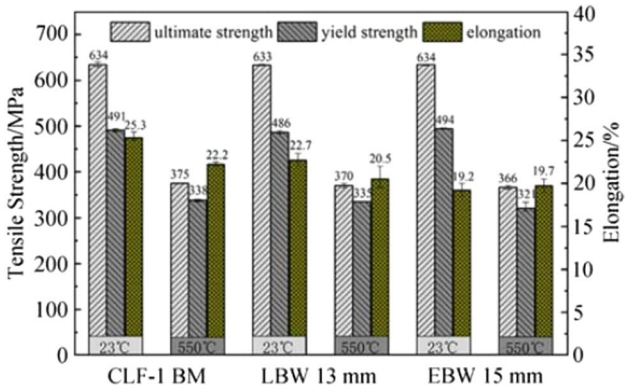

Fig. 21 Tensile strength and elongation results for LBW and EBW joints. [102]

indicate that heat input significantly influences the depth of the weld and the width of the HAZ. Figure 22 displays macrographs of cross-sectional weld beads developed at various heat inputs. At a heat input of 800 J/mm, a weld with favorable macroscopic morphology and microstructure can be achieved. However, the weld's ductility is compromised compared to the BM due to elevated microhardness and residual tensile stresses in the weld fusion and HAZ. This may be attributed to substantial changes in the α-phase and the residual β-phase in the melting zone and HAZ.

2.3.2.3 Other welding methods application in nuclear power These methods may offer unique advantages in joint strength, efficiency, or the ability to join dissimilar materials. A typical example involves using Inconel 625 as the BM for nuclear power plant protection, with GTAW employed for the welding process [107]. Inconel 625, known for its corrosion resistance and high-temperature strength, is a suitable choice for such critical applications.

Moreover, the integration of computer technology and virtual reality into welding processes is a noteworthy trend. Luo and others explored the application of virtual reality technology to nuclear power welding [108]. They used Unity3D and UG software to construct a virtual reality system for riser automation equipment welding. As shown in Fig. 23, this system includes virtual representations of welding carts, welding rails, welding power supply, virtual cameras, and other equipment. User interface graphical user interface systems were employed to create human–machine interface scenarios, facilitating human–machine collaboration. Through this technology, operators can visualize and interact with a virtual welding environment in real time. This has implications for training, simulation, and even remote operation.

The use of virtual reality in radiation environments offers several advantages, enabling real-time monitoring and control of the welding process. In the maintenance of nuclear power plants, certain areas are restricted from manual welding due to radiation. The use of automation and virtual reality improves the precision of welding operations and guarantees the safety of the operators. This trend aligns with broader developments in automation technology, making it a potentially effective means for not only nuclear power plant maintenance but also for applications in space structure construction, marine engineering, and other fields where extreme conditions may pose challenges for human workers.

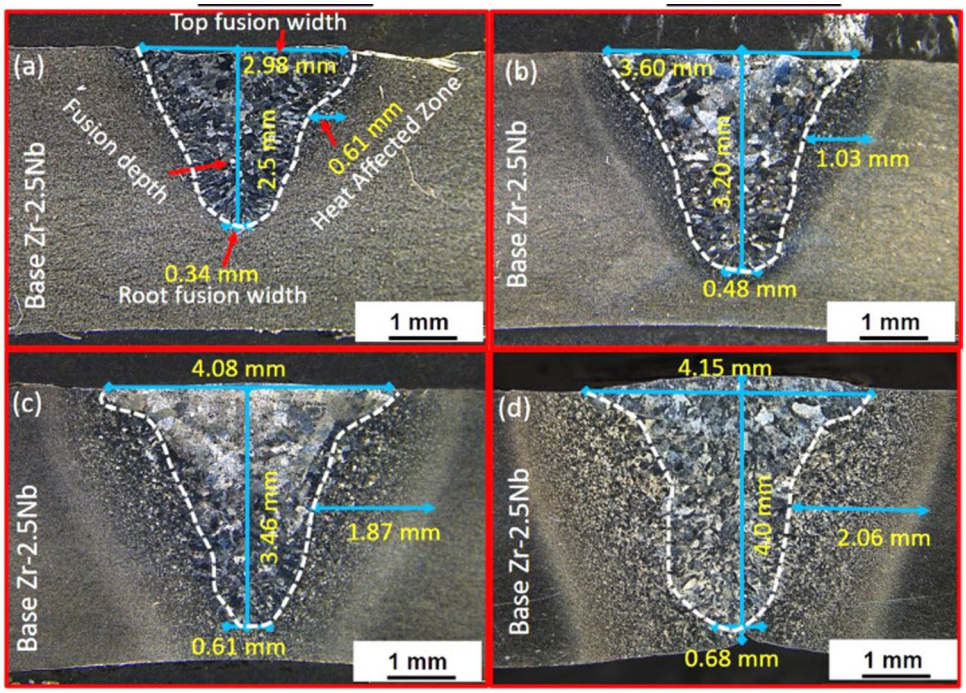

Fig. 22 Macrographs of the cross section of weld beads developed at different heat inputs. **a** 312 J/mm. **b** 520 J/mm. **c** 650 J/mm. **d** 800 J/mm [106]

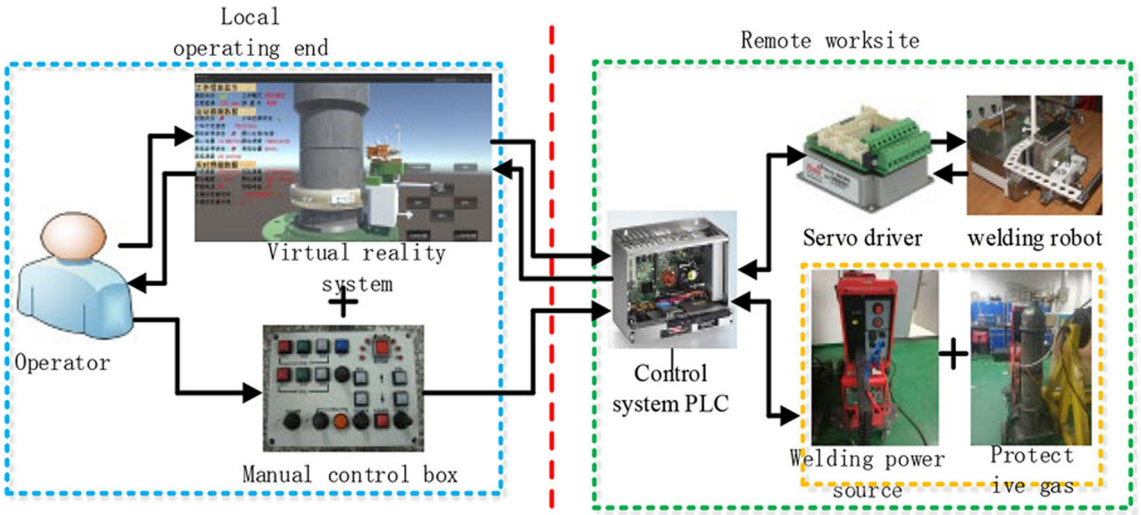

Fig. 23 Test system structure diagram [108]

While welding in radiation environments has been extensively researched, there is a lack of studies on the effects of various types of radiation on welding materials. These effects include deformation, damage, and gas injection, and may impact the performance of welded joints. Therefore, further research is needed to fully understand the impact of radiation on welding materials. Due to the specificity of the radiation environment, it is a new research direction to study the combination of welding materials with radiation protection materials to improve the radiation resistance of welded joints. Addressing these research gaps can improve the feasibility and reliability of welding in radiation environments.

2.4 Research and application progress of welding technology in the deep sea environment

Underwater welding is considered an extreme manufacturing technique in the marine industry. This technology is used for ship repair, energy pipeline laying, and infrastructure maintenance, which involves joining materials in a deep sea environment. Complex marine environments can

have a significant negative impact on welded structures and materials.

2.4.1 Effects of the deep sea environment on welded structures

The deep sea environment is characterized by dynamic loads, low temperatures, high pressure, and intense corrosion [109]. Metal materials used in marine engineering typically possess considerable size and thickness. The truss structures are commonly employed in construction, leading to intricate welded joints and notable stress concentration. These factors significantly impact the comprehensive performance of materials and welded structures, and the main influencing factors and mechanisms are as follows:

2.4.1.1 High-water pressure Water pressure in the deep sea increases sharply with depth. The high-water pressure environment not only limits the application of welding methods but also impedes the release of gasses from the molten metal. These gasses lead to cracks and pores, reducing the sealing and strength of the weld [109, 110].

2.4.1.2 Dynamic loads Dynamic loads are prevalent in the deep sea, such as ocean waves and currents. The cyclic action of these loads can result in fatigue cracking and structural damage in welded joints over repeated loading cycles [111]. At the same time, the welding process may be disturbed by water flow, which affects the welding quality and stability.

2.4.1.3 Corrosive environment The high salinity of seawater, coupled with other chemical substances, poses a significant risk for the corrosion of welded joints. Welded joints are typically vulnerable points to corrosion in materials [109]. Welded structures exposed to marine environments for extended periods may experience corrosive damage, heightening the risk of corrosion fatigue and reducing the overall structural lifespan [112].

2.4.1.4 Bubbling effect Underwater welding causes water to decompose into hydrogen, which dissolves within the weld seam. The gas is less quickly expelled as the molten metal solidifies, making the joints susceptible to cracking and complicating the weld quality assurance [110].

2.4.1.5 Temperature fluctuations Water exerts a pronounced cooling influence on both the WM and the BM within the HAZ. The rapid cooling at the weld induces the formation of thermal stresses, resulting in cracks due to the embrittlement of the weld tissue.

2.4.1.6 Limited visibility Water exhibits strong light reflection and absorption, leading to noticeable light attenuation. Simultaneously, a significant number of bubbles are generated during the underwater welding process. These bubbles form around the welding area and cannot dissipate quickly, reducing visibility in the underwater environment. This visibility reduces the precision of the worker's operation, with deviations and leakage of soldering.

These complex factors place high demands on the development of underwater welding technology. Currently, commonly used techniques for underwater welding include conventional arc welding, explosion welding, friction welding, and various other methods. These methods are classified into three categories based on the welding environment, including wet welding, local dry welding, and dry welding.

2.4.2 Wet welding technology

The wet welding is performed directly in water without any waterproof measures. This technology is commonly employed in marine engineering, underwater pipeline repairs, and other welding operations beneath the water surface. Figure 24a illustrates the scenario of a welder engaging

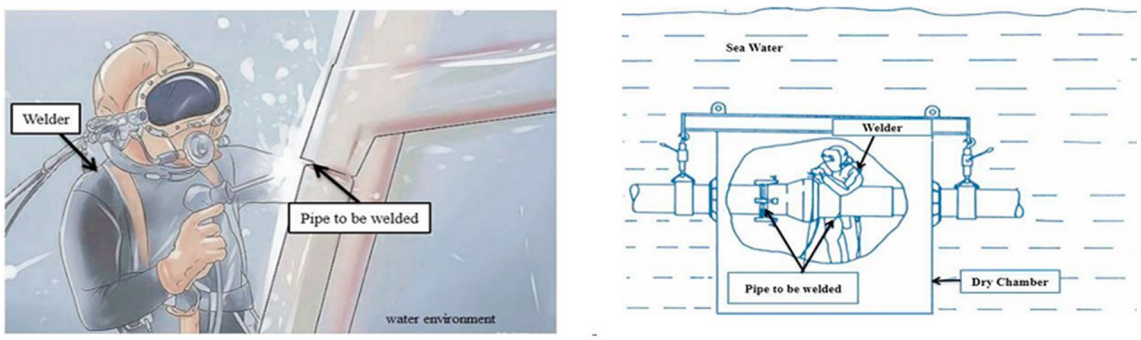

Fig. 24 The different welding techniques in the underwater environment. **a** Wet welding. **b** Dry welding. [113]

in underwater wet welding. Welders need to wear special equipment, and welds are formed directly in the water. In comparison to welding on land, the microscopic structure of wet welding joints is also more prone to the occurrence of welding defects [113].

Wet welding can produce severe defects and problems, such as porosity and cracks. Porosity is caused by the dissolution of gasses, such as H_2 and O_2, in the molten pool metal at high temperatures. The internal metallurgical reactions produce gasses, such as CO and H_2S, which are insoluble in the metal. These gasses gradually escape during the solidification process of the molten metal. However, the cooling effect of water causes the molten bath to cool rapidly, preventing the gasses from escaping in time. After solidification, these gasses may form pores or other defects in the metal, which can result in reduced density, plasticity, and strength of the weld joint [114].

Electrode welding and flux-cored wire arc are the most commonly used welding methods for wet welding. In the 1970s, underwater flux-cored wire welding technology was developed by the PWI to replace the wet welding technique of underwater electrode welding. Due to the higher welding efficiency and more substantial scope of application, this method has become the most promising underwater wet welding method [115]. Liu et al. [116] used flux-cored welding wire as the welding material for TIG welding. This method ensures a uniform distribution of the arc temperature field, resulting in a more stable welding process than conventional unfilled TIG welding. Chen et al. [117] incorporated multiple alloying elements, such as Nb and Ti, into conventional flux-cored wires and used these wires to weld Q235 steel. The impact of different alloyed flux-cored wires on the microstructure of Q235 steel joints was investigated. The research findings revealed that a significant amount of brittle martensitic structure formed after adding alloying elements. As the content of the Cr element decreases, plate-like and lath-like martensite become the primary constituents of the microstructure. Liu et al. [118] developed a self-shielded flux-cored wire containing Cr elements and investigated the influence of Cr elements on the WM. Numerous experiments were conducted using this self-shielded flux-cored wire. The results indicate that the wire demonstrated high slag coverage and excellent removal performance.

In addition to optimizing and enhancing the welding wire, the wet welding process is also a key area of research. Hu et al. [119] successfully executed an underwater wet multilayer welding process, employing different joint configurations. The results indicate that the welded joints exhibit no slag or other defects. However, these joints do display cladding, porosity, and unfused elements. Despite these blemishes, all mechanical properties meet the required standards. Cai et al. [120] used wet laser welding technology to fabricate TC4 titanium alloy joints and studied the influence of different process parameters on the microstructure and mechanical properties of the joints. The results indicate that underwater laser welding can form an effective joining when the water depth is less than 7m. The microstructure of the weld consists mainly of brittle lath martensite. Compared with conventional laser welding, underwater wet laser welding produces narrower welds with finer grains.

Although wet welding technology is highly mature and can meet the joining requirements of various materials, the adaptability to specific materials and alloys still needs to be investigated. Wet welding increases the risk of corrosion because direct exposure to the underwater environment exposes the weld and the surrounding metal structure. Therefore, it is necessary to develop underwater wet welding materials to reduce the adverse effects of hydrogen and oxygen on welding joints and enhance the corrosion resistance of welds. These welding materials will extend the service life of the equipment and encourage the use of underwater welding in diverse fields.

2.4.3 Local dry welding technology

Local dry welding represents an advanced underwater welding method, combining the benefits of both wet welding and dry welding, leading to a high-quality welded joint [121]. The commonly employed techniques in local dry welding include underwater TIG welding, MIG/MAG welding, and LW.

TIG welding is a highly versatile technique that is gradually being applied in the deep sea environment. Hamasaki et al. [122] demonstrated successful welded seams at a depth of 200 m underwater using a drainage device with a modified dual-nozzle structure. The device effectively released argon gas, which contributed to the stability of the welding process. Lyons et al. [123] utilized an orbital tungsten inert gas high-pressure oxygen welding system to repair submarine pipelines and similar tasks. This approach demonstrates the versatility and adaptability of TIG welding techniques in challenging underwater conditions. Zhai et al. [124] introduced the concept of flux-cored local dry underwater tungsten electrode welding and systematically investigated the metal transfer mode in this process. The study analyzed metal transfer mode, weld morphology, and microstructure, confirming interactions between electrode gap, metal transfer mode, and microstructure. Researchers are exploring the use of high-frequency oscillation generators to initiate the arc. Process parameters are optimized by selecting the appropriate tungsten wire tip cone angle. These efforts aim to expand the application of local dry underwater TIG welding, making it more versatile and efficient for various underwater welding scenarios.

In addition, MIG/MAG technology is also a significant research area in local dry welding. MIG/MAG welding

for underwater applications dates back to the 1960s, and substantial experience been has accumulated in practical applications. Gülenç et al. [125] contributed to the understanding of this welding method by emphasizing the importance of shielding gas. Their work involved using argon doped with varying levels of hydrogen as shielding gas, revealing its influence on welding outcomes.

In 2001, Hitachi Ltd. [126] made significant strides in underwater welding technology by pioneering localized dry underwater laser welding. This innovation involved expanding the study of water curtain localized dry underwater welding, with the noteworthy step of replacing the original arc welding method with a laser torch. This transition marked a milestone in the evolution of underwater welding techniques, showcasing the adaptability of laser technology in challenging underwater environments. Zhang et al. [127] further advanced the field by demonstrating the substantial advantages of local dry underwater laser welding. Their work highlighted the use of laser substance and process inspection techniques to achieve high-quality welds. Localized dry underwater laser welding provides precision and control, making it a valuable technique for underwater applications where maintaining weld quality is crucial.

Guo et al. [128] used underwater laser welding equipment to weld 304 stainless steels. The experimental system is illustrated schematically in Fig. 25a. As shown in Fig. 25b, they utilized self-developed air curtain nozzles to exclude water and air, forming a localized cavity to protect the laser welding environment. Mechanical property testing revealed that the mechanical properties of laser-welded joints in the controlled environment were nearly conventional. This accomplishment is noteworthy for its potential real-world applications, highlighting the feasibility and effectiveness of local dry laser welding in underwater environments.

Therefore, laser welding is a research focus for local dry welding technology. However, the amplitude and phase will change due to the absorption and refraction of laser light by water, resulting in phenomena such as changes in spot size and scattering. These phenomena can lead to laser attenuation and even failure. These factors significantly constrain the welding effectiveness of underwater laser welding [129]. Currently, underwater laser welding is mainly confined to basic experimental research in shallow water depths. One of the future research directions is how to acquire correction data and perform laser attenuation correction.

2.4.4 Dry welding technology

Dry welding uses gas to displace water from around the weld zone, creating a dry or partially dry environment for the welding process, as shown in Fig. 24b. This technology offers several advantages over wet welding, including higher welding quality and better joint performance, leading to an increased focus on dry welding in various applications [130].

Dry welding is classified into high-pressure and atmospheric-pressure dry welding based on internal pressure. High-pressure dry welding occurs in a chamber where internal and external pressures are nearly equal. Water within the chamber is expelled by injecting compressed air, argon, or helium, creating a dry space to optimize the air environment for welding [112]. Research in this field has concentrated on constructing high-pressure chamber welding devices, with institutions like the Brazil Cenpes Center, the Marine Engineering Center of UK Cranfield University, and Norway's Sintef actively involved in such endeavors [129].

High-pressure dry underwater welding has successfully achieved automatic monitoring, ensuring excellent weld quality and efficiency. However, a critical limitation of this technology is its dependence on diving welders. Essential

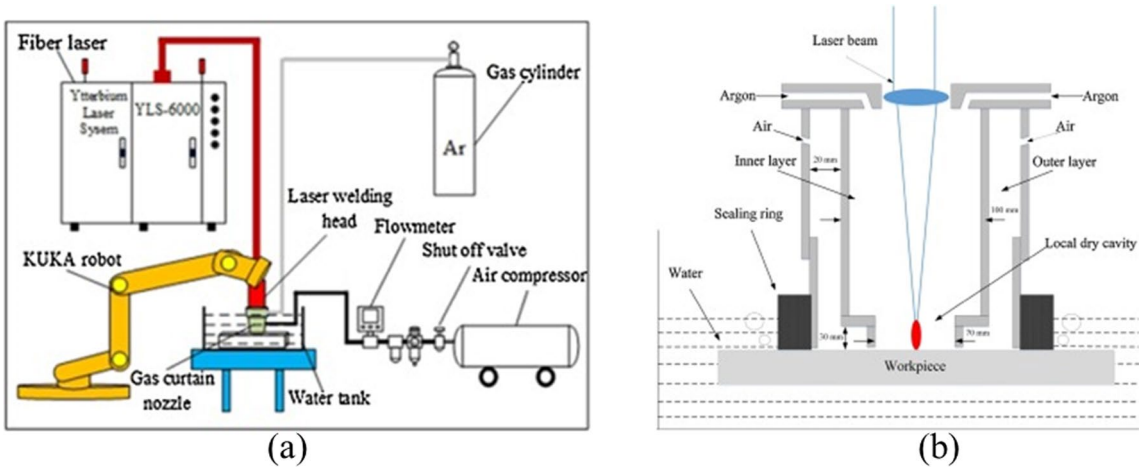

Fig. 25 The experiment system. **a** Schematic of the experiment system. **b** Schematic of the double-layer gas curtain nozzle [128]

tasks, such as equipment installation, maintenance, and testing, require the direct involvement of human divers. This reliance on manual intervention imposes depth restrictions, and the current welding system faces a notable constraint, unable to operate beyond 650 m. Moreover, the professional and technical requirements for underwater welders are notably demanding.

The development of intelligent welding robots is widely acknowledged as a crucial area of research to meet the growing requirements of marine engineering in greater depths. These robots could potentially overcome the problems posed by deep sea environments, enabling more efficient and reliable welding at greater depths in the challenging conditions of the deep sea. The integration of automation and intelligent technology into welding processes could revolutionize underwater welding and contribute to advancements in deep sea exploration and infrastructure development.

2.5 Research and application progress of welding technology in the high-pressure environment

2.5.1 Effects of high-pressure environment on welded structure

In a high-pressure environment, the arc tends to contract, which exacerbates the disorderliness of the arc column and leads to deteriorating arc stability [130]. Simultaneously, plasma velocity decreases under high pressure, resulting in more erratic movement of the arc root on the electrode surface. Differences in current density between the arc column and the arc root give rise to the formation of counter-electron plasma jets. These jets cause pressure disparities around the weld pool, hindering droplet transition and consequently causing spattering and process instability [131].

Wu et al. [132] revealed the effect of different environmental pressures on the arc characteristics of GTAW using a self-built high-pressure GTAW experimental system. Figure 26 illustrates the arc characteristic at 0.1 to 2.3 MPa. The results indicate that increasing pressure makes ionization more challenging, especially with higher currents. Treutler et al. [133] investigated the impact of different environmental pressures on the weld depth. During this experiment, the welded joints were fabricated at environmental pressures of 2 bar and 16 bar. Figure 27 shows the cross section and microstructure of the weld in different environment pressures. It can be observed that as the environmental pressure increases, the width of the weld increases. This result suggests a significant increase in penetration depth under high-pressure conditions. Moreover, Azar et al. [134] proposed a mathematical model based on extensive high-pressure experimental data. The model was able to accurately predict the electrical behavior and stability of the arc in a high-pressure environment.

In summary, welding in a high-pressure environment requires comprehensive consideration of the material, equipment, gas protection, and operating techniques, and the adoption of appropriate measures to ensure the quality and safety of welding.

2.5.2 Development of welding in the high-pressure environment

Research institutions have extensively delved into high-pressure welding technologies, mainly focusing on high-pressure

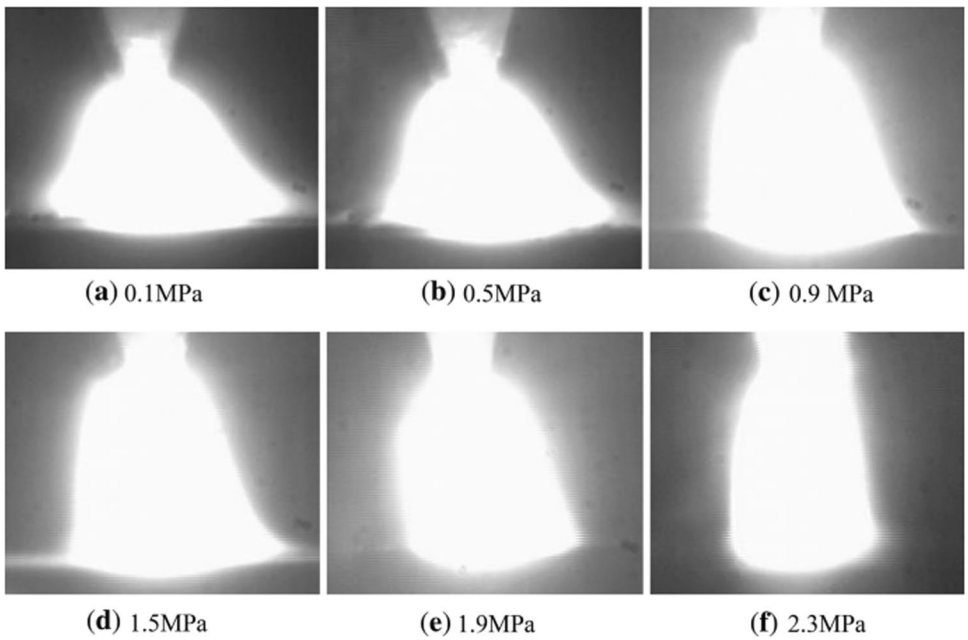

Fig. 26 The arc characteristic in different environmental pressures [132]

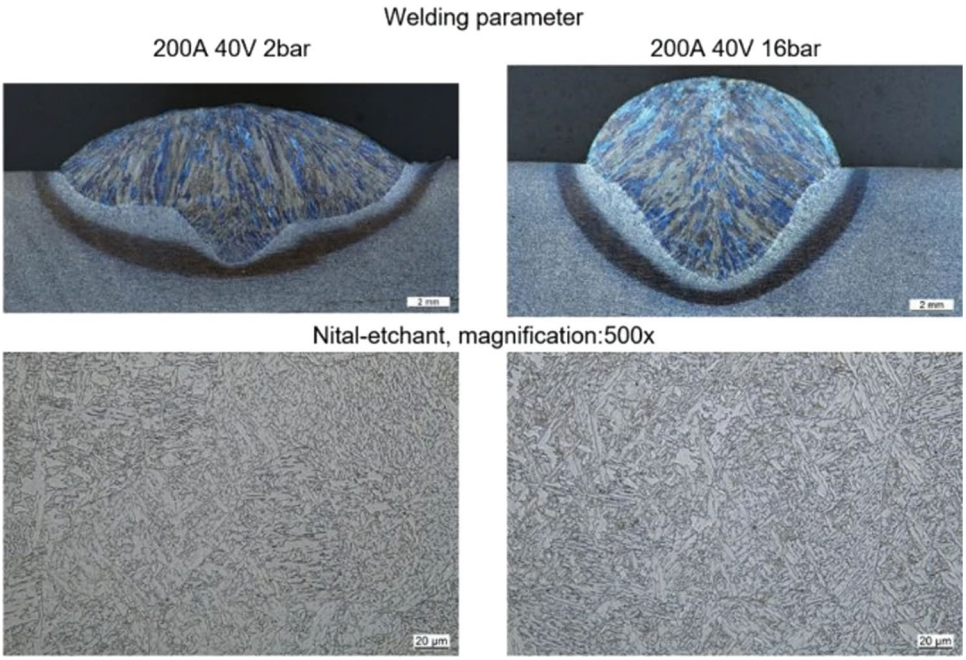

Fig. 27 The cross-section and microstructure of the weld in different environment pressures [133]

dry welding techniques within the 500 to 1000 m underwater depth range. Key contributors in this field include GKSS in Germany, the Federal Defense University in Germany, Sinteff in Norway, and Cranfield University in the United Kingdom. While the specific details of these projects may vary, they collectively arrive at consistent conclusions. Within this depth range, two arc welding methods have proven effective: PAW and MIG welding.

PAW is characterized by the concentration of energy in a small diameter arc column. This welding technique is in contrast to the unrestricted arc spread in hydrogen tungsten arc welding [135]. This compression results in a high concentration of arc energy, elevating both arc temperature and stability. Cranfield University has concluded a significant research initiative on high-pressure plasma arc welding. Findings indicate that the plasma arc maintains stability under ambient pressures equivalent to a water depth of 1000 m. Moreover, it demonstrates a smooth and reliable arc initiation under this substantial pressure [136].

In the mid-1970s, MIG welding was initially applied in a high-pressure environment. In a high-pressure environment, flux-cored arc welding demonstrated success through the use of tubular electrodes [137]. The evolution of high-performance power supplies has prompted a reevaluation of the MIG welding process [138]. GKSS [139] and Cranfield [136] universities have pioneered the development of welding power control systems explicitly tailored for high-voltage welding processes. While there may be nuances in the specifics, these systems follow conventional design concepts by regulating the static and dynamic output characteristics of the welding power supply to optimize welding process stability. The integration of this control system with a high-performance welding power supply empowers the MIG welding process to execute all-position welding under environmental pressures equivalent to a water depth of 1000 m. This setup attains satisfactory stability and fusion rates [140]. Extensive research conducted at Cranfield University has demonstrated the capability of the MIG welding process to effectively fuse materials under high pressures, reaching up to 25 MPa. The process exhibits stability, reliability, and repeatability that align with practical requirements.

In summary, there are still some research gaps in welding technology in high-pressure environments, which need to be studied and solved in depth. First, welding materials under a high-pressure environment may experience different stresses and deformations. The study of stress–strain behavior, plastic deformation, and fracture behavior of welding materials under high pressure is deemed necessary. The generation and distribution of stresses in the welding process is also a focus that needs to be researched. Secondly, conventional welding processes cannot be used in high-pressure environments, and the optimization and development of welding processes, materials, and equipment are urgent research gaps that need to be addressed. Finally, the reliability assessment methods for welded structures under high pressure, mainly including life prediction and new energy detection, are also an area that needs to be investigated. Through in-depth research on these aspects, more comprehensive and feasible solutions can be provided for high-pressure welding technology.

2.6 Research and application progress of welding technology in the corrosive environment

2.6.1 The corrosion mechanism of welded structures in the corrosive environment

The impact of a corrosive environment on welded structures is a lengthy and intricate process. During the process, the material is lost and destroyed due to the effects of the surrounding medium, which results in an overall decrease in the structural integrity. The forms of corrosion on welded structures include electrochemical corrosion, intergranular corrosion, stress corrosion cracking, and localized corrosion [141]. In a corrosive environment, welded structures may undergo electrochemical corrosion, particularly in electrolytes such as water. Different regions within the welded joints (dissimilar metal contact points, defects, oxides) may form electrochemical cells, resulting in localized corrosion and damage to the surface of the welded structure [142]. During the welding process, the interaction between carbon and chromium elements within the high-temperature zone leads to the formation of brittle carbides. These carbides are distributed along the grain boundaries, compromising the integrity of the metal grain boundaries and making the grain boundary region more susceptible to corrosion. When metal materials are exposed to external corrosive media, corrosion occurs at a faster rate at the grain boundaries compared to the interior regions, resulting in the phenomenon of intergranular corrosion [143]. When welded structures are exposed to a stress-inducing environment, corrosion can trigger stress corrosion cracking. This phenomenon typically occurs in high-stress areas exposed to gasses, liquids, or salt solutions, making the material more prone to corrosion-induced cracking under stress [144]. Localized corrosion occurs when the corrosive environment targets specific areas on the surface of welded structures, such as weld seams, defects, or vulnerable metal surfaces, leading to corrosion damage. The corrosion mechanism of welded joints in corrosive environments is depicted in Fig. 28 [145].

Previous studies have indicated that corrosive environments corrosive environments exert diverse effects on welded structures. The initial defects of welded joints, such as residual stresses, cracks, and porosity, are exacerbated. Moreover, the fatigue limit of welded joints is reduced, making the structure more prone to fatigue failure. Corrosion accelerates the generation and propagation of cracks, further worsening the fatigue-related deterioration of welded joints. These phenomena pose a threat to the reliability and safety of structures.

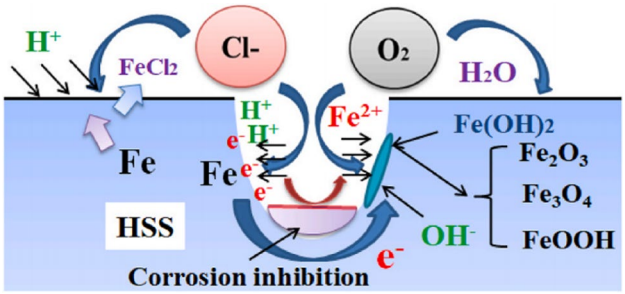

Fig. 28 Schematic diagram of corrosion mechanism [145]

2.6.2 The effects of the chemical composition of steel on the corrosion resistance of welded structures.

The alloy element content and microstructure in the material have a significant impact on the corrosion resistance of the welded structures. Wei et al. [145] conducted a comparative study on the corrosion performance of ordinary steel and Q690 joints in a marine environment. The results indicate that with increasing corrosion time, the corrosion resistance of Q690 joints is significantly superior to that of ordinary steel. In a separate study conducted by Song et al. [141], the corrosion resistance of low-alloy high-strength steel (HSAL) WM with different compositions in atmospheric and marine environments was examined. Both the BM and WM underwent Scanning Kelvin Probe (SKP) and corrosion weight loss tests. The test results, as depicted in Fig. 29, revealed that the HSAL WM sample with a strength of 980 MPa exhibited the highest level of corrosion resistance according to the SKP test. Particularly noteworthy was the significantly elevated voltaic potential observed in this sample, especially at the weld interface, surpassing that of the other two samples. As shown in Fig. 29b, the corrosion weight loss tests on the three welding samples further validate this conclusion.

Wei [146] and Zhang et al. [147] compared the corrosion resistance of steel materials under static corrosion and wear corrosion conditions. The wear corrosion behavior of 30CrNi2MoVA steel and S31254 steel structures subjected to gravel and seawater was investigated. Tafel curves, as shown in Fig. 30, were obtained through electrochemical tests. By comparing results, it was observed that the current intensity of wear corrosion was lower than that of static corrosion. Table 2 illustrates the corrosion potentials of 30CrNi2MoVA steel and S31254 steel. The corrosion potentials of these materials under static corrosion were − 0.6502 V and − 0.074V, while during wear corrosion, they were − 0.8646 V and − 0.504 V. These observations indicate that materials corrode more severely in seawater environments compared to normal conditions.

Somervuori et al. [148] compared the corrosion resistance of austenitic stainless steels with different grades

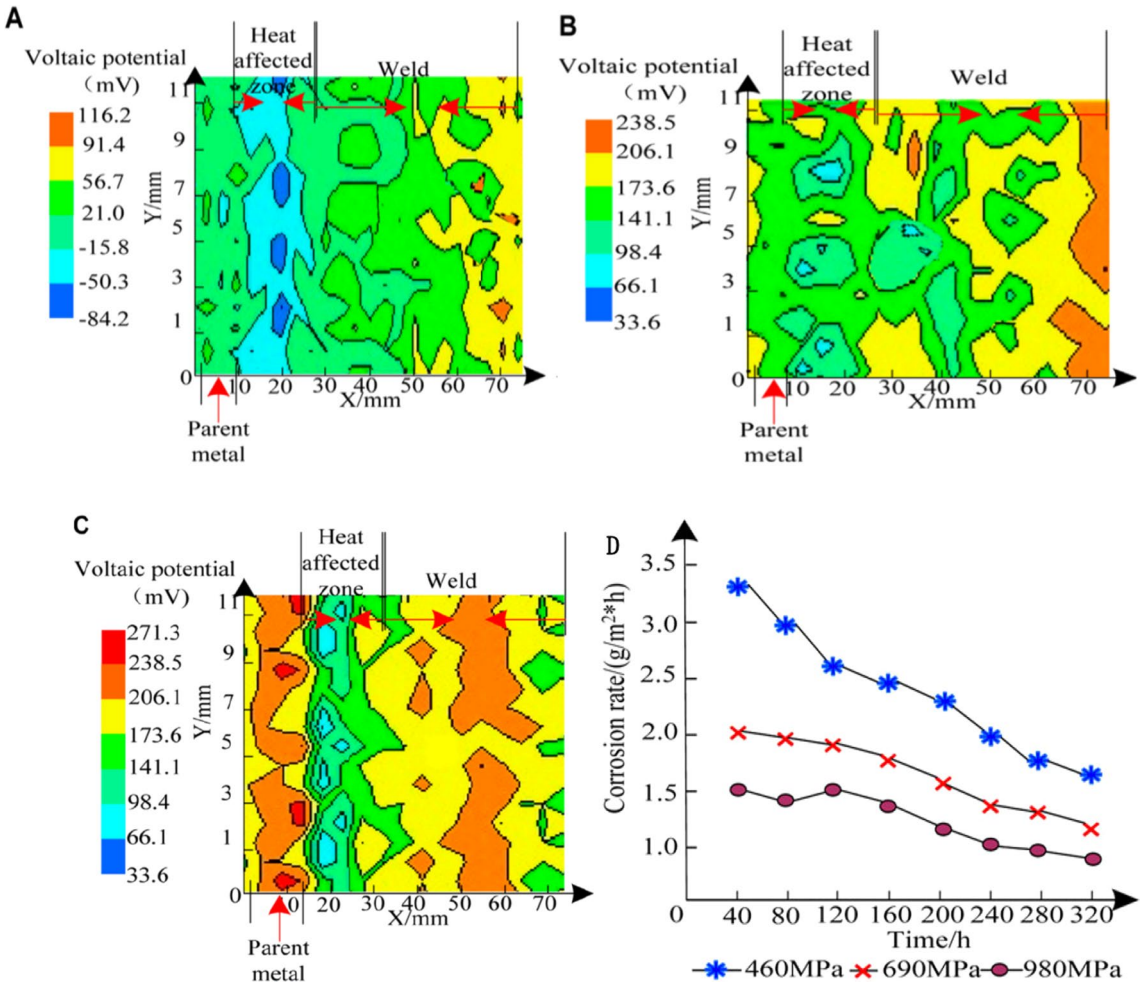

Fig. 29 Experimental results of HSAL with different compositions. **A** 460 MPa HSAL. **B** 690 MPa HSAL. **C** 980 MPa HSAL. **D** The results of weight loss tests [141]

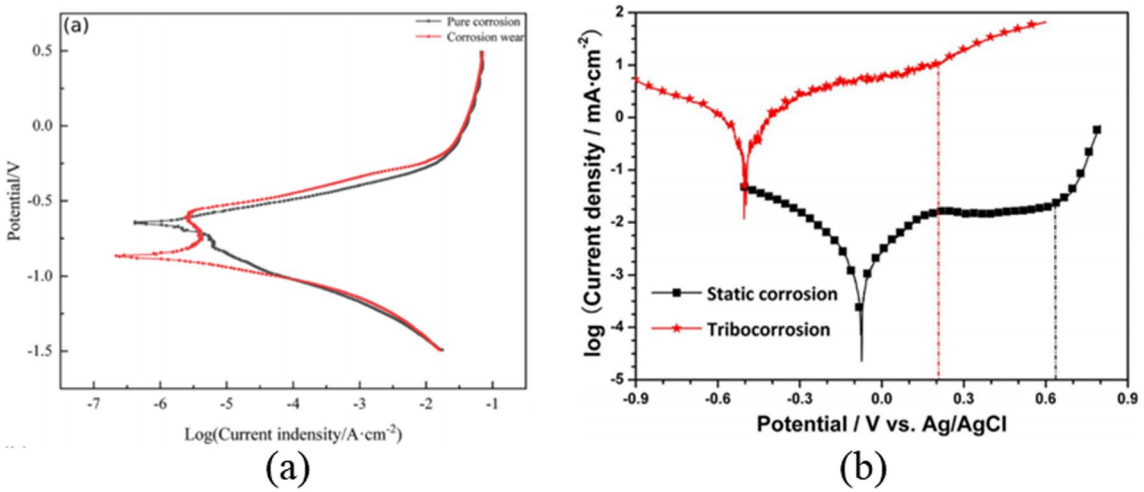

Fig. 30 Polarization curves. **a** 30CrNi2MoVA steel. [146] **b** S3125 steel [147]

Table 2 Electrochemical parameters for static and wear corrosion [146, 147]

Material	Status	Potential/V	Current intensity / A·cm^{-2}
30CrNi2MoVA steel	Static corrosion	− 0.6502	4.17×10^{-7}
	Corrosion wear	− 0.8646	2.18×10^{-7}
S31254 steel	Static corrosion	− 0.074	0.7×10^{-7}
	Corrosion wear	− 0.504	514.4×10^{-7}

(EN1.43.1 and EN1.4318) and levels (2B, 2F, and 2H) under different corrosion conditions. In this study, they investigated the effects of composition, surface quality, and chloride on the corrosion resistance of steel. Their research indicated that the type of chloride has a minimal impact on fatigue strength, and the corrosion resistance of 2B grade spot-welded specimens is better than that of the 2H grade. Ha et al. [149] explored the corrosion behavior of S32101 with different phase fractions. They achieved two phases (α phase and γ phase) by subjecting samples to different temperatures. Figure 31 shows the microstructures corresponding to different phase fractions. At a heat treatment temperature of 1040 °C, the fraction of the γ phase is significantly higher than that of the α phase. However, the α phase gradually becomes the predominant phase as the temperature increases. Figure 32 shows the results of the Scanning Kelvin Probe Force Microscopy (SKPFM). As illustrated by the potentiodynamic polarization curves, the corrosion potential of the specimen decreases progressively with an increase in the fraction of the *α* phase. This suggests that the lower corrosion resistance with higher α phase fractions.

In summary, alloy composition directly influences the corrosion resistance of welded joints. The addition of alloying elements, such as Cr, Ni, and Mo, effectively mitigates corrosion propagation. In corrosive environments, surface defects serve as initiation points for corrosive media attack, accelerating corrosion progression. Furthermore, the distribution of phases, grain size, and precipitates during welding also affect corrosion resistance. Therefore, it is necessary to

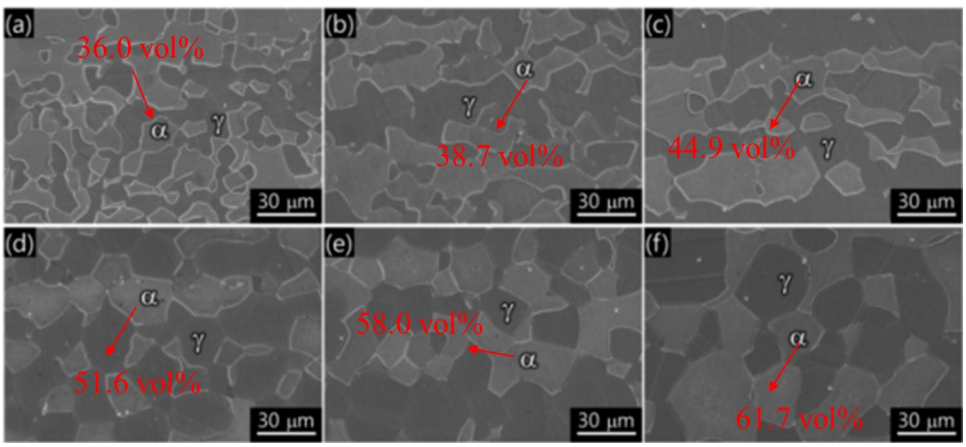

Fig. 31 The microstructure of S32101 at different temperatures. **a** 1040 °C. **b** 1080 °C. **c** 1110 °C. **d** 1140 °C. **e** 1170 °C. **f** 1200 °C [149]

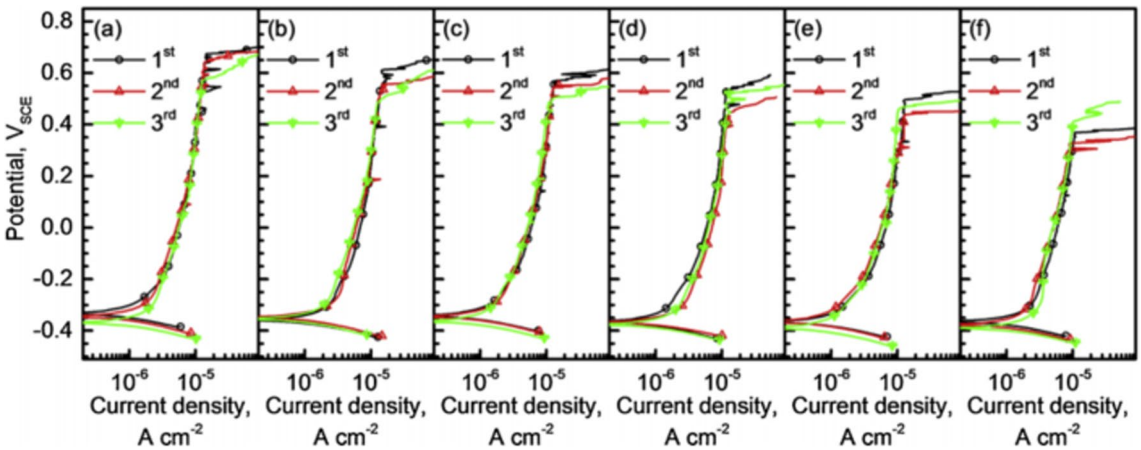

Fig. 32 Kelvin probe force microscopy scan results of the S32101 with different α fractions**. a** 36.0 vol%. **b** 38.7 vol%. **c** 44.9 vol%. **d** 51.6 vol%. **e** 58.0 vol%. **f** 61.7 vol% [149]

consider these factors comprehensively during welding to ensure clean and smooth joint surfaces.

2.6.3 The effects of the welding processes of steel on the corrosion resistance of welded structures

To investigate the influence of different welding processes on the corrosion behavior of welded joints, Gnanarathinam et al. [150] employed arc welding, MIG welding, and TIG welding techniques on 316 steel. Three strong acids, Ferric chloride ($FeCl_3$), Oxalic acid ($H_2C_2O_4$), and Nitric acid (HNO_3), were used to corrode the welds. After a 12-day corrosion test, the results indicated that 316 steel corroded fastest in $FeCl_3$ solution, while corrosion was slower in $H_2C_2O_4$ and HNO_3 solutions. The research highlights the crucial role of chloride ions (Cl^-) in corroding steel. These ions disrupt the passivation film on the steel's surface, prompting a reaction between Cl^- and the steel specimen's surface, initiating an active corrosion process. $H_2C_2O_4$ exhibits mild corrosiveness toward this type of stainless steel. Interestingly, in the $FeCl_3$ solution, TIG welding and arc welding showed lower levels of corrosion compared to other welding processes. This suggests that the choice of welding process can influence the corrosion resistance of the welded structure, with TIG welding and arc welding demonstrating better corrosion resistance in the specific corrosive environment of $FeCl_3$ solution.

The mechanical properties of welded structures under corrosive environments are crucial indicators of their corrosion resistance. Omiogbemi et al. [151] summarized the variations in the mechanical properties of joints in acidic corrosion environments. Their study focused on mild steel and examined its corrosion rate in 0.5 M HNO_3. Figure 33 shows the mechanical properties of the joints after different treatments. A significant reduction in the tensile strength and elongation of the corroded joints can be observed. This conclusion indicates a reduction in the ductility of the joints under acidic corrosion conditions. In their study, Wang et al. [152] aimed to improve the corrosion resistance of welded joints of 2024 aluminum alloy in a corrosive environment. They compared the variations in mechanical properties under different conditions. FSW was employed to join 2024 aluminum alloy in the study and the welded samples were subjected to corrosion by exposure to atmospheric and a 3.5% NaCl solution. The experimental results suggest a significant decrease in the overall performance of joints made with 2024 aluminum alloy in corrosive environments.

To investigate the influence of different process parameters on the corrosion performance of austenitic stainless steel, Zhang et al. [153] employed EBW for joining. Welding was conducted at heat input levels of 0.43, 0.46, and 0.5 kJ/mm, followed by corrosion testing in a 3.5% NaCl solution. The current density curves of the joint samples are shown in Fig. 34. The results indicate a significant decrease in the corrosion resistance of the joint when the current density exceeds 100μA. This result may be due to excessive heat input during the welding process, causing changes in the microstructure and chemical composition of the joint area.

2.6.4 The effects of the post-weld heat treatment of steel on the corrosion resistance of welded structures

Nyrkova et al. [154] subjected Al–Mg–Si–Cu alloy joints to heat treatment and tested the corrosion performance of the joints. The test results suggest that the mechanical performance of the joint decreased by approximately 1%

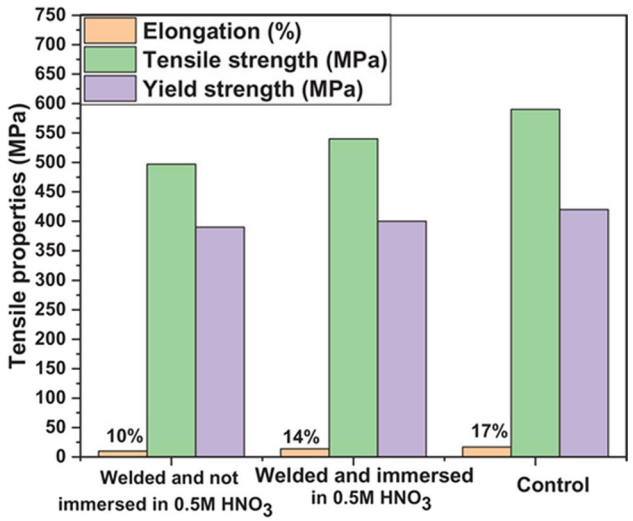

Fig. 33 The mechanical properties of joints under different corrosion conditions. [151]

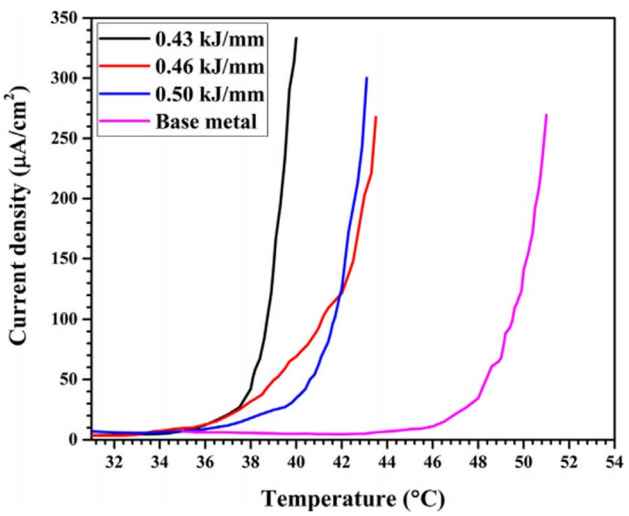

Fig. 34 The current density curves of the WM with different heat input and BM. [153]

to 2% within 14 days. With increasing test duration, the intensity decreased by an additional approximately 11%. During the corrosion-mechanical impact testing, the form of fracture of the joints primarily exhibited ductile failure. Kumar et al. [155] employed FSW to join AA7075 alloy and subjected it to peak aging (T6) and retrogression and re-aging (RRA) heat treatments. Dynamic polarization performance testing revealed that the weld exhibited higher hardness and strength under peak aging conditions, albeit with reduced corrosion resistance. The RRA treatment significantly improved the corrosion resistance of the weld while maintaining its mechanical properties. This dual enhancement in corrosion resistance and mechanical performance highlights the effectiveness of the RRA treatment in optimizing the overall performance of the AA7075 alloy weld.

In addition, Fereidooni et al. [156] explored the influence of ultrasonic treatment on materials. TIG welding was employed to weld 316 SS and 347 SS, with ultrasonic treatment applied near the weld zone. The polarization curves after ultrasonic treatment are depicted in Fig. 35. It can be observed that after ultrasonic treatment, the BM becomes the anode, protecting the weld zone from corrosion. This effect is primarily attributed to the ultrasonic treatment's ability to refine the grain structure and eliminate residual stresses, resulting in improved corrosion resistance of the treated weld.

To mitigate the impact of corrosion on steel structures, the selection of materials with excellent corrosion resistance is crucial, such as stainless steel or steel covered with anti-corrosive coatings. Regular inspections of steel structures are essential to promptly identify and address potential corrosion issues, thereby extending the structural lifespan.

2.6.5 Development of welding technology in the corrosive environment

Different welding methods indeed have varying impacts on the corrosion performance of welded joints. The TIG-shielded welding process tends to facilitate a more adequate transformation of ferrite into austenite. This results in a weld zone with a phase ratio of austenite to ferrite that is closer to the ideal phase balance. Numerous researchers have recently explored special welding techniques, such as FSW, LW, EBW, and PAW, to enhance welding efficiency and ensure high-quality outcomes.

FSW stands out due to its characteristics like low energy consumption, minimal pollution, and excellent welding quality. It can circumvent issues commonly associated with conventional fusion welding, such as coarse weld zones and high ferrite content [157]. LW offers a negligible heat input, resulting in a narrow weld with a higher ferrite content. This technique produces minimal HAZ in the weld, leading to increased resistance to uniform corrosion, although it might have relatively lower resistance to pitting corrosion [158].

Research and development of corrosion-resistant materials is an effective way to deal with corrosion. Gong et al. [159] systematically investigated the corrosion behavior of welds containing different alloying elements in a CO_2/H_2S environment. They utilized welding wires with Cr, Ni, Cu, and Mo to weld seamless steel pipes and the alloying element content of the WM and BM, as shown in Table 3. After corrosion, the microstructure was analyzed and Figs. 36 and 37 illustrate the SEM morphology and 3D topography of localized corrosion on weld WM. As shown in Fig. 36, the depth and the quantity of corrosion pits in WM4 are significantly less than those in the other samples. The average sizes of corrosion pits in WM1 were 0.13 mm and 17 μm, while the average diameters and depths of pits in WM2 and

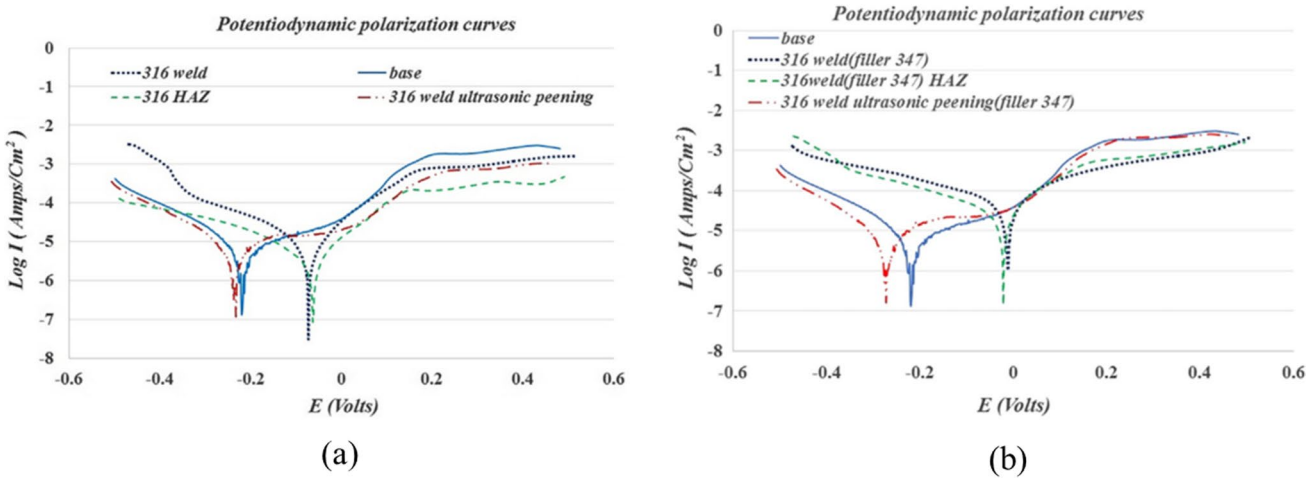

Fig. 35 The polarization curves of different materials after ultrasonic treatment. **a** 316 SS, **b** 347 SS [156]

Table 3 Alloy element content of BM and WM (wt.%) [159]

Composition	C	Mn	Si	S	P	Cr	Ni	Cu	Mo	Fe
Base Metal	0.12	1.28	0.29	0.005	0.012	0.04	0.03	0.05	0.03	Balance
WM1	0.11	1.42	0.45	0.006	0.021	0.05	0.04	0.04	0.02	Balance
WM2	0.11	1.08	0.58	0.010	0.017	0.41	0.23	0.23	–	Balance
WM3	0.09	0.94	0.50	0.011	0.013	0.96	0.20	–	–	Balance
WM4	0.14	0.44	0.71	0.010	0.012	9.61	1.80	–	1.33	Balance

WM1 = CHE507SHA, WM2 = CHE507CuP, WM3 = CHE507CrNi, WM4 = CHR507Mo

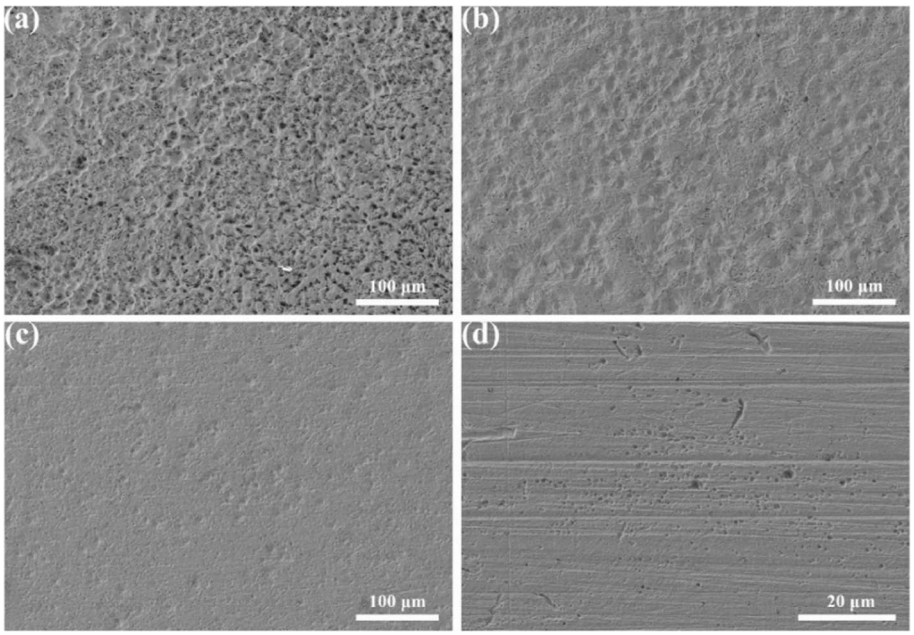

Fig. 36 SEM morphology of WM surface. **a** WM1. **b** WM2. **c** WM3. **d** WM4 [159]

WM3 were 0.10 mm/8 μm and 0.06 mm/6 μm, respectively. In WM4, both the diameter and depth were less than 1 μm, suggesting that the addition of Cr element enhances the corrosion resistance of the WM.

Research by Xu et al. [160] confirmed that Cr and Cu have synergistic effects on increasing the corrosion of the weld due to Cu promoting the enrichment of Cr in pearlite. This suggests that the content, distribution, and structure of alloying elements affect the corrosion behavior of welded structures. Avazkonandeh-Gharavol et al. [161] investigated the influence of Cu content on the corrosion resistance of Cr–Ni–Cu low alloy steel weld metal. They observed that when the Cu content ranged from 0.14 to 0.94 wt.%, the microstructure of the weld joint became refined, leading to improved overall performance of the weld. Adding Ni and Mo to welding materials also serves to prevent corrosion in welded joints. Bhole et al. [162] incorporated Ni and Mo into the filler metal, and experimental findings indicate that the combination of Ni and Mo significantly reduced the content of grain-boundary ferrite in the WM, thereby enhancing both the toughness and corrosion resistance of the weld. Ti alloys and Cu-Ni alloys have broad application prospects in the field of marine engineering due to their excellent corrosion resistance and comprehensive mechanical properties. Wu et al. [163] joined Ti80 (Ti-6Al-2Nb-2Zr-1Mo) and B10 (CuNi90/10) to investigate the galvanic corrosion behavior of B10/Ti80 in simulated seawater environments. Figure 38 shows the polarization curve of the sample in a 3.5% NaCl solution for 28 days. The potential difference between Ti80 and B10 exceeded 300 mV, indicating that severe galvanic coupling corrosion of B10 occurred when the two materials were in contact. Figure 39 shows the EIS diagram of B10/Ti80 coupling with different cathode/anode area ratios. As depicted in Fig. 39, the combination of B10 and Ti80 does not accelerate the corrosion of B10 at the initial stage. This is because Ti80 generates an oxide film that protects the surface of B10. However, due to the significant potential difference between the two materials, Ti80 eventually accelerates the corrosion of B10 until reaching a steady state with increasing corrosion time. As the cathode/anode area ratio increases, the corrosion rate also increases. Therefore, alloying elements can effectively modulate the electrochemical activity and electronic structure of welded joints, thereby enhancing their corrosion resistance.

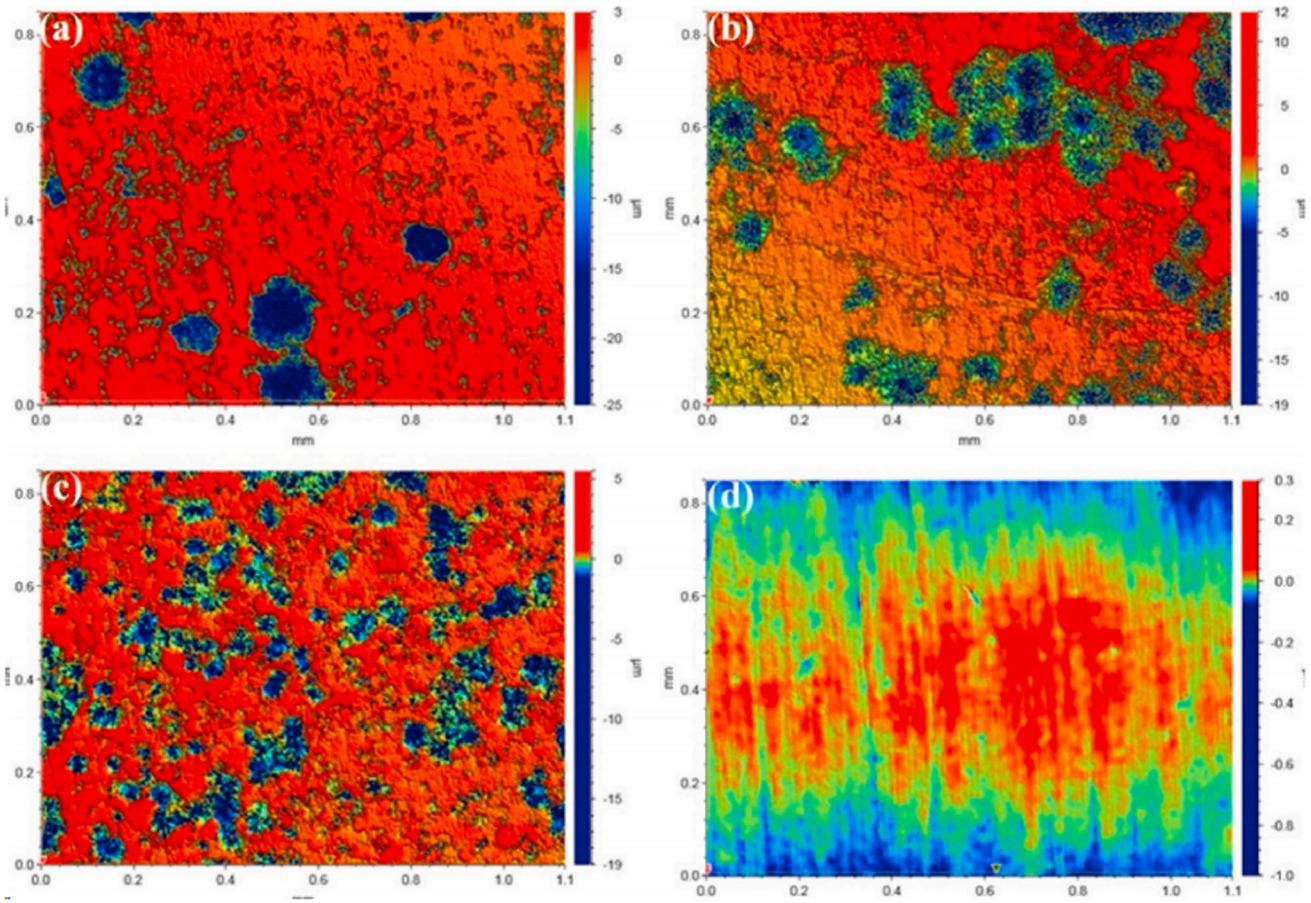

Fig. 37 3D topography of WM surface. **a** WM1. **b** WM2. **c** WM3. **d** WM4 [159]

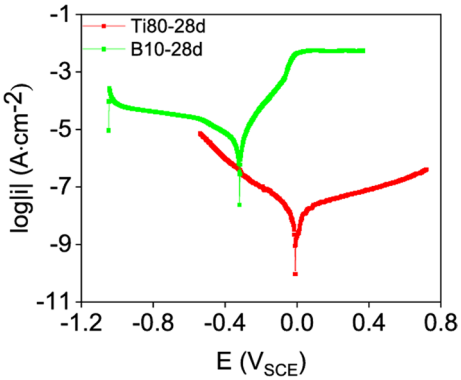

Fig. 38 Potentiodynamic polarization curve of B10 and Ti80 in a 3.5% NaCl solution for 28 days [163]

Overall, these studies show that the alloy composition, surface quality, and microstructure are critical factors in ensuring welded joints exhibit excellent corrosion resistance. PWHT, surface treatment and chemical protection measures are also effective ways to solve this problem. Presently, strategies, such as coating protection, alloy selection, and anodic protection, are commonly used to prevent corrosion in welded structures and base materials. These methods are critical focus areas in future welding technology research.

2.7 Research progress of other extreme service environments

2.7.1 Strong-wind environment

The effects of strong winds are an unavoidable challenge in the construction and marine industries. Strong winds cause frictional wear on materials and reduce weld strength and sealing. Meanwhile, the strong wind can blow away the welding arc, disrupt the stability of the arc, and result in uneven microstructure and metal distribution in the weld.

Moreover, strong winds can weaken gas shielding, exposing the weld area to the atmosphere and increasing the potential for oxidation and contamination. Temperature control in the welding area also becomes difficult in strong wind conditions. This leads to high or uneven temperatures in the welded joints, which in turn affects

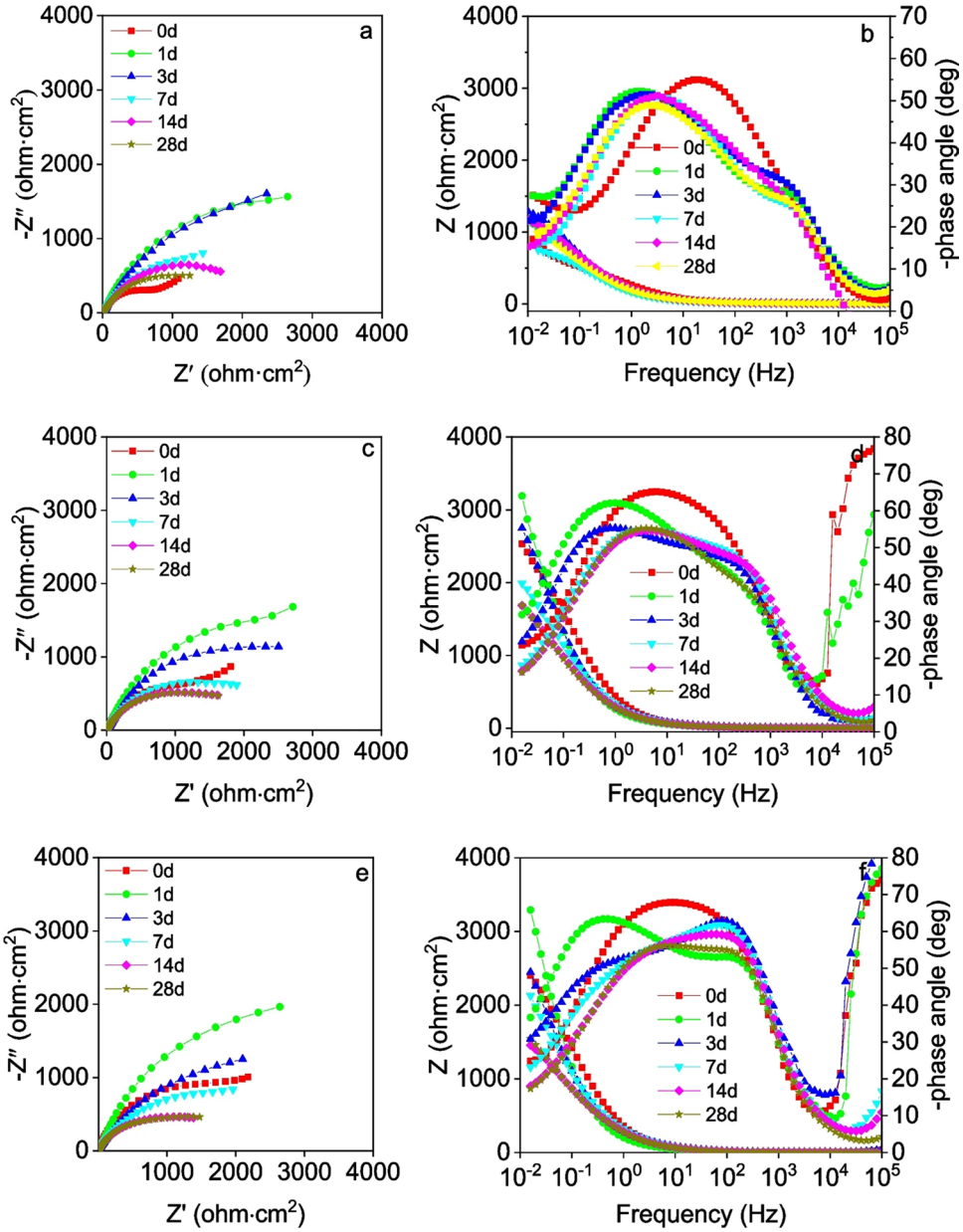

Fig. 39 EIS plots of B10/Ti80 coupling with different cathode/ anode area ratios. **a**, **c**, **e** Nyquist plots for cathode/ anode area ratio of 1, 3, and 5. **b**, **d**, **f** Bode plots for cathode/ anode area ratio of 1, 3, and 5 [163]

the strength and organization. Su et al. [164] conducted TIG welding experiments with different wind speeds. The experiments revealed that higher wind speeds correlated with a decrease in hardness values in both the weld zone and the HAZ. These results are attributed to the varying cooling rates and heat inputs in the WM and the HAZ. Therefore, the effect of wind speed must be carefully considered when using gas-shielded welding. While constructing wind shelters is a simple and effective method of mitigating the effects of wind in welding zones, it may be challenging for high-altitude projects in confined spaces. In such cases, alternative methods like LW, which are less affected by wind speed, should be explored.

2.7.2 Wear environment

Wear is a major factor in the failure of base materials and welds, and frictional wear is the most common form of wear [165]. Wear significantly changes the surface roughness and shape of the joint and affects its chemical composition and organizational structure. Nasresfahani et al. [166] investigated the influence of wear on the internal structure and mechanical properties of friction stir-welded joints. The experimental results showed that intense wear increased the brittleness of the joints, leading to a 40% decrease in mechanical strength.

Li et al. [167] delved into the wear behavior and mechanisms of welded joints, focusing on rail joints. Wear

experiments conducted on welded joints revealed that the degree of impact wear escalated with increasing impact cycles and loads. As the impact load and cycle intensified, the impact wear of rail welded joints underwent processes, such as plastic deformation, localized pitting damage, and fatigue crack expansion. The combined impact of fatigue and oxidative wear causes this phenomenon. Future research endeavors can explore the impact of different treatments on the material properties to improve the quality and performance of welded joints. It is important to consider material, process, and design factors to ensure welded joints have good wear resistance and long-term stability.

2.7.3 Electromagnetic environment

In an electromagnetic environment, welding equipment is exposed to a magnetic field that can cause arc shaking and drifting. These changes in arc behavior can result in increased melt droplet spatter, diminished arc stability, and increased operational challenges. Additionally, metal materials may experience electromagnetic induction, resulting in induced currents that can cause localized heating or electromagnetic forces around welded joints. These combined effects pose significant obstacles in achieving high-quality welded structures within such an environment. Mitigating the impact of electromagnetic interference on welding processes is crucial for ensuring high-quality welds. Strategies may involve shielding and grounding techniques, as well as the use of specialized equipment designed to minimize the effects of electromagnetic fields on welding operations.

2.7.4 Petrochemical environment

In the petrochemical industry, welding equipment is designed to meet the demands of different usage conditions [168]. This equipment often operates in high-temperature, high-pressure, and corrosive environments, requiring welding methods that can withstand these challenging conditions effectively. Moreover, the welding requirements can differ significantly based on the application, whether it involves plant manufacturing, on-site installation welding, or maintenance procedures. Given the stringent demands, the petrochemical sector has been proactive in embracing welding technologies that offer high efficiency and reliability. Among the widely adopted welding methods in this industry are:

2.7.4.1 Friction welding This technique involves joining metals through the generation of heat resulting from mechanical friction between the components. Due to material melting is not involved in the process, friction welding produces minimal deformation and residual stresses, which reduces the occurrence of voids and solidification cracks. This technique can effectively join dissimilar materials that are difficult to weld due to differences in melting points or properties. These advantages make friction welding an ideal choice for petrochemical industries.

2.7.4.2 Gas-shielding welding Gas-shielded welding creates a stable atmosphere, preventing molten metal from reacting with oxygen and nitrogen in the surrounding air, thus ensuring high-quality welds. Gas-shielded welding finds extensive applications in chemical engineering environments due to its ability to produce high-quality welds and maintain the integrity of materials under harsh conditions. In chemical plants, where corrosion resistance and leak-proof connections are paramount, gas shielding welding techniques are employed to join various components, such as pipes, tanks, and structural elements. Additionally, gas shielding welding offers precise control over the welding parameters, allowing for the customization of welds to meet the specific requirements of chemical processes.

2.7.4.3 Plasma and Tig composite welding Utilizing a plasma arc alongside TIG welding creates a composite welding process that offers high precision and control. This technique is beneficial for welding materials requiring fine detailing and high-quality finishes.

The evolution of "green" welding technologies has also influenced the welding practices of the petrochemical industry. Environmental protection and energy conservation are important trends in the petrochemical industry. Future welding technology is likely to focus more on reducing energy consumption, reducing waste generation, and using more environmentally friendly welding materials and processes. Moreover, automation technology plays a crucial role in enhancing welding efficiency and precision in the petrochemical industry. Advancements in automated welding systems, robotics, and computerized controls have contributed to improved weld quality, productivity, and safety. These automated systems enable precise and repeatable welds, reducing human error and ensuring consistent results, which is particularly valuable in petrochemical operations where reliability and safety are paramount.

In summary, high-performance, durable, and environmentally friendly welding technology is required in the petrochemical industry. Automation technology can effectively meet the challenges. Welding technology will continue to develop toward automation, intelligence, high-performance materials, environmental protection, and energy efficiency in the petrochemical industry.

3 Welding technology development under extreme conditions

Conventional welding technology may not be sufficient for manufacturing and maintaining equipment under extreme conditions due to advancements in extreme manufacturing technology. This paper aims to integrate existing welding methods with the distinctive features of extreme environments, highlighting areas for future research:

(1) Advancing the theoretical underpinnings is crucial, especially in the context of welding in space. Despite the growing interest in space welding, there is a lack of foundational theoretical exploration in this area. This scarcity extends to facets such as understanding the physical characteristics of electron beam or laser beam flow, delineating the metallurgical principles governing welding under microgravity conditions, comprehending heat and mass transfer dynamics along with molten pool flow, analyzing the distribution of temperature field and stress field, and unraveling the mechanisms behind defect formation, among other critical areas. Simultaneously, the welded structures experience a complex interplay within extreme temperature environments. Researchers navigate this challenge by adjusting welding processes and altering material compositions to mitigate the adverse impact on mechanical properties from these extreme temperature conditions. While these efforts yield specific research outcomes, future developments may require addressing a broader spectrum of temperatures, imposing more demanding requirements on welding theory.

(2) Research on welding materials, processes, and equipment remains a top priority. The current approach using molten metal particles faces several challenges, including spatter, electromagnetic interference, low energy conversion efficiency, and poor adaptability to the space environment. Hence, it is necessary to conduct further research into welding technologies that are safer, more stable, and highly efficient to address these challenges. In space materials, the selection of welding wires, brazing fluxes, and coating powders is restricted due to their predominantly lightweight metal or composite composition. Therefore, specialized development is necessary to create materials seamlessly integrated with the unique wire-feeding and powder-feeding equipment used in space welding. As an illustrative example, brazing materials must contain a specific proportion of reaction exothermic elements. This composition enables the utilization of self-propagating exothermic reactions, which reduces the energy input required for welding. Research is dedicated to developing new alloys and composite materials with enhanced performance advantages to meet the demands of various industries for high-strength, corrosion-resistant, and high-temperature-resistant materials. In terms of welding equipment, intelligent welding robots will become the primary carrier of welding automation, with autonomous perception and decision-making capabilities, capable of completing complex welding tasks. Integrated welding systems will also be widely used to monitor and optimize the welding process. In addition, portable and modular equipment will become the development trend in the welding field, improving the flexibility and adaptability of welding operations.

(3) Modeling and simulation of welding tests are also important areas of research. The testing of various welding processes on land is feasible. However, due to constraints and limitations, welding operations cannot be performed in extreme conditions, such as space and underwater. Therefore, welding simulation trials and process simulations must be performed on welding simulation and simulation systems. These simulations can be applied in actual welding scenarios by employing appropriate process parameters, adjusting design parameters, and implementing backup procedures.

(4) The assessment of weld seam quality in nuclear power and aerospace equipment is primarily based on conventional experimental validation due to a lack of actual performance data in radiation environments. Mechanical testing, fracture testing, and non-destructive testing are commonly used in a laboratory setting. It is important to note that test results may be uncertain due to the inability to test in a natural operating environment. Additionally, manual welding is unsuitable for equipment joining and maintenance environments, which require welding equipment to have extremely high reliability. As a result, researchers are working to develop new technologies and methods to more accurately assess the performance of welded joints in radiation environments to improve the safety and reliability of nuclear power and aerospace equipment. The mechanical welding industry is moving toward automation, remote techniques, and visual technologies. These advancements are poised to replace conventional welding methods.

(5) The technology of welding robots has reached a highly mature stage. Equipped with vision and perception systems, these mobile machines can operate autonomously or be remotely controlled to perform tasks using manipulators and other tools. They can work independently or collaborate with human operators. Combining virtual reality technology and artificial intelligence, we can anticipate further enhancements in the capabilities of welding robots. The advancement of underwater weld-

ing robots relies on improved sensing and perception systems, more sophisticated control algorithms, and the ability to adapt to various welding scenarios. These technologies will expand the application of underwater welding robots and play a critical role in future welding technology.

In conclusion, it is crucial to fill the research gaps in welding technology to promote technological development, improve safety, adapt to unique environments, and broaden application areas. Through in-depth research and theoretical exploration, we can better understand the welding process, optimize existing technologies, and lay a solid foundation for future development.

4 Summary

In the field of extreme manufacturing, durability and reliability have become pressing requirements for modern equipment. As the fundamental technology for joining materials, welding is widely used in various fields, including aerospace and energy. However, intricate manufacturing and service environments have resulted in aging patterns and failure mechanisms on welded structures that differ from those in conventional environments, presenting significant challenges for the development of welding technology. A thorough analysis of the current situation is the premise for looking forward to the future. Therefore, this paper focuses on researching and applying welding technology in extreme environments, providing a comprehensive summary and analysis of the current research status of welding technology.

After conducting an in-depth investigation into extreme welding technology, the typical environmental characteristics under extreme conditions were precisely identified. Key indicators, such as weld quality, microstructure, and mechanical properties, were combined to perform a detailed analysis of the influence mechanisms of various environmental factors on welding structures. The challenges associated with welding technology in such environments were also analyzed. Previous research suggests that welding technology encounters challenges in extreme environments like space, deep sea, polar, corrosive, and radiation environments. The research is mainly concerned with the effects of environmental factors, such as temperature, pressure, corrosive substances, and radiation, on the properties of welding materials and joints. The improvement and the optimization of welding processes, as well as the selection of welding equipment and materials, emerge as crucial aspects requiring attention.

Additionally, this paper combines examples of various welding technologies to highlight the advancements made by researchers in tackling extreme environmental obstacles. In deep sea conditions, some studies focus on developing welding materials and processes resilient to high pressure and high temperatures, aiming to enhance the reliability and the corrosion resistance of welded joints. In polar environments, researchers investigate the performance and behavior of welding materials under low-temperature conditions and develop welding equipment and processes tailored for polar conditions. In space environments, welding technology must account for the effects of vacuum and radiation on materials and joints. These studies have significantly contributed to developing welding processes, materials, and equipment.

Furthermore, researchers are exploring environmentally friendly materials and sustainable welding technologies to mitigate the environmental impact of the welding process. These research outcomes provide technical support for welding in extreme environments and propel welding technology toward a safer, more reliable, and sustainable direction.

After analyzing the existing research, it is evident that significant strides have been made in developing welding technology for extreme environments. Despite the progress, several challenges still need to be solved. Therefore, it is imperative to intensify research efforts and continuously innovate and refine welding techniques to meet the demands of engineering projects in extreme environments. This paper serves as a valuable reference for researchers and engineers engaged in related fields, inspiring further advancements in welding technology.

Acknowledgements This research work is supported by the National Natural Science Foundation of China (Grant No. 52275398), Central South University Innovation-Driven Research Programme (2023CXQD068), the Project of State Key Laboratory of High Performance Complex Manufacturing, Central South University (Grant No. ZZYJKT2022-01), Huxiang Young Talents Program of Hunan Province (No.2021RC3024), and Central South University Graduate Student Self-Discovery and Innovation Programs (No. 2024ZZTS0483)

Data availability The data supporting this study's findings are available from the corresponding author upon reasonable request.

Declarations

Conflict of interest The authors declare that there is no conflict of interest.

References

1. Wharry JP, Salvati E. Advanced welding and joining technologies—a commentary. Mater Today Commun. 2023;35: 105563. https://doi.org/10.1016/j.mtcomm.2023.105563.
2. Jeong SE, Yoon JW. Intermetallic compound transformation and mechanical strength of Ni-Sn transient liquid phase sinter-bonded joints in an extreme high-temperature environment. J Mater Sci-Mater El. 2022;33(9):6616–26. https://doi.org/10.1007/s10854-022-07836-3.

3. Wang JN, Wu ZZ, Han B, Zhang T, Zhou BS, Song KL, Jin X, Ren SZ, Chen JR, Zhao XN. Exploration on the materials quality control of railway vehicle weld structure based on service safety demand. J Phys Conf Ser. 2021;2109(1): 012014. https://doi.org/10.1088/1742-6596/2109/1/012014.
4. Gao XL, Chen C. High-strength joining of silica glass and 2024 aluminum alloy by ultrasonic-assisted soldering with Sn-Bi low temperature solder. J Manuf Process. 2023;101:1482–96. https://doi.org/10.1016/j.jmapro.2023.07.010.
5. Zhang HY, Chen C. Research on material flow in flat clinching process and joint failure mechanism. J Cent South Univ. 2023;30:3975–90. https://doi.org/10.1007/s11771-023-5502-6.
6. Wu YM, Wan YQ, Shi YJ, Jiang JJ. Effects of low temperature on properties of structural steels. J Univ Sci Technol Beijing. 2004;11(5):442–8.
7. Kodur VKR, Dwaikat MMS. Effect of high temperature creep on the fire response of restrained steel beams. Mater Struct. 2010;43(10):1327–41. https://doi.org/10.1617/s11527-010-9583-y.
8. Murty KL. Role and significance of source hardening in radiation embrittlement of iron and ferritic steels. J Nucl Mater. 1999;270(1–2):115–28. https://doi.org/10.1016/S0022-3115(98)00766-1.
9. New scientific factors in industry.1918. Nature 102, 32–34. https://doi.org/10.1038/102032b0.
10. Ma B, Gao XD, Huang YJ, Gao PP, Zhang YX. A review of laser welding for aluminium and copper dissimilar metals. Opt Laser Technol. 2023;167: 109721. https://doi.org/10.1016/j.optlastec.2023.109721.
11. Meng XC, Huang YG, Cao J, Shen JJ, Santos DJF. Recent progress on control strategies for inherent issues in friction stir welding. Prog Mater Sci. 2021;115: 100706. https://doi.org/10.1016/j.pmatsci.2020.100706.
12. Lange A, Widomski P, Kaszuba M, Boryczko B. Influence of gas shielding type and welding parameters on weld geometry and selected properties of welded joints from INCONEL 600. Archiv Civ Mech Eng. 2022;22(4):150. https://doi.org/10.1007/s43452-022-00470-0.
13. Zhan XH, Yu HS, Feng XS, Pan P, Liu ZM. A comparative study on laser beam and electron beam welding of 5A06 aluminum alloy. Mater Res Express. 2019;6(5):056563. https://doi.org/10.1088/2053-1591/ab0562.
14. Jiang M, Chen X, Chen YB, Tao W. Mitigation of porosity defects in fiber laser welding under low vacuum. J Mater Process Technol. 2020;276: 116385. https://doi.org/10.1016/j.jmatprotec.2019.116385.
15. Zhou ZW, Li HJ, Chen C. Microstructural transformation and mechanical properties of Cu-sputtered alumina ceramic/Zn5Al/AA2024 ultrasonic soldering joints. Intermetallics. 2024;165: 108153. https://doi.org/10.1016/j.intermet.2023.108153.
16. Chen J, Chen Q, Wu CS. Study of high-speed pulsed gas metal arc welding assisted by external magnetic-field. Sci Technol Weld Joining. 2020;25(7):564–70. https://doi.org/10.1080/13621718.2020.1774994.
17. Rhode M, Richter T, Schroepfer D, Manzoni AM, Schneider M, Laplanche G. Welding of high-entropy alloys and compositionally complex alloys—an overview. Weld World. 2021;65(8):1645–59. https://doi.org/10.1007/s40194-021-01110-6.
18. Bond D, Lussoli RJ, Neto JBR, D'Oliveira ASCM. Co-based superalloy (Stellite 6) powder with added nanoparticles to be molten by PTA. Soldag Insp. 2020;25:E2514. https://doi.org/10.1590/0104-9224/SI25.14.
19. Li YX, Chen C, Yi RX, He L. The brazing of Al2O3 ceramic and other materials. Int J Adv Manuf Technol technology.2022; 120: 9–84. https://doi.org/10.1007/s00170-022-08789-x.
20. Ren XQ, Chen C. Analysis of mechanical properties and defect failure of clinched joints for joining AA5052 sheets with sandwich structures. J Market Res. 2023;25:5650–62. https://doi.org/10.1016/j.jmrt.2023.06.242.
21. Suita Y, Tanaka K, Ohtani M, Shobako S, Terajima N, Noboru T, Hiraoka N. Technique to prevent metal deposition on optical components in space diode laser welding for space applications. Trans Jpn Soc Aeronaut Space Sci. 2011;4(183):67–73. https://doi.org/10.2322/tjsass.54.67.
22. Xue ZH, Liu JG, Wu CC, Tong YC. Review of in-space assembly technologies. Chinese J Aeronaut. 2021;34(11):21–47. https://doi.org/10.1016/j.cja.2020.09.043.
23. Liu XM, Dong QL, Wang PF, Chen H. Review of electron beam welding technology in space environment. Optik. 2020;225: 165720. https://doi.org/10.1016/j.ijleo.2020.165720.
24. Nogi K, Aoki Y, Fujii H, Nakata K. Behavior of bubbles in weld under microgravity. Acta Mater. 1998;46(12):4405–14. https://doi.org/10.1016/S1359-6454(98)00084-6.
25. Kim S, Damle N, Mudawar I, Hartwig J. Cryogenic flow boiling in microgravity: Effects of reduced gravity on two-phase fluid physics and heat transfer. Int J Heat Mass Transf. 2024;218: 124751. https://doi.org/10.1016/j.ijheatmasstransfer.2023.124751.
26. Fragomeni JM, Nunes AC. A study of the effects of welding parameters on electron beam welding in the space environment. Aerosp Sci Technol. 2003;7(5):373–84. https://doi.org/10.1016/S1270-9638(03)00031-2.
27. Luo Y, Wu W, Wu GF, Ye H. Influence of gravity state upon bubble flow in the deep penetration molten pool of vacuum electron beam welding. Vacuum. 2013;89:26–34. https://doi.org/10.1016/j.vacuum.2012.08.008.
28. Krichel T, Olschok S, Reisgen U. Influence of working pressure on laser beam welding in vacuum of electrical steel sheets. Vacuum. 2023;207: 111659. https://doi.org/10.1016/j.vacuum.2022.111659.
29. Ma XT, Xu SM, Wang FF, Zhao YB, Meng XC, Xie YM, Wan L, Huang YX. Effect of temperature and material flow gradients on mechanical performances of friction stir welded AA6082-T6 joints. Materials. 2022;15(9):6579. https://doi.org/10.3390/ma15196579.
30. Smith T. Review, analyses, and recommendations related to modern international use of nuclear space technologies with focus on united states and russia. J Br Interplanet Soc. 2012;65(11–12):360–72.
31. Qi H, Shi QS, Qian YH, Li YM, Xu JJ, Xu CH, Zhang Z, Xie XB. The atomic oxygen erosion resistance effect and mechanism of the perhydropolysilazane-derived SiOx coating used on polymeric materials in space environment. Polymers. 2022;14(2):322. https://doi.org/10.3390/polym14020322.
32. Tong PY, Wei Q, Hu N, Chen XG. Asynchronous synergistic damage effect of atomic oxygen and space micro debris on kapton film. Coatings. 2022;12(2):179. https://doi.org/10.3390/coatings12020179.
33. Jing PY, Wang HJ, Chen WA, Chen L, Yin HZ, Wu HJ, Li DY. Effect of Ti addition on microstructure and tribological properties of laser cladding Ni35/WC coating in an oxygen-free environment. Surf Coat Technol. 2022;440: 128480. https://doi.org/10.1016/j.surfcoat.2022.128480.
34. Long WM, Liu DS, Wu AP, Wang DC, Huang GQ. Influence of laser scanning speed on the formation property of laser brazing diamond coating. Diam Relat Mater. 2020;110: 108085. https://doi.org/10.1016/j.diamond.2020.108085.
35. Liu Y, Liu ZM. Correlation of reflected plasma angle and weld pool thermal state in plasma arc welding process. J Manuf Process. 2022;75:1111–22. https://doi.org/10.1016/j.jmapro.2022.01.066.

36. Nunes AC, Russell C, Bhat B, Fragomeni JM. Assessment of molten metal detachment hazards for electron beam welding in the space environment: Analysis and Test Results.
37. Bunton PH. Particulate electron beam weld emission hazards in space. 1996.
38. Fragomeni JM. An assessment of molten metal detachment hazards during electron beam welding in the space Shuttle Bay at LEO for the international space welding experiment.1996.
39. Jogender S, Anil K, Namhyun K. Welding in space. Adv Mater Process. 2005;163(6):54–7.
40. Xiao QS, Han X, Pei YF. Ultra-low temperature effect on electron beam welding process. IOP Conf Ser Mater Sci Eng. 2020;2020(770): 012067. https://doi.org/10.1088/1757-899X/770/1/012067.
41. Das D, Pratihar DK, Roy GG. Effects of space charge on weld geometry and cooling rate during electron beam welding of stainless steel. Optik. 2020;206: 163722. https://doi.org/10.1016/j.ijleo.2019.163722.
42. Zhai YT, Huang B, Zhang JY, Zhang BR, Liu SJ, Huang QY. Effect of weld spacing on microstructure and mechanical properties of CLAM electron beam welding joints. Fusion Eng Des. 2016;112:440–9. https://doi.org/10.1016/j.fusengdes.2016.06.027.
43. McCay TD, Bible JB, Mueller RM, McCay MH, Sharp CM, Hopkins JA. Space applications industrial laser system (SAILS). 25th Plasmadynamics and Lasers Conference. (Colorado Springs, CO, USA.).1994. https://doi.org/10.2514/6.1994-2448.
44. Gong JF, Peng GC, Li LQ, Xia HB, Meng SH, Wang JM. Effect of plasma plume produced by vacuum laser welding on energy transmission. Opt Laser Technol. 2021;136: 106744. https://doi.org/10.1016/j.optlastec.2020.106744.
45. Suita Y, Tabakodani E, Sugiyama S, Terajima N, Tsukuda Y, Fujisawa S, Imagawa K. Development of space DL welding process for construction and repair of space structures in Space. Trans Jpn Soc Aeronaut Space Sci. 2005;48(160):86–91. https://doi.org/10.2322/tjsass.48.86.
46. Luo Y, Tang XH, Lu FG, Chen QT, Cui HC. Effect of subatmospheric pressure on plasma plume in fiber laser welding. J Mater Process Technol. 2015;215:219–24. https://doi.org/10.1016/j.jmatprotec.2014.08.011.
47. Suita Y, Tsukuda Y, Terajima N, Hatta T, Kono T, Inokuma R, Kawata K, Oji T, Nishikawa H, Yoshida K, Masubuchi K. Gas hollow tungsten arc welding experiments in aircraft borne simulated space environment. Weld Int. 2001;15(2):100–7. https://doi.org/10.1080/09507110109549325.
48. Suita Y, Matsushita K, Terajima N. Arc initiation phenomena by space GHTA welding process using touch start technique in a vacuum. Weld Int. 2006;20(9):707–12. https://doi.org/10.1533/wint.2006.3652.
49. Suita Y, Ohara M, Sogawa H, Matsushita K, Shobako S, Terajima N, Tsukuda Y, Masubuchi K, Yamauchi S. Welding experiments of aluminium pipe by space GHTA welding in aircraft-borne simulated space environment. Weld Int. 2009;23(5):369–75. https://doi.org/10.1080/09507110802542767.
50. Cho DW, Lee SH, Na SJ. Characterization of welding arc and weld pool formation in vacuum gas hollow tungsten arc welding. J Mater Process Technol. 2013;213(2):143–52. https://doi.org/10.1016/j.jmatprotec.2012.09.024.
51. Prater T. Welding in space: a comparative evaluation of candidate welding technologies and lessons learned from on-orbit experiments. J Br Interplanet Soc. 2015;68(1):33–46.
52. Ding J, Carter B, Lawless K, Nunes A, Russell C et al. A decade of friction stir welding R and D at NASA's Marshall Space Flight Center and a glance into the future. (NASA Marshall Space Flight Center). 2019.
53. Daly S, Hardyman M, Ragan J, Toombs J, Prater T, Grugel NR. MMaJIC, an experimental chamber for investigating soldering and brazing in microgravity. Gravit Space Res. 2017;5(2):28–34. https://doi.org/10.2478/gsr-2017-0008.
54. Ting W, Wu YF, Chong G, Jiang SY. Feasibility study on feeding wire electron beam brazing of pure titanium using an electron gun for space welding. Vacuum. 2020;180:109575. https://doi.org/10.1016/j.vacuum.2020.10957.
55. Flom Y. Brazing in space: enabling the next frontier. Weld J. 2005;84(10):25–9.
56. Zheng W, Qiao GF. Brazing of SiC ceramic with extraterrestrial regolith simulant in ISRU and ISRF applications. Adv Space Res. 2022;70(3):752–61. https://doi.org/10.1016/j.asr.2022.05.015.
57. Jacoby BR. Fundamental mechanisms affecting friction welding under vacuum. Naval Postgraduate School at California in USA. 2018.
58. Abbasi M, Baghei B. New attempt to improve friction stir brazing. Mater Lett. 2021;304:10688. https://doi.org/10.1016/j.matlet.2021.130688.
59. Ouyang X, Zhang HY, Chen C. Recycling of scrap sheet material enhanced joining mechanical properties of aluminum alloys by a novel auxiliary sheet flat-clinching process. J Mater Res Technol. 2023;25:4609–21. https://doi.org/10.1016/j.jmrt.2023.06.209.
60. Sahoo A, Tripathy S. Development in plasma arc welding process: a review. Mater Today Proc. 2021;41(2):363–8. https://doi.org/10.1016/j.matpr.2020.09.562.
61. Lv XQ, Qu ZQ, Su HY, Xu LY, Jing HY. Study on arc characteristics of different defects in pulsed micro-plasma arc welding. J Mater Process Technol. 2022;302: 117514. https://doi.org/10.1016/j.jmatprotec.2022.117514.
62. Trydell K, Persson KA, Fuertes N, Siewert E, Hussary N, Pfreuntner M, Bengtsson P, Janiak P, Vishnu R, Frodigh M. Ferrite fraction in duplex stainless steel welded with a novel plasma arc torch. Weld World. 2023;67(3):805–17. https://doi.org/10.1007/s40194-022-01447-6.
63. Song Y, Chai MY, Han ZL, Liu P. High-temperature tensile and creep behavior in a crmov steel and weld metal. Materials. 2021;15(1):109. https://doi.org/10.3390/ma15010109.
64. Yang B, Xuan FZ. Creep behavior of subzones in a CrMoV weldment characterized by the in-situ creep test with miniature specimens. Mater Sci Eng A. 2018;723:148–56. https://doi.org/10.1016/j.msea.2018.03.051.
65. Xue BQ, Tan JB, Zhang ZY, Wang X, Wu XQ, Han EH, Ke W. Effect of temperature on low cycle fatigue behavior of T91 steel in liquid lead-bismuth eutectic environment at 150–550°C. Int J Fatigue. 2023;167: 107344. https://doi.org/10.1016/j.ijfatigue.2022.107344.
66. Ma L, Guo J, Liu QY, Wang WJ. Fatigue crack growth and damage characteristics of high-speed rail at low ambient temperature. Eng Fail Anal. 2017;82:802–15. https://doi.org/10.1016/j.engfailanal.2017.07.026.
67. Burns JT, Gupta VK, Agnew SR, Gangloff RP. Effect of low temperature on fatigue crack formation and microstructure-scale propagation in legacy and modern Al-Zn-Mg-Cu alloys. Int J Fatigue. 2013;55:268–75.
68. Bian YY, Guo SQ, Xu YL, Tang K, Lu XG, Ding WZ. Recovery of rare earth elements from permanent magnet scraps by pyrometallurgical process. Rare Met. 2022;41(5):1697–702. https://doi.org/10.1007/s12598-015-0554-x.
69. Guo Z, Jia X, Qiao W. Mechanical properties of butt weldments made with Q345B steel and E5015 Elec trodes at different temperatures. J Mater Civil Eng. 2019;31(9):04019185. https://doi.org/10.1061/(ASCE)MT.1943-5533.0002845.

70. Huang YY, Luo XW, Zhan YC, Chen Y, Yu LP, Feng W, Xiong JK, Yang JP, Mao GJ, Yang L, Nie FH. High-temperature creep rupture behavior of dissimilar welded joints in martensitic heat resistant steels. Eng Fract Mech. 2022;273: 108739. https://doi.org/10.1016/j.engfracmech.2022.108739.
71. Pe˘si˘cka J, Ku˘zel R, Dronhofer A, Eggeler G. The evolution of dislocation density during heat treatment and creep of tempered martensite ferritic steels. Acta Mater. 2003;51(16):4847–62.
72. Kumar R, Varma A, Kumar YR, Jain J, Neelakantan S. Microstructure anomaly upon high temperature exposure and its influence on the mechanical properties of a modified 9Cr-1Mo steel weld. Mater Charact. 2022;189: 111937. https://doi.org/10.1016/j.matchar.2022.111937.
73. Sung HJ, Moon JH, Jang MJ, Kim HS, Kim S-J. Microstructural and finite element analysis of creep failure in dissimilar weldment between 9Cr and 2.25 Cr heat-resistant steels. Metall Mater Trans A. 2018;49(11):5323–32. https://doi.org/10.1007/s11661-018-4859-x.
74. Cao J, Gong Y, Yang Z-G. Microstructural analysis on creep properties of dissimilar materials joints between T92 martensitic and HR3C austenitic steels. Mater Sci Eng A. 2011;528(19–20):6103–11. https://doi.org/10.1016/j.msea.2011.04.057.
75. Forni D, Chiaia B, Cadoni E. High strain rate response of S355 at high temperatures. Mater Des. 2016;94:467–78. https://doi.org/10.1016/j.matdes.2015.12.160.
76. Borgioli F. The corrosion behavior in different environments of austenitic stainless steels subjected to thermochemical surface treatments at low temperatures: an overview. Metals. 2023;13(4):776. https://doi.org/10.3390/met13040776.
77. Stephens RI, Chung JH, Glinka G. Low temperature fatigue behavior of steels—a review. SAE Trans. 1979;88:1892–904. https://doi.org/10.4271/790517.
78. Shul'ginov BS, Matveyev VV. Impact fatigue of low-alloy steels and their welded joints at low temperature. Int J Fatigue. 1997;19(8):621–7. https://doi.org/10.1016/S0142-1123(97)00066-2.
79. Liao XW, Wang YQ, Qian XD, Shi YJ. Fatigue crack propagation for Q345qD bridge steel and its butt welds at low temperatures. Fatigue Fract Eng Mater Struct. 2018;41(3):675–87. https://doi.org/10.1111/ffe.12727.
80. Jeong D, Park T, Lee J, Kim S. Ambient and cryogenic S-N fatigue behavior of Fe15Mn steel and its weld. Met Mater Int. 2015;21:453–60. https://doi.org/10.1007/s12540-015-4397-7.
81. Peral LB, Zafra A, Blasón S, Rodríguez C, Belzunce J. Effect of hydrogen on the fatigue crack growth rate of quenched and tempered crmo and crmov steels. Int J Fatigue. 2019;120:201–14. https://doi.org/10.1016/j.ijfatigue.2018.11.015.
82. Fu RD, Wu SF, Zhou WH, Zhang WH, Yang YQ, Zhang FC. Effects of heat treatment processes on microstructure and properties of 2.25Cr-1Mo-0.25V HSLA steels. Mater Sci Technol. 2009;25:50–5. https://doi.org/10.1179/174328407X213143.
83. Jiang ZH, Wang P, Li DZ, Li YY. The evolutions of microstructure and mechanical properties of 2.25Cr-1Mo-0.25V steel with different initial microstructures during tempering. Mater Sci Eng A. 2017;699:165–75. https://doi.org/10.1016/j.msea.2017.05.095.
84. Turichin G, Kuznetsov M, Sokolov M, Salminen A. Hybrid laser arc welding of X80 steel: influence of welding speed and preheating on the microstructure and mechanical properties. Phys Procedia. 2015;78:35–44. https://doi.org/10.1016/j.phpro.2015.11.015.
85. Sklenička V, Kuchařová K, Svobodová M, Kvapilová M, Král P, Horváth L. Creep properties in similar weld joint of a thick-walled P92 steel pipe. Mater Charact. 2016;119:1–12. https://doi.org/10.1016/j.matchar.2016.06.033.
86. Bae S, Kim Y, Liu SP. A study on creep and mechanical properties at high temperature of SMAW welds for a Cr–Mo-X steel. Weld World. 2023;67(9):2153–62. https://doi.org/10.1007/s40194-023-01560-0.
87. Lee EH, Yoo MH, Byun TS, Hunn JD, Farrell K, Mansur LK. On the origin of deformation microstructures in austenitic stainless steel: Part II—mechanisms. Acta Mater. 2001;49(16):3277–87. https://doi.org/10.1016/S1359-6454(01)00194-X.
88. Lee EH, Byun TS, Hunn JD, Yoo MH, Farrell K, Mansur LK. On the origin of deformation microstructures in austenitic stainless steel: part I—microstructures. Acta Mater. 2001;49(16):3269–76. https://doi.org/10.1016/S1359-6454(01)00193-8.
89. Cárcel-Carrasco FJ, Pascual-Guillamón M, Pérez-Puig MA. Effects of X-rays radiation on AISI 304 stainless steel weldings with AISI 316L filler material: a study of resistance and pitting corrosion behavior. Metals. 2016;6(5):102. https://doi.org/10.3390/met6050102.
90. Sun LB, Wang MQ, Huang LJ, Fang NW, Wu PB, Huang RS, Xu K, Wang XX, Qin J, Li S, Long WM. Comparative study on laser welding thick-walled TC4 titanium alloy with flux-cored wire and cable Wire. Metals. 2023;16(4):369. https://doi.org/10.3390/ma16041509.
91. Zhang XH, Hatter K, Chen YX, Shao L, Li J, Sun C, Yu KY, Li N, Taheri ML, Wang HY, Wang J, Nastasi M. Radiation damage in nanostructured materials. Progr Mater Sci. 2018;96:217–321. https://doi.org/10.1016/j.pmatsci.2018.03.002.
92. Arora H, Basha KM, Abhishek DN, Devesh B. Welding simulation of circumferential weld joint using TIG welding process. Materials Today: Proceedings. 2022;50:923–9. https://doi.org/10.1016/j.matpr.2021.06.315.
93. Venkateswaran S, Mageshwaran G, Balakrishnan K, Bharadwaj RR, Saiteja R, Sasipraba T, Subramaniam P, Jayaprabakar J, Joy N, Anish M, Ganesan S, Kavitha KR. Experimental investigation on the strength of dissimilar joints between MONEL400 and stainless steel using pulsed TIG and interpulsed TIG welding. AIP Conf Proc. 2020;2311(1):1–9. https://doi.org/10.1063/5.0034414.
94. Aqeel M, Gautam JP, Shariff SM. Comparative study on autogenous diode laser, CO2 laser-MIG hybrid and multi-pass TIG welding of 10-mm thick Inconel 617 superalloy. Mater Sci Eng A. 2022;856: 143967. https://doi.org/10.1016/j.msea.2022.143967.
95. Vidyarthy R, Dwivedi DK. Activating flux tungsten inert gas welding for enhanced weld penetration. J Manuf Process. 2016;22:211–28. https://doi.org/10.1016/j.jmapro.2016.03.012.
96. Tanaka M, Tashiro S, Kashima T, Lowke JJ, Murphy AB. A CO_2 gas shielded gas tungsten arc and its application to welding of steel sheets. Mater Sci Forum. 2007;539:3926–30. https://doi.org/10.4028/0-87849-428-6.3926.
97. Kumar A, Sundarrajan S. Optimization of pulsed TIG welding process parameters on mechanical properties of AA 5456 Aluminum alloy weldments. Mater Des. 2009;30(4):1288–97. https://doi.org/10.1016/j.matdes.2008.06.055.
98. Yu WW, Fan MY, Shi JH, Xue F, Chen X, Liu H. A comparison between fracture toughness at different locations of SMAW and GTAW welded joints of primary coolant piping. Eng Fract Mech. 2018;202:135–46. https://doi.org/10.1016/j.engfracmech.2018.09.021.
99. Yu WW, Fan MY, Jia WQ, Xue F, Yu M, Liu H, Chen X. Thermal aging effect on the tensile and fatigue properties of the narrow-gap TIG welded joints in offshore floating nuclear power plants. Int J Fatigue. 2019;126:143–54. https://doi.org/10.1016/j.ijfatigue.2019.05.002.
100. Wang RR, Welsch GE. Joining titanium materials with tungsten inert gas welding, laser welding, and infrared brazing. J

Prosthet Dent. 1995;74(5):521–30. https://doi.org/10.1016/S0022-3913(05)80356-7.
101. Wu SK, Zhang JC, Yang JX, Lu JX, Liao HB, Wang XY. Investigation on microstructure and properties of narrow-gap laser welding on reduced activation ferritic/martensitic steel CLF-1 with a thickness of 35 mm. J Nucl Mater. 2018;503:66–74. https://doi.org/10.1016/j.jnucmat.2018.02.038.
102. Wu SK, Shi YL, Liao HB, Wang Y. Microstructure and mechanical properties of LBW and EBW weld joints of CLF-1 steel: a comparative analysis. J Nucl Mater. 2021;549: 152914. https://doi.org/10.1016/j.jnucmat.2021.152914.
103. Rudling P, Adamson R, Cox B, Garzarolli F, Strasser A. High burnup fuel issues. Nucl Eng Technol. 2008;40(1):1–8. https://doi.org/10.5516/NET.2008.40.1.001.
104. Srivastava D, Mani KK, Neogy S, Dey GK, Samajdar I, Banerjee S. Evolution of microstructure, microtexture and texture in dilute zirconium based structural components of pressurised heavy water reactors. In 17th International Conference on Nuclear Engineering. 2009; 401–409. (Springer, Brussels, Belgium)
105. Slobodyan M. Resistance electron-and laser-beam welding of zirconium alloys for nuclear applications: A review. Nucl Eng Technol. 2021;53(4):1049–78. https://doi.org/10.1016/j.net.2020.10.005.
106. Bharadwaj V, Rai AK, Upadhyaya BN, Singh R, Rai SK, Bindra KS. A study on effect of heat input on mode of welding, microstructure and mechanical strength in pulsed laser welding of Zr-2.5 wt.% Nb alloy. J Nucl Mater. 2022;564:153685. https://doi.org/10.1016/j.jnucmat.2022.153685.
107. German CS, Lin X. GTAW welded inconel 625 alloy fuel cladding for the canadian scwr: microstructure and mechanical property characterization. J Nucl Eng Radiat Sci. 2021;7(3): 031304. https://doi.org/10.1115/1.4049278.
108. Luo Y, Fang ZW, Guo JZ, Lu H, Li J. Research on the virtual reality technology of a pipeline welding robot. Ind Rob. 2021;48(1):84–94. https://doi.org/10.1108/IR-04-2020-0074.
109. Shen C, Li ZZ, Ma YH, Sun LM. Research and application of underwater wet welding technology. Mater Sci Eng. 2019;562(1): 012161. https://doi.org/10.1088/1757-899X/562/1/012161.
110. Morita I, Owaki K, Yamaoka H, Kim CC. Study of underwater laser welding repair technology. Weld World. 2007;50(7–8):37–43. https://doi.org/10.1007/BF03266534.
111. Wang JF, Sun QJ, Zhang S, Wang CJ, Wu LJ, Feng JC. Characterization of the underwater welding arc bubble through a visual sensing method. J Mater Process Technol. 2018;251:95–108. https://doi.org/10.1016/j.jmatprotec.2017.08.019.
112. Łabanowski J. Development of under-water welding techniques. Weld Int. 2011;25(12):933–7. https://doi.org/10.1080/09507116.2010.540847.
113. Surojo E, Putri EDWS, Budiana EP, Triyono. Recent developments on underwater welding of metallic material. Procedia Struct Integr. 2020; 27: 14–21. https://doi.org/10.1016/j.prostr.2020.07.003.
114. Wang MQ, Fang NW, Sun LB, Wu PB, Huang RS, Xu K, Wang XX, Qin J, Zhou ZZ, Li S, Su JH, Long WM. Study of the microstructure and properties of the butt joint of laser-welded titanium alloy with flux-cored wire. Metals. 2023;13(2):369. https://doi.org/10.3390/met13020369.
115. Vashishtha P, Wattal R, Pandey S, Bhadauria N. Problems encountered in underwater welding and remedies-a review. Mater Today Proc. 2022;64:1433–9. https://doi.org/10.1016/j.matpr.2022.04.634.
116. Liu Y, Yang LJ, He TX, Zhai YL, Liu T. Spectral analysis of arc characteristics of flux cored wire TIG welding. Spectrosc Spectr Anal. 2017;37(07):2171–6. https://doi.org/10.3964/j.issn.1000-0593(2017)07-2171-06.
117. Chen JC, Xie WP, Liu RP, Wei YH. Microstructure and wear resistance of Fe-based hardfacing layer prepared by fux-cored wire feeding MAG welding process. Welding in the World. 2022;66:175–85. https://doi.org/10.1007/s40194-021-01209-w.
118. Liu DS, Long WM, Wu MF, Li LJ, Wang JY, Zhang Y. Microstructure and wear performance of Cobalt-Containing Iron-based slag-free self-shielded flux-cored wire. J Mater Eng Perform. 2019;28(4):2158–66. https://doi.org/10.1007/s11665-019-04002-5.
119. Hu Y, Shi YH, Shen XQ, Wang ZM. Microstructure evolution and selective corrosion resistance in underwater multi-pass 2101 duplex stainless steel welding joints. Metall Mater Trans A. 2018;49(8):3306–20. https://doi.org/10.1007/s11661-018-4686-0.
120. Cai ZH, Du X, Zhu JL, Wang K, Zhao XX, Liu J, Li J, Liu J, Wang J, Wang HD. Research on underwater wet laser self-fusion welding process and analysis of microstructure and properties of TC4 Titanium alloy weld. Materials. 2022;15(9):3380. https://doi.org/10.3390/ma15093380.
121. Varley RJ, Leong KH. Polymer coatings for oilfield pipelines. Ser Mater Sci. 2016;233:385–428. https://doi.org/10.1007/978-94-017-7540-3_14.
122. Hamasaki M, Sakakibara J. Underwater dry TIG welding using wire brush nozzle. Underwater Welding. 1983. https://doi.org/10.1016/B978-0-08-030537-0.50013-2.
123. Lyons RS, Middleton TB. Orbital TIG system simplifies underwater welding. Metal construction. 1984;16(10):627–31.
124. Zhai YL, Yang LJ, He TX, Liu Y. Weld morphology and microstructure during simulated local dry underwater FCTIG. J Mater Process Technol. 2017;250:73–80. https://doi.org/10.1016/j.jmatprotec.2017.07.010.
125. Gülenç B, Develi K, Kahraman N, Durgutlu A. Experimental study of the effect of hydrogen in argon as a shielding gas in MIG welding of austenitic stainless steel. Int J Hydrog Energy. 2005;30(13–14):1475–81. https://doi.org/10.1016/j.ijhydene.2004.12.012.
126. Yamashita Y, Kawano T, Mann K. Underwater laser welding by 4 kW CW YAG laser. J Nucl Sci Technol. 2001;38(10):891–5. https://doi.org/10.3327/jnst.38.891.
127. Zhang XD, Ashida E, Shono S, Matsuda F. Effect of shielding conditions of local dry cavity on weld quality in underwater Nd: YAG laser welding. J Mater Process Technol. 2006;174(1–3):34–41. https://doi.org/10.1016/j.jmatprotec.2004.12.009.
128. Guo N, Fu YL, Xing X, Liu YK, Zhao SX, Feng JC. Underwater local dry cavity laser welding of 304 stainless steel. J Mater Process Technol. 2018;260:146–55. https://doi.org/10.1016/j.jmatprotec.2018.05.025.
129. Liao HP, Zhang WX, Xie HM, Li XY, Zhang Q, Wu XM, Tian JY, Wang ZM. Effects of welding speed on welding process stability, microstructure and mechanical performance of SUS304 welded by local dry underwater pulsed MIG. J Manuf Process. 2023;88:84–96. https://doi.org/10.1016/j.jmapro.2023.01.047.
130. Huang J, Xue L, Huang J, Zou Y, Niu H. Arc behavior and joints performance of CMT welding process in hyperbaric atmosphere. Acta Metall Sin. 2016;52(1):93–9. https://doi.org/10.11900/0412.1961.2015.00204.
131. Miholca C, Nicolau V. Pressure influence upon the welded metal geometry on the MAG hyperbaric procedure by estimating the spectral power of the electrical ARC signals. Weld World. 2005;49:276–7.
132. Wu SJ, Gong S, Gao HM. Arc characteristics of GTAW under high pressure. Sadhana Acad P Eng S. 2019; 44(3): 70. https://doi.org/10.1007/s12046-019-1053-9.
133. Treutler K, Brechelt S, Wiche H, Wesling V. Beneficial use of hyperbaric process conditions on the welding of high-strength low alloy steels. Sci Rep. 2022;12(1):12434.

134. Azar AS, Woodward N, Fostervoll H, Akselsen OM. Statistical analysis of the arc behavior in dry hyperbaric GMA welding from 1 to 250 bar. J Mater Process Technol. 2012;212(1):211–9. https://doi.org/10.1016/j.jmatprotec.2011.09.006.
135. Burke MH. Future developments in plasma arc welding. Aircr Eng Aerosp Technol. 1968;40(12):13–5. https://doi.org/10.1108/eb034452.
136. Richardson IM. Properties of the Constricted Gas Tungsten Plasma Welding Arc at Elevated Pressures. 1991. (Cranfield University at Bedfordshire in UK).
137. Lythall DJ. New underwater welding process proved for continental shelf depths. In Offshore Technology Conference. 1977. (Houston, Texas).
138. Wu KY, Huang H, Chen ZW, Zeng M, Yin T. Novel and simplified implementation of digital high-power pulsed MIG welding power supply with LLC resonant converter. Circuit World. 2022. https://doi.org/10.1108/CW-03-2022-0068.
139. Nixon JH, Richardson IM. Deepwater welding and intervention technology. Underw Technol. 1995;21(3):3–7. https://doi.org/10.3723/175605495783326432.
140. Dos SJ, Szelagowski P, Schafstall H. Mechanical and metallurgical properties of robotic underwater welds performed within a depth range of 100 to 1100 msw. In: Proceedings of the 7th International Conference on Offshore Mechanics and Arctic Engineering. 1988. (Houston, USA).
141. Song L, Peng Y, Zhao HY, Cao Y, Fang Q. Corrosion resistance analysis of the weld metal of low-alloy high-strength steel considering different alloy compositions. Front Mater. 2022;9:957669. https://doi.org/10.3389/fmats.2022.957669.
142. Wahab MA, Sakano M. Experimental study of corrosion fatigue behaviour of welded steel structures. J Mater Process Technol. 2001;118(1):116–21. https://doi.org/10.1016/S0924-0136(01)00902-5.
143. Wahab MA, Sakano M. Corrosion and biaxial fatigue of welded structures. J Mater Process Technol. 2003;143:410–5. https://doi.org/10.1016/S0924-0136(03)00412-6.
144. Xu FF, Zhao Y, Xu Y. Preparation and corrosion resistance of rare earth–silane composite conversion coatings on magnesium–lithium alloy surface. Rare Met. 2023;42(2):1011–7. https://doi.org/10.1007/s12598-015-0657-4.
145. Wei HH, Tang YQ, Chen C, Xi PF. Corrosion behavior and microstructure analysis of butt welds of Q690 high strength steel in simulated marine environment. J Build Eng. 2024;84: 108509. https://doi.org/10.1016/j.jobe.2024.108509.
146. Wei A, Feng YJ, Wu LY, Li YY, Xie ZW. Corrosion wear behavior of 30CrNi2MoVA steel in simulated seawater. Mater Lett. 2023. https://doi.org/10.1016/j.matlet.2023.134750.
147. Zhang Y, Yin XY, Yang FY. Tribocorrosion behaviour of type S31254 steel in seawater: identification of corrosion–wear components and effect of potential. Mater Chem Phys. 2016;179:273–81. https://doi.org/10.1016/j.matchemphys.2016.05.039.
148. Somervuori ME, Alenius MT, Kosonen T, Karppi R, Hänninen HE. Corrosion fatigue of weld-bonded austenitic stainless steels in 3.5% NaCl solution. Mater Corros. 2006;57(7):562–7. https://doi.org/10.1002/maco.200503950.
149. Ha HY, Lee TH, Lee CG, Yoon H. Understanding the relation between pitting corrosion resistance and phase fraction of S32101 duplex stainless steel. Corros Sci. 2019;149:226–35. https://doi.org/10.1016/j.corsci.2019.01.001.
150. Gnanarathinam A, Palanisamy D, Gangaraju M, Arulkirubakaran D, Balachander E. Investigation of corrosion behavior of welded area of austenitic stainless steel under different environments. Mater Today: Proceedings. 2022;68:1737–41. https://doi.org/10.1016/j.matpr.2022.09.351.
151. Omiogbemi IM, Faci ND, Gummadi AK. The influence of arc welding process on the mechanical and microstructural characteristics of low carbon steel in a corrosive environment. Macromol Symp. 2022;402(1):2100362. https://doi.org/10.1002/masy.202100362.
152. Wang L, Hui L, Song Z, Xu L, He B. Effect of corrosive environment on fatigue property and crack propagation behavior of Al 2024 friction stir weld. Trans Nonferrous Met Soc China. 2016;2016(26):2830–7. https://doi.org/10.1016/S1003-6326(16)64411-4.
153. Zhang ZQ, Jing HY, Xu LY, Han YD, Zhao L, Lv XQ, Zhang JY. Influence of heat input in electron beam process on microstructure and properties of duplex stainless steel welded interface. Appl Surf Sci. 2018;435:352–66. https://doi.org/10.1016/j.apsusc.2017.11.125.
154. Nyrkova L, Goncharenko L, Osadchuk S, Labur T, Yavorska M. Influence of exposure in a corrosive environment on ultimate stress of heat-treated welded joints of Al-Mg-Si-Cu alloy. Corros Rev. 2023;41(4):485–96. https://doi.org/10.1515/corrrev-2022-0076.
155. Kumar PV, Reddy M, Rao KS. Microstructure, mechanical and corrosion behavior of high strength AA7075 aluminium alloy friction stir welds—effect of post weld heat treatment. Defence Technology. 2015;11(4):362–9. https://doi.org/10.1016/j.dt.2015.04.003.
156. Fereidooni B, Morovvati MR, Sadough-Vanini SA. Influence of severe plastic deformation on fatigue life applied by ultrasonic peening in welded pipe 316 Stainless Steel joints in corrosive environment. Ultrasonics. 2018;88:137–47. https://doi.org/10.1016/j.ultras.2018.03.012.
157. Sinhmar S, Dwivedi DK. A study on corrosion behavior of friction stir welded and tungsten inert gas welded AA2014 aluminium alloy. Corros Sci. 2018;133:25–35. https://doi.org/10.1016/j.corsci.2018.01.012.
158. Kwok CT, Fong SL, Cheng FT, Man HC. Pitting and galvanic corrosion behavior of laser-welded stainless steels. J Mater Process Technol. 2006;176(1–3):168–78. https://doi.org/10.1016/j.jmatprotec.2006.03.128.
159. Gong Q, Wu H, Yang F, Tang ZH. Corrosion of pipeline steel weld metals containing alloying elements in CO_2/H_2S environment. J Nat Gas Sci Eng. 2023;109: 104846. https://doi.org/10.1016/j.jngse.2022.104846.
160. Xu QF, Gao KW, Lv WT, Pang XL. Effects of alloyed Cr and Cu on the corrosion behavior of low-alloy steel in a simulated groundwater solution. Corros Sci. 2016;2015(102):114–24. https://doi.org/10.1016/j.corsci.2015.09.025.
161. Avazkonandeh-Gharavol MH, Haddad-Sabzevar M, Haerian A. Effect of copper content on the microstructure and mechanical properties of multipass MMA, low alloy steel weld metal deposits. Mater Des. 2009;30(6):1902–12. https://doi.org/10.1016/j.matdes.2008.09.023.
162. Bhole SD, Nemade JB, Collins L, Liu C. Effect of nickel and molybdenum additions on weld metal toughness in a submerged arc welded HSLA line-pipe steel. J Mater Process Technol. 2006;173(1):92–100. https://doi.org/10.1016/j.jmatprotec.2005.10.028.
163. Wu S, Ning YJ, Xie H, Tian HY, Lv JM, Liu B. Study on the galvanic corrosion behavior of copper-nickel/titanium alloys under simulated seawater environment. J Solid State Electrochem. 2023. https://doi.org/10.1007/s10008-023-05769-3.
164. Su HN, Rosidah AA, Lillahulhaq Z, Ridhlo IA, Wardani I. The experiment of ambient wind speed and argon flow rate on tig welding process. Mater Sci Eng. 2021;1010(1):012023. https://doi.org/10.1088/1757-899X/1010/1/012023.
165. Ren XQ, Chen C. Research on mechanical clinching process for dissimilar aluminum alloy sheets with inclined surface. J Manuf

Process. 2023;89:362–70. https://doi.org/10.1016/j.jmapro.2023.01.073.
166. Nasresfahani AR, Soltanipur AR, Farmanesh K, Ghasemi A. Effects of tool wear on friction stir welded joints of Ti–6Al–4V alloy. Mater Sci Technol. 2017;33(5):583–91. https://doi.org/10.1080/02670836.2016.1237065.
167. Li W, Chang KR, Zeng PY, Zuo CG. Impact wear of flash-and aluminothermic-welded hypereutectoid steel rail joints. Tribol Trans. 2021;64(4):644–57. https://doi.org/10.1080/10402004.2021.1893874.
168. Qin DL, Chen C. Failure behavior and mechanical properties of novel dieless clinched joints with different sheet thickness ratios. J Cent South Univ. 2022;29:3077–87. https://doi.org/10.1007/s11771-022-5120-8.